Deep well injection at the Langerak and Nieuwegein sites in the Netherlands: chemical reactions and their modeling

CLIENTs
Water Supply Zuid-Holland Oost (WZHO)
European Commission

ORDER NUMBERs
30.1460.016, 30.1110.018 (ENV4-CT95-0071)

AUTHORs
P.J. Stuyfzand[1] & H. Timmer[2]

DEPARTMENTs
[1] Water Resources and Water Management, Kiwa Research and Consultancy, Nieuwegein, Netherlands
[2] Production, Water Supply Zuid-Holland Oost, Gouda, Netherlands

Nieuwegein, May 1999

Research & Consultancy

Groningenhaven 7
P.O. Box 1072
3430 BB Nieuwegein
Phone 31 30 60 69 511
Fax 31 30 60 61 165

ISBN 90-74741-70-3

© 1999 Kiwa NV, Research & Consultancy
All rights reserved. No part of this publication may be reproduced, stored in a retrieval system or transmitted in any form or by any means, electronic, mechanical, magnetic tape, photocopying, recording or otherwise, without permission from the publisher, kiwa nv.

SWE 99.006

PRODUCT DESCRIPTION

Title:'Deep well injection at the Langerak and Nieuwegein sites in the Netherlands: chemical reactions and their modeling'
Authors: dr. P.J. Stuyfzand & drs. H. Timmer
Editor: Kiwa Research and Consultancy, Nieuwegein, the Netherlands
Series no: Kiwa-SWE 96.006
Clients: Water Supply Company Zuid-Holland Oost (WZHO) and European Commission
Specification: with 15 tables, 47 figures and 44 pages
Key words: artificial recharge / deep well injection / quality changes / aquifer passage / pyrite oxidation / heavy metals / chemical reactions / sorption / retardation / leaching / well clogging.

ISBN 90-74741-70-3

Contents

Preface

Water supply company South-Holland East (WZHO) considers deep well injection of pretreated Rhine river water as an attractive technique to meet growing drinking water demands within its supply area. In order to explore the feasibility of this technique, one experimental injection well and 2-3 monitoring wells were drilled on each of two sites: near Langerak and near Nieuwegein, both in the fluvial plain of the Rhine River.

WZHO built the test site, performed the hydrological and hydrochemical measurements, and constructed a hydrological model. Kiwa Research and Consultancy advised on the experimental set-up, performed the geochemical analyses, built the parallel columns, elaborated the chemical data and made various progress reports and a final report on the hydrochemical aspects.

WZHO's main objective of both injection experiments was to know whether pretreated Rhine river water can be injected into a deep sandy aquifer without serious clogging of the injection well. WZHO's second most important objective was to know and understand the water quality changes during aquifer passage.

Water quality changes also formed the scope of the work packages 'Redox dynamics' and 'Water-rock interaction' within the EU-project 'Artificial Recharge'. This project was financed by the European Union within the framework of the Environment and Climate program, under contract ENV4-CT95-0071. This combined interest (WZHO and EU) resulted in a more profound analytical program and elaboration of data, collected in this report. In addition the experimental results presented here, formed the basis of studies on chemical transport modelling in connection with (a) the above-mentioned EU-project, and (b) a joint project of Kiwa and NITG-TNO sponsored by 9 Dutch drinking water companies.

The help of Frans Lüers (Kiwa) in all the data manipulation is greatly acknowledged.

Abstract

Characterization of the target aquifer

Prior to deep well injection the target aquifer was examined on both field sites: Langerak and Nieuwegein in the Rhine fluvial plain of the Netherlands.

The target aquifer is composed on both sites of Middle Pleistocene sands belonging to the same sedimentary unit (mainly Harderwijk Formation). It is composed, in the middle and lower parts, of deep anoxic, mainly quartz sands, poor in organic carbon (0.09-0.12%), containing a small amount of pyrite (70-200 mg S/kg) and calcite (0.3-0,6%). CEC is low (8-12 meq/kg), dominated by Ca^{2+} (69-77% of CEC) and Mg^{2+} (17%). The top layer contains on both sites 2-30 times more organic carbon, calcite and pyrite.

The maximum trace element content of pyrite was estimated by linear regression of the pyrite content (expressed as S) and the amounts of As, Co, Ni and Zn extracted with aqua regia. This yielded the following most probable stoichiometry of pyrite: $Fe_{0,98}Co_{0,0037}Ni_{0,01}Zn_{0,01}S_2As_{0,0053}$.

Batch experiments were carried out with 5 aquifer samples. For 72 hours the samples were shaken with pretreated Rhine River water in closed vials, with and without addition of 2 mmol $NaNO_3$/l. The main reaction was the oxidation of pyrite; this reaction was kinetically hindered. Arsenic and nickel, from oxidizing pyrite, were largely fixed in solid phases again, probably in neoformed ironoxyhydroxides.

On both sites the native groundwater shows a very high pre-industrial quality, which is characterized further as 'chloride-poor, deep anoxic (high in methane, without any oxygen, nitrate and sulphate) and calcite-saturated.

The target aquifer on both sites compared very well, notwithstanding minor differences.

The injection experiments

In the period July 1996 till March 1998 Water Supply Company WZHO carried out 2 deep well recharge experiments, one in Langerak and the other in Nieuwegein (Netherlands). At both test sites the influent was oxic and the anoxic sandy target aquifer contained pyrite. Both experiments revealed a typical quality evolution due to sequential leaching of aquifer constituents. The main processes were, in mean order of increasing duration: displacement of native groundwater, cation exchange, pyrite oxidation, acid-buffering by calcite dissolution, and oxidation of organic matter. Differences in quality changes between both sites relate to their deviating aquifer geochemistry and influent quality. The reactions were quantified using the mass balance approach (also called 'inverse modeling').

Pyrite oxidation was kinetically hindered, it took about 10 days to deplete O_2 and 100 days to deplete NO_3^- in the influent. Oxygen was reacting faster with pyrite than with labile organic matter, for nitrate the reverse was true. Pyrite oxidation led to mobilization of As, Ni and Zn, but they were largely fixed by neoformed $Fe(OH)_3$. The main geochemical heterogeneity was related to variations in the reactivity of both pyrite (high in lower parts of aquifer) and organic matter (high in upper parts of aquifer).

The water quality changes during aquifer passage and the leaching of reactive solid phases from the aquifer have been successfully simulated for each site, using Kiwa's model EASY-LEACHER. The main reactions included were: pyrite oxidation, oxidation of organic matter, cation exchange and calcite dissolution. In addition, the model was used to predict the quality development over 100 years, for the raw water recovered by a fictive deep well injection plant on the Langerak site.

Some conclusions of practical interest

Reactions of pretreated Rhine river water with the aquifer and mixing with native groundwater necessitate to post-treat the water recovered, in order to remove methane, iron, manganese and ammonium for obtaining drinking water quality. This can be achieved by aeration and rapid sand filtration. Water softening prior to injection is dissuaded, if the calcite saturation index of the influent is maintained at 0 (equilibrium), because of calcite dissolution in the aquifer. However, water softening prior to injection can be applied if the influent is kept calcite supersaturated (SI > +0.3), because this will buffer the acid produced in the aquifer.

The presence of oxidizable pyrite and organic matter in the aquifer are expected to protect the recovery wells in a future plant from a cumbersome clogging (by mixing of aerobic with anaerobic, ferrogenous water) for at least 50 years.

1 Introduction

Pieter J. Stuyfzand
Kiwa Research and Consultancy, Nieuwegein, Netherlands

1.1 DEEP WELL INJECTION

In general

Artificial recharge of aquifer systems can be achieved by way of injection through deep wells (Huisman & Olsthoorn, 1983). In general surface water is used after a thorough pretreatment in order to remove suspended fines which otherwise will clog the injection well.

Deep well injection, in contrast to ASR (Aquifer Storage and Recovery) consists of separate injection and recovery wells. It uses single purpose wells (for either injection or recovery), and aims at quality improvement. ASR uses a dual purpose well (first for injection, later for recovery), and aims at storage without quality changes!

Aquifer passage thus is considered an essential advantage of deep well injection, for reasons discussed in section 1.2. The beneficial quality improvements make deep well recharge an interesting option in preparing drinking water from polluted surface water, especially in areas where space is too scarce for open recharge or storage reservoirs.

In the Netherlands

Space restrictions predominate in the densely populated Netherlands and stimulated several water supply companies to study the feasibility of deep well recharge since 1970, and in two cases a production plant has been realized in 1989-1990 (Stuyfzand, 1998b). Although clogging of the injection well, being the most critical factor, was the main target of these studies, water quality changes in the aquifer were also given importance. This is mainly for two practical reasons:

(a) water quality changes in the aquifer determine which post-treatment will be necessary and whether water softening can be included in the pretreatment or not. Where deep well recharge is to be applied on an already existing well field, its water treatment may need modifications when the quality of the raw water will change due to the recovery of 'renovated groundwater'. The water-aquifer interactions are likely to result in an unsteady water quality of the infiltrate recovered, which needs to be quantified in order to schedule adaptations of the existing treatment facility; and

(b) the mixing of various water qualities in recovery wells poses serious clogging hazards (Van Beek, 1989). This clogging may shorten the life time of the pumping wells and thereby reduce the economic feasibility of the project. Due to heterogeneity of the aquifer and diverging flow velocities and travel distances in the artificial flow domain between injection and recovery wells, mixing of water types will occur in the recovery well. In this mixing the following watertypes are involved: (1) the native anoxic groundwater (slowly replaced, never completely depleted), (2) anoxic infiltrate (the first to arrive at the recovery well), and in a later stage (3) oxic infiltrate (reaching the recovery well only after depletion of the reactive aquifer phases). The mixing of watertype 3 with either 1 or 2 will cause the clogging of the recovery well.

In Langerak and Nieuwegein

Water supply company South-Holland East (WZHO) supplies drinking water to 0.7 million inhabitants in the Rhine fluvial plain in the Netherlands, in between Amsterdam, Rotterdam and Utrecht. The main source is Rhine bank filtrate, requiring advanced purification techniques. WZHO considers deep well injection of pretreated river Rhine water as an attractive technique to meet growing drinking water demands within its supply area. To test this technique prior to large scale application, two experimental injection wells were constructed, one in Largerak and the other in Nieuwegein (about 20 km apart). The chemical results obtained with these wells are reported in chapters 3-5. The test sites, set-up and goals of the experiments and analytical program are described in Ch.2.

1.2 CHEMICAL AND MICROBIOLOGICAL ADVANTAGES OF AQUIFER PASSAGE

From a hygienic point of view, aquifer passage is the most essential part of artificial recharge and related techniques like bank filtration (induced recharge). It has proved to be capable of transforming polluted surface and waste waters into hygienically save groundwater of a relatively constant water quality in many parts of the world (Olsthoorn & Huisman, 1983; Asano, 1985; Stuyfzand, 1989a,b, 1998a; Frycklund, 1998).

Stuyfzand & Lüers (1996) mention the following advantages:

(1) a nearly 100% elimination of suspended fines and the attached heavy metals, trace organic contaminants, and pathogens, by filtration;
(2) a full 100% elimination of the non-silt-bound pathogens, by filtration, sorption, and dying-off, if distance and time in the underground suffice (Gerba & Goyal, 1985);
(3) attenuation of quality fluctuations (including temperature) in the influent, by spreading the detention times, dispersion, sorption, elimination, and dilution with native groundwater (Huisman & Olsthoorn, 1983; Stuyfzand, 1989, 1998c; Sontheimer, 1991);
(4) a reduction of the radio-activity, especially by prolongation of the detention times in the aquifer through sorption (Haberer, 1989; Stuyfzand, 1998c);
(5) a more or less permanent lowering of the concentration of many organic micropollutants and colour, taste and odour compounds, by breakdown or degradation, and dilution with native groundwater (Bouwer, 1985; Piet & Smeenk, 1985; Stuyfzand, 1998);
(6) a natural hardness and pH correction in case of an acidic, soft influent passing through a calcareous aquifer;
(7) a natural denitrification in case of surface water contaminated with nitrate passing through an anoxic aquifer with reactive organic material or pyrite (Stuyfzand, 1998a,b);
(8) a lowering of the toxicological effects in connection with 1 and 4-7 (Kool, 1983; Noordsij et al., 1985); and
(9) storage in a medium protected from atmospheric fall-out, microbiological infection, and algal blooms.

The environmental profits of this 'natural' purification method, as compared to chemical water treatment, are many. The following is considered most important: a reduced application of undesired chemicals like coagulants, active carbon and ozone or chlorine.

1.3 CHEMICAL DISADVANTAGES OF AQUIFER PASSAGE

Stuyfzand & Lüers (1996) mention the following disadvantages of aquifer passage from a chemical point of view:

(a) the accumulation of fine particles in a clogging layer either at the floor of a basin or at the bore hole wall of an injection well (see Ch.5). This layer is harder to remove than the clogging layer in a purification plant;
(b) the accumulation of pollutants in the aquifer. This is more difficult to remove than in a treatment plant and may deteriorate a larger volume of natural, although subterranean, space;
(c) the leaching of natural reactive solid phases from the aquifer. Although this may proceed very slowly, on the long run (sometimes centuries) specific beneficial processes like complete denitrification and hardness or pH correction will stop. This reactivity cannot be restored easily in contrast with a purification plant; and
(d) undesired changes in water quality which require post-treatment after recollection. These may consist of an increase in concentration of Ca^{2+}, HCO_3^-, SiO_2, SO_4^{2-}, Fe^{2+}, Mn^{2+}, NH_4^+, CH_4, As, DOC and PO_4^{3-} (Stuyfzand, 1998a).

The disadvantages under a and b can be reduced by a selective intake and intensive pretreatment.

1.4 PROCESSES AND FACTORS AFFECTING QUALITY CHANGES

Water quality changes during aquifer passage are related to the 7 main processes listed in Table 1.1. These processes mainly depend on factors connected with either the aquifer (the presence of an unsaturated zone, the grain size, travel distance and travel time), or the water it self prior to infiltration (temperature, pH, electrical conductivity or ionic strength, and complexation, for instance with DOC).

Of course, the processes are also governed to a large extent by the concentration levels of the substances involved in each process: the concentration levels in the influent as well as the aquifer's content of reactive phases like organic matter, carbonates, silicates, phosphates, hydroxides, and sulphides. Aquifers containing gypsum or halites haven been excluded from Table 1.1, because they are not considered a suitable target aquifer for drinking water supply.

TABLE 1.1 Review of the most important processes during aquifer passage and their dependency on aquifer and water factors.

PROCESS	SUBSTANCES INVOLVED @	AQUIFER FACTORS				WATER FACTORS				
		unsatur zone	grain size	distance	time	temp.	pH	EC	complex.	oxidation capacity
FILTRATION	Suspended solids	o	--	+	o	o	o	o	o	o
	hydrophobic OMPs and TEs	o	--	+	+	o	o	o	o	o
	B&V	o	--	+	+	o	o	o	o	o
OXIDATION or REDUCTION	O_2, NO_3, SO_4, NH_4, Fe, Mn, CH_4	++/--	--	++	++	++	+	+?	-?	++/--
	As, Cr, Cu, Sb, Se, V	++/--	--	++	++	++	+	+?	-?	++/--
	DOC, OMPs	++/--	--	++	++	++	+	+?	-?	++/--
SORPTION	cations (also OMPs/TEs^+)	o	--	++	o	-	++	--	--	o
	anions (F, PO_4, OMPs/TEs^-)	o	--	++	o	-	--	--	--	o
	OMPs (uncharged)	o	--	++	o	-	-	?	?	o
	B&V	?	--	++	o	-	+/-	+/?	o	o
DISSOLUTION	carbonates (Ca, Sr, HCO_3, PO_4, Fe, Mn)	o	--	o	o	--	--	+	+	o
	silicates (SiO_2, Al, Ca, Na, K)	o	--	++	++	++	--	+	++	+
	sulfides (Fe, H_2S, TEs)	++	-	o/+	o/+	+	--	+	+	++
	phosphates (PO_4, Ca, Fe, F)	o	--	+	+	+	--	+	++	-
	hydroxides (Fe, Al)	-	--	+	+	+	--	+	++	--
PRECIPITATION	carbonates (Ca, Sr, HCO_3, PO_4, Fe, Mn)	o	-	o	o	++	++	-	-	o
	sulfides (Fe, H_2S, TEs)	--	-	o/+	o/+	-	++	-	--	--
	phosphates (PO_4, Ca, Fe, F)	o	-	+	+	-	++	-	--	+
	hydroxides (Fe, Al)	++	-	+	+	-	++	-	--	++
DECAY	^3H, ^{14}C, ^{60}Co, ^{90}Sr, ^{106}Ru, ^{131}I, ^{137}Cs	o	o	o	++	o	o	o	o	o
	B&V (die off)	?	o	?	++	++	?	o	o	?
MIXING	all	o	--	++	++	+	o	o	o	o

o = no/little influence; - = moderate influence (negative relation); -- = strong influence (negative relation); + moderate influence (positive relation); ++ = strong influence (positive relation).
@: OMPs = Organic MicroPollutants; TEs = Trace Elements; B&V = Bacteria and Virusses.

1.5 OBJECTIVES OF THIS REPORT

The main objectives

The main objectives of this report are to:

(a) quantify the migration rate of the nitrate and oxygen fronts in the anoxic target aquifer and relate their retardation to the relevant redox reactions and the initial amount of the reactive redox constituents of the aquifer material.

(b) quantify all relevant water-aquifer interactions and thereby predict the dynamic water quality evolution in the recovery well.

The quality changes of injected drinking or waste water during movement in aquifer systems, and particularly the extinction of these changes with time, were never quantitatively linked to the initial amounts of reactive phases in the aquifer material. This linking is attempted here, and is a prerequisite for predicting the quality of the water being recovered on the long term. This linking results ideally in a model which only requires the input of soil chemical data, the quality of the water to be injected and various hydrological data (like the various transit times in the aquifer and mixing), and subsequently generates the prediction. Knowing the (approximate) answers before starting injection experiments, means that the experiment can be optimized a priori (for instance by selecting a more appropriate aquifer or another surface water quality), and that the experimental run can be shortened, thus saving time and money.

Scientific issues

Experiments during artificial recharge form an ideal compromise between laboratory experiments and field studies. They unify the advantages of both: most experimental conditions are well defined (like flow and quality of in- and effluent), the scale of operation is large enough to contain the natural heterogenities (in general an aquifer volume of about 40 m high, 20 m wide and 150 m long is addressed), and the time scale is also sufficient (1-3 years) for detection of specific trends.

The main scientific questions today, regarding the behaviour and modelling of solutes in a raw water source for drinking water preparation, as in case of artificial recharge and bank infiltration, are connected with:

- unknown reaction kinetics in complex natural environments;
- uncertainties in the contribution of enhanced or facilitated transport by particles or dissolved

organic macro-molecules (lumped together in DOC-analysis);
- a further need to identify hard-to-detect organic micropollutants (like pharmaceutical compounds, metabolites of pesticides, and xeno-oestrogens); and
- the difficult quantification of reactive constituents of the aquifer matrix, especially the fraction of reactive organic material and the trace element content of for instance pyrite.

This study addresses some of these scientific issues, especially: (a) the kinetics of denitrification, pyrite oxidation, the oxidation of organic matter; and (b) the quantification of the reactive fraction of organic matter and of the trace element content of pyrite.

1.6 RELATION WITH OTHER REPORTS

This report is in fact a collection of various contributions of Kiwa and WZHO to the final EU-report on Artificial Recharge (Jensen et al. 1999).

Contributions to this EU-report, which also elaborate on the experiments at Langerak and Nieuwegein, but which are not included here, are:

on the clogging of the injection wells by Timmer et al. (1999), and by Perez-Paricio & Carrera (1999); and on chemical transport modelling by Saaltink (1999).

Furthermore, there were several contributions to the third international symposium on artificial recharge (TISAR) in Amsterdam (21-25 September 1998), which were based on the experiments at Langerak and Nieuwegein as well. These were on various results by Timmer & Stuyfzand (1998), and on chemical transport modelling by Brun et al (1998) and by Saaltink et al (1998).

1.7 REFERENCES

ASANO, T. [ed] (1985). Artificial recharge of groundwater. Butterworth Publ., Boston, 767p.

BALL, J.W. & D.K. NORDSTROM 1991. User's manual for WATEQ4F, with revised thermodynamic data base and test cases for calculating speciation of major, trace and redox elements in natural waters. US Geol. Surv., Open-File Report 91-183.

BOSMA, T.N.P., E.M.W. BALLEMANS, N.K. HOEKSTRA, R.A.G. TE WELSCHER, J.G.M.M. SMEENK, G. SCHRAA & A.J.B. ZEHNDER 1996. Biotransformation of organics in soil columns and an infiltration area. Ground Water 34, 49-56.

BOUWER, H. 1985. Renovation of wastewater with rapid-infiltration land treatment systems. Ch.8 in 'Artificial Recharge of Groundwater', T. Asano (ed), Butterworth Publ. Boston, 249-282.

BRUN, A., F.D. CHRISTENSEN, J.S. CHRISTIANSEN, P.J. STUYFZAND & H. TIMMER 1998. Water quality modelling at the Langerak deep-well recharge site. In: Peters J.H. (ed), Artificial Recharge of groundwater, Proc. 3rd Intern. Symp. on Artificial Recharge, Amsterdam the Netherlands, Balkema, 305-310.

FRYCKLUND C. 1998. Artificial recharge of groundwater for public water supply; potential and limitations in Boreal conditions. Ph.D. Thesis, Royal Inst. Technology (KTH), Stockholm.

GIGER W. ET AL. 1983. Das verhalten organischer Wasserinhaltstoffe bei der Grundwasserbildung und im Grundwasser. Gas-Wasser-Abwasser, 63, 517-531.

HABERER, K. 1989. Umweltradioaktivität und Trinkwasserversorgung. R. Oldenbourg Verlag, München, 142p.

HRUBEC, J., A. LUIJTEN, W.C.M.M. LUIJTEN & G.J. PIET 1986. A pilot plant study on water quality changes during groundwater recharge. Water Research 20, 1119-1127.

HRUBEC, J., G. DEN ENGELSMAN, A.C. DE GROOT & R.S. DEN HARTOG, 1995. Behaviour of organic micropollutants during groundwater recharge. Intern. J. Environ. Anal. Chem. 58, 185-198.

HUISMAN, L. & T.N. OLSTHOORN 1983. Artificial Groundwater Recharge. Pitman Books Ltd, London, 320p.

KARICKHOFF S.W., D.S. BROWN & T.A. SCOTT, 1979. Sorption of hydrophobic pollutants on natural sediments. Water Res. 13, 241-248

KOOL, H.J. 1983. Organic mutagens in drinking water in the Netherlands. Proefschrift LU-Wageningen, 116p.

NOORDAM, P.C. 1985. Toxicologische aspecten van oevergrondwater. Ch.9 in KIWA-Meded. 89, 42p.

NOORDSIJ, A., L.M. PUIJKER & M.A. VAN DER GAAG 1985. The quality of drinking water prepared from bank-filtered river water in the Netherlands. Sci. Total Environm. 47, 273-292.

PEREZ-PARICIO, A. & J. CARRERA 1999. Modelling of physical clogging in a recharge well: the Langerak site. Section 9.7 in EU-report on Artificial Recharge, contract ENV4-CT95-0071, K.H. Jensen et al., in prep.

PIET, G.J. & J.G.M.M. SMEENK 1985. Behaviour of organic pollutants in pretreated Rhine water during dune infiltration. In "Ground water quality", C.H. Ward, W. Giger & P.L. McCarthy (eds), J. Wiley & Sons, NY, 122-144.

PIET, G.J. & B.C.J. ZOETEMAN 1980. Organic water quality changes during sand bank and dune filtration of surface waters in The Netherlands. J. AWWA, July 1980, 400-404.

SAALTINK, M.W. 1999. Modelling deep well recharge at Langerak using RETRASO. Section 9.6 in EU-report on Artificial Recharge, contract ENV4-CT95-0071, K.H. Jensen et al., in prep.

SAALTINK, M.W., C. AYORA, P.J. STUYFZAND & H. TIMMER 1998. Modelling the effects of deep artificial recharge on groundwater quality. In: Peters J.H. (ed), Artificial Recharge of groundwater, Proc. 3rd Intern. Symp. on Artificial Recharge, Amsterdam the Netherlands, Balkema, 423-425.

SCHWARZENBACH R.P. and J. WESTALL, 1981. Transport of nonpolar organic compounds from surface water to groundwater. Laboratory sorption studies. Env. Sci. and Techn. 15, 1360-1367.

SCHWARZENBACH R.P., W. GIGER, E. HOEHN & J. SCHNEIDER, 1983. Behavior of organic compounds during infiltration of river water to groundwater; Field studies. Envir. Sci. and Techn. (17), 472-479.

SONTHEIMER, H. 1991. Trinkwasser aus dem Rhein?. Academia Verlag, Sankt Augustin, BRD, 295p.

STUYFZAND P.J., 1989a. Quality changes of river Rhine and Meuse water upon basin recharge in The Netherlands' coastal dunes: 30 years of experience. In "Artificial recharge of groundwater", Johnson & Finlayson (eds), Am. Soc. Civ. Eng., New York, 235-247.

STUYFZAND, P.J. 1989b. Hydrology and water quality aspects of Rhine bank ground water in The Netherlands. J. Hydrol. 106, 341-363.

STUYFZAND, P.J. 1993. Hydrochemistry and hydrology of the coastal dune area of the Western Netherlands. Ph.D Thesis Vrije Univ. Amsterdam, published by KIWA, ISBN 90-74741-01-0, 366 p.

STUYFZAND, P.J. 1994. Behavior of phosphate in eutrophic surface water upon artificial recharge in the Western Netherlands. In : "Artificial recharge of Groundwater", Proc. Int. Symp. Orlando USA, 17- 22 July 1994, Johnson, A.I. & D.J. Finlayson (eds), Am. Soc. Civil Eng., New York, in press; tevens als Kiwa-rapport SWI 95.135, 10p.

STUYFZAND, P.J. 1998a. Fate of pollutants during artificial recharge and bank filtration in the Netherlands. In: Peters J.H. (ed), Artificial recharge of groundwater, Proc. 3rd Intern. Symp. on Artificial Recharge, Amsterdam the Netherlands, Balkema, 119-125.

STUYFZAND, P.J. 1998b. Quality changes upon injection into anoxic aquifers in the Netherlands: evaluation of 11 experiments. In: Peters J.H. (ed), Artificial recharge of groundwater, Proc. 3rd Intern. Symp. on Artificial Recharge, Amsterdam the Netherlands, Balkema, 283-291.

STUYFZAND, P.J. 1998c. Simple models for reactive transport of pollutants and main constituents during artificial recharge and bank filtration. In: Peters J.H. (ed), Artificial recharge of groundwater, Proc. 3rd Intern. Symp. on Artificial Recharge, Amsterdam the Netherlands, Balkema, 427-434.

STUYFZAND, P.J. & F. LÜERS 1996. Behaviour of environmental pollutants during bank filtration and artificial recharge; effects of aquifer passage as measured along flow paths. Kiwa-Meded. 125, in dutch, 272p.

TIMMER, H. & P.J. STUYFZAND 1998. Experiments with deep well infiltration along the river Rhine, for drinking water supply. In: Peters J.H. (ed), Artificial Recharge of groundwater, Proc. 3rd Intern. Symp. on Artificial Recharge, Amsterdam the Netherlands, Balkema, 181-185.

TIMMER, H., J.D. VERDEL & P.J. STUYFZAND 1999. Deep recharge clogging in Langerak (The Netherlands). Section 5.7 in EU-report on Artificial Recharge, contract ENV4-CT95-0071, K.H. Jensen et al., in prep.

VAN DER GAAG, M.A. 1984. Some toxicological aspects of dune infiltration. KIWA-Meded. 81, in dutch, 260-283.

VAN DER GAAG, M.A., J.P. ORANJE & M.E.F. BOLMAN 1985. Mutagenity of bank filtrated - groundwater. Ch.8 in KIWA-Meded. 89, in dutch, 6.1-6.24.

VAN HAAREN, F.W.J. 1964. Das Verhalten radioaktiver Isotope im Boden (Grundwasser). Informationsblatt F.E.G. 10, 56-61.

WABER, U.E., C. LIENERT & H.R. VON GUNTEN 1990. Colloid-related infiltration of trace metals from a river to shallow groundwater. J. Contaminant Hydrol. 6, 251-265.

2 Description of test sites Langerak and Nieuwegein (Netherlands)

Pieter J. Stuyfzand
Kiwa Research and Consultancy, Nieuwegein, Netherlands
Harrie Timmer
Water Supply Zuid-Holland Oost, Gouda, Netherlands

ABSTRACT: Water Supply Zuid-Holland Oost has tested deep well injection of oxic water into a deep anoxic aquifer on 2 sites in the Netherlands: Langerak and Nieuwegein. Both sites are close to the Rhine River, which is considered to deliver the influent after pretreatment. The experiments were run for 1.5 years and included hydrological, geochemical end hydrochemical monitoring.

2.1 INTRODUCTION

Drinking water supply by WZHO and testing deep well recharge

Water supply company South-Holland East (WZHO) supplies drinking water to 0.7 million inhabitants in the Rhine fluvial plain in the Western Netherlands, in between Amsterdam, Rotterdam and Utrecht. The main source is Rhine bank filtrate, requiring advanced purification techniques. WZHO considers deep well injection of pretreated river Rhine water as an attractive technique to meet growing drinking water demands within its supply area.

The idea evolved to inject the water prepared at Nieuwegein by the Water Transport Company Rijn-Kennemerland (WRK) at WZHO's well field 'De Steeg' near Langerak (Fig.2.1). WRK pretreats 100 Mm^3/y of river Rhine water, for artificial recharge in the coastal dunes (by spreading) and for industrial water supply.

The distance between Nieuwegein and Langerak is about 20 km, which would necessitate an expensive pipe line for transport of pretreated Rhine water to the test area Langerak. The risk of failure due to clogging was considered too high so that field tests with WRK-water were inevitable. Lacking any pipe line, the main tests with WRK-water had to be done on site at Nieuwegein, where about the same deep aquifer is present as in Langerak. In order to be able to savely extrapolate the tests at Nieuwegein to the Langerak area the following additional experiments were carried out:

(a) a nearly identical injection test was done in the same aquifer at the Langerak site, however using drinking water. In order to make drinking water more similar to WRK-water, Na-NO$_3$ was added continuously;
(b) anoxic sediment cores from both the Langerak and Nieuwegein site were placed in a column at Nieuwegein and flushed with the same WRK-water which was injected in the deep well; and
(c) anoxic sediment cores from both the Langerak and Nieuwegein site were shaken for 3 days with WRK-water in the laboratory. After filtration this water was analysed.

Thus WZHO's main objective of both injection experiments is to know whether WRK-water can be injected into a deep sandy aquifer without serious clogging of the injection well. WZHO's second most important objective was to know and understand the water quality changes during aquifer passage.

Test site Langerak

The village of Langerak is situated in a polder area along the Rhine River tributary 'Lek'. Since 1992 WZHO is pumping groundwater from a well field close to this village, for drinking water supply (Fig.2.2 left). About 5 Mm^3/a is pumped annually by 21 wells from a semiconfined aquifer. Adjacent to the well field is the treatment plant (De Steeg), where the groundwater is transformed in drinking water by aeration and rapid sand filtration.

In the period February - April 1996 one injection well and 3 observation wells were drilled by the auger hole system, in the southern part of the well field. The locally prepared drinking water was injected from 22 June 1996 till 23 February 1998.

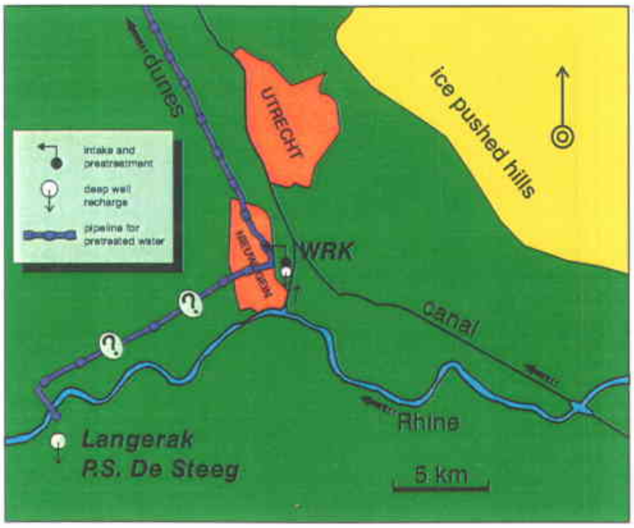

FIG. 2.1 Large scale situation of the test sites Langerak and Nieuwegein (WRK) for deep well injection, with the possible future pipe line for transport of pretreated Rhine River water from the pretreatment plant WRK to the well field at Langerak (De Steeg).

Test site Nieuwegein

The city of Nieuwegein is situated in a similar polder area along the Rhine River tributary 'Lek'. Since 1957 the Water Transport Company Rijn-Kennemerland (WRK) is pretreating 100 Mm^3/a of River Lek water -- actually taken from a canal flushed with this water -- to a near drinking water quality. WRK-water is distributed for artificial recharge in the coastal dunes (by spreading) and for industrial water supply. WRK's standard purification consists of subsequently: aeration, sedimentation, coagulation (with aluminium sulphate), rapid sand filtration and a pH-correction. In addition about 5% of local high quality groundwater is admixed when needed to reduce the chlorinity (<150 mg Cl^-/l) or to overcome periods with a too high pollution load of the Lek River. This water is pumped by the 6 wells indicated in Fig.2.2 (right). In the period February - April 1996 one injection well and 2 observation wells were drilled by the auger hole system, in the northern part of WRK's well field (Fig.2.2). For injection the WRK-water had to be polished up by filtration over granular activated carbon in a provisional unit, in order to remove some trace organic contaminants. This was necessary to comply with the Dutch standards for soil protection. Injection took place from 19 August 1996 till 23 February 1998.

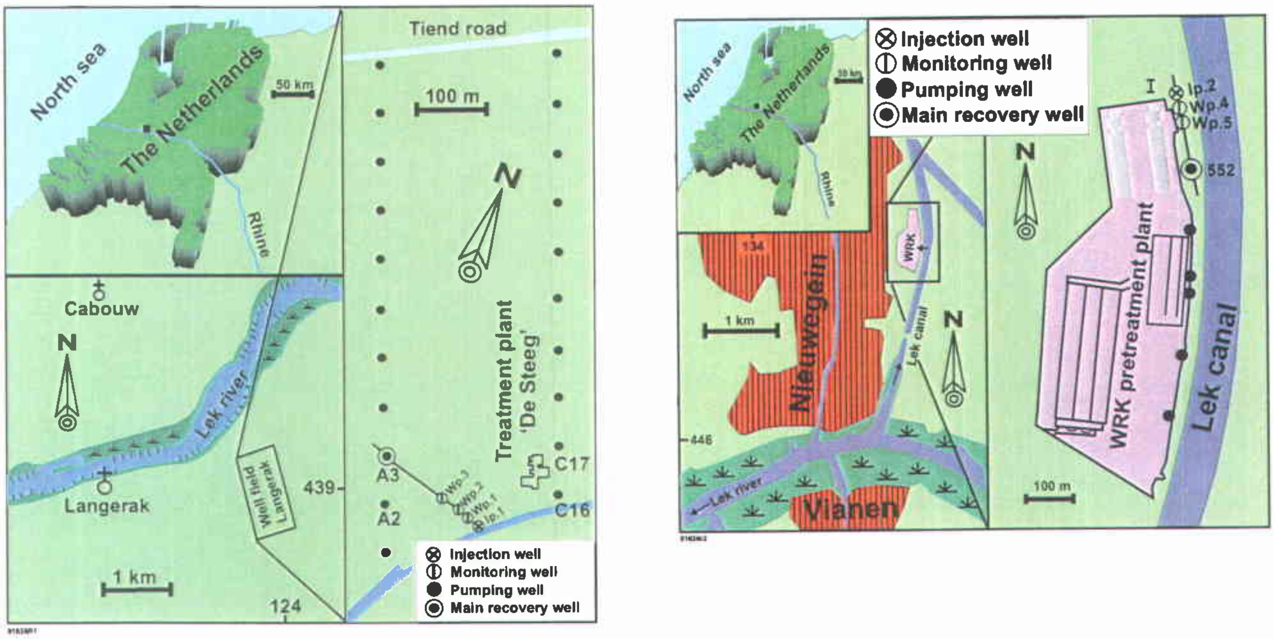

FIG. 2.2 Detailed situation of test sites Langerak (left) and Nieuwegein (right) for deep well injection, with their existing well field for groundwater pumping, treatment plant (resp. De Steeg and WRK), and the section of observation wells used for monitoring the quality changes.

2.2 HYDROGEOLOGY

On both sites the target aquifer is composed of fluvial sands of Middle Pleistocene age, belonging to the so-called Kedichem and/or Harderwijk Formation. The interfingering of both formations is shown in Fig.2.3. The Kedichem Formation contains on average more calcite, feldspar and fine particles than the Harderwijk Formation.
A schematized cross section over the Langerak (Fig.2.4 above) and Nieuwegein site (Fig.2.4 below) shows resp. 3 and 10 distinct strata. The indicated permeabilities were calculated from the total transmissivity of the aquifer as derived from a pumping test, and sedimentological characteristics like modal grain size, gravel content and sorting degree (Stuyfzand et al., 1997). The porosity of the aquifer was measured in 5 cores and averaged 31%.

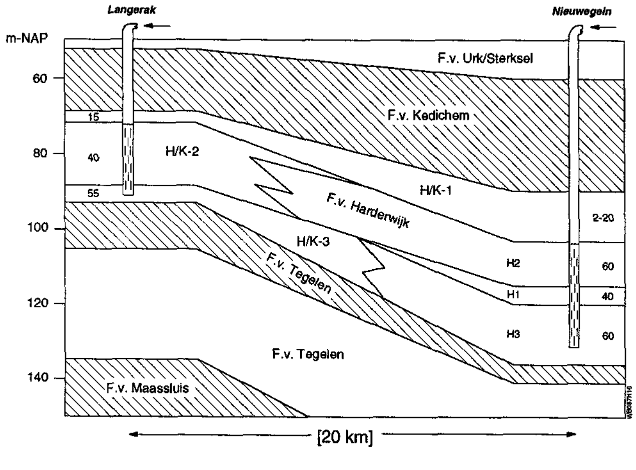

FIG. 2.3 Relation between the discerned strata within the target aquifer at Nieuwegein (WRK) and Langerak (De Steeg), as based on grain size distribution and calcite content. Hatched = clayey aquitards; White = sandy aquifers; 40 = horizontal permeability [m/d]; H/K = transition zone of Kedichem and Harderwijk sands (Middle Pleistocene).

2.3 OPERATION

Test site Langerak

The injection water was composed of the local groundwater which has been transformed into drinking water by aeration and rapid sand filtration (without chlorination). Sodium nitrate was added continuously in order to make the oxidation capacity of this water comparable to WRK-water. Several problems occurred with its dosage, resulting in a variable nitrate concentration. Only during the first month of injection NaCl was added to the drinking water (Cl^- rose from 10 to 100 mg/l) for tracing purposes.

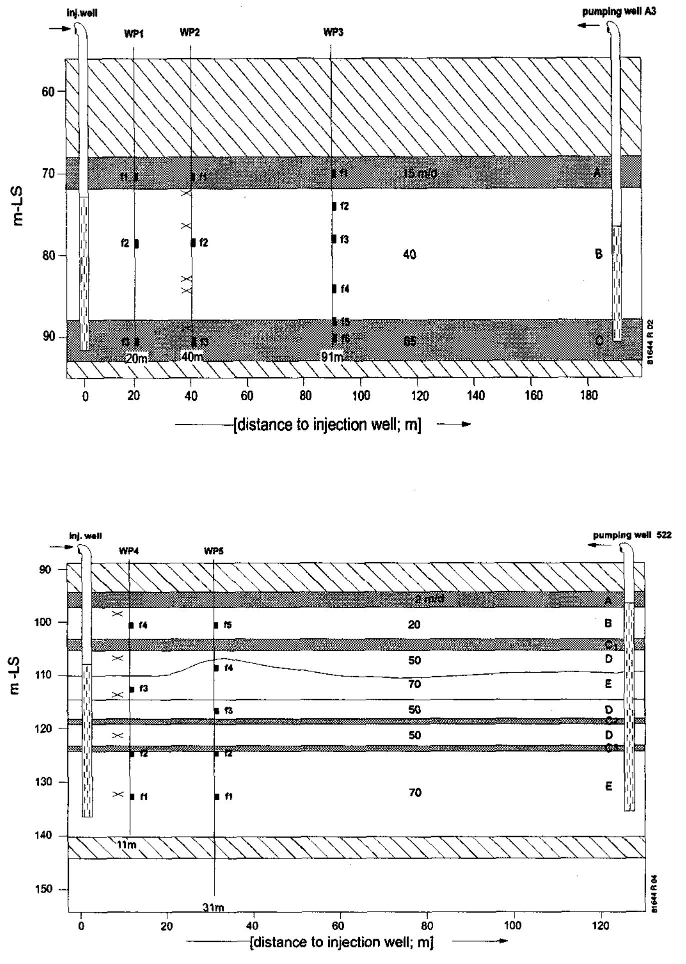

FIG. 2.4 Schematized section of the target aquifer at the Langerak (above) and Nieuwegein (below) test sites, with the position of all well screens and the geochemical samples. LS = Land Surface; K_h = horizontal permeability [m/d]. Position of sections shown in Fig.2.2.

Injection (35 m^3/h) and recovery were hardly interrupted. In total the injection was obstructed for a few days. Clogging of the injection well IP.1 can be noticed since May 1997. During the last half year of injection the well was regenerated first by surging and later by using H_2O_2, both with little results (Timmer & Stuyfzand, 1998). The clogging is probably caused by $Fe(OH)_3$ colloids which pass the rapid sand filters.
Injection and recovery occur within an operational well field (21 wells pumping from the target aquifer) which provides 5 Mm^3/a of groundwater. During the whole injection period wells C16 and C17 were closed off, wells A2 and A3 pumped at a higher rate (60 m^3/h), and all other wells operated with a normal discharge (ca. 30 m^3/h), in order to force the main flow of injected water along the section of observation wells 1-3.
Some detailed information on the injection well, the 3 monitoring wells and the main recovery well is collected in Table 2.1.

TABLE 2.1 Some important data on the 5 observation wells, 2 injection wells and 2 recovery wells, which constitute the monitoring facilities in the injection experiments at Langerak and Nieuwegein.

well no.	well type	distance to IP.1/2 [m]	depth of screens# m-MSL	Drilling [date; type@]
LANGERAK (DE STEEG)[1]				
IP.1	**injection**	**0**	**73-92**	**Apr.96; Z + f + ϕ**
WP.1	**monitoring**	**20**	**71, 79, 92**	**Mar.96; P**
WP.2	**monitoring**	**40**	**71, 79, 91**	**Mar.96; P + †**
WP.3	**monitoring**	**91**	**70, 74, 78, 84, 88, 91**	**Feb.96; P**
P.A3	**recovery**	**190**	**78-91**	**Apr.92; Z**
NIEUWEGEIN (WRK)[2]				
IP.2	**injection**	**0**	**104-132**	**Apr.96; Z + f + ϕ**
WP.4	**monitoring**	**11**	**96, 108, 120, 128**	**Feb.96; P + †**
WP.5	**monitoring**	**31**	**96, 104, 112, 121, 129**	**Feb.96; P**
P.522	**recovery**	**130**	**92-132**	**Oct.79; Z + ϕ**

1 = land surface at 1 m-MSL; 2 = land surface at 3.8 m+MSL; MSL = Mean Sea Level.
 # = screened interval for injection and recovery wells, center of 1 m long screen for monitoring wells;
@: Z = rotary-suction; P = auger; ϕ = geophysical bore hole logging; f = flow logging;
†: aquifer cores from 2-3 depths were placed in the chemical parallel filters (resp. no. 1-3 and 4-5), and were used in a batch experiment (shaking for 72 hours) with 2 solutes.

Test site Nieuwegein

The injection water was essentially composed of Rhine River water, which received the normal pretreatment by WRK (see above) and subsequently GAC-filtration (over Granular Activated Carbon) in a provisional unit constructed by WZHO. The GAC-filtration had a very positive effect on the MFI (Membrane Filtration Index reduced form 6 to 3 s/L^2) and turbidity (from 0.10 to 0.06 NTU). Injection and recovery were hardly interrupted. In total the injection was obstructed for few hours, and injection well IP.2 did not clog at all (Timmer & Stuyfzand, 1998). Injection and recovery occured within an operational well field (6 wells pumping from the target aquifer) which provides 5 Mm^3/a of groundwater to WRK, when needed (see above). During the whole experiment, however, only the recovery well pumped 40 m^3/h (the other 5 wells did not pump). Some detailed information on the injection well, the 3 monitoring wells and the main recovery well is collected in Table 2.1.

Part of the injection water was diverted to flush on site, 4 hydrological and 5 hydrochemical parallel columns. The hydrological parallel columns were flushed with different flow rates to simulate and stimulate clogging processes. Results obtained with them are dealt with by Timmer et al. (in prep). The hydrochemical parallel filters, shown in Fig.2.5, were used to simulate a very short passage of aquifer material, in order to (a) quantify reaction kinetics more precisely and (b) achieve more pore volume flushings as compared to the observation wells, which require more time for the water to flush one pore volume.

2.4 DATA COLLECTION

The original monitoring program and the elaboration of the resulting data were strongly extended and intensified thanks to financial support by the EU-project. Separating all efforts is useless, and we therefore give here a brief listing of all major activities regarding data collection. The activities are grouped together into those connected with chemical reactions and those with clogging.

Regarding chemical reactions:

1. Collection of 10 anoxic aquifer samples (5 from each site), determination of grain size distribution and porosity, and quantitative chemical analysis for total element content (by XRF), ironsulfides, calcium carbonate, exchangeable cations, organic matter, and organic carbon.
2. Batch experiments with these aquifer samples, using synthetic infiltration water, in order to obtain data on reaction kinetics and to compare sediment reactivity.
3. Sampling of the native groundwater on both sites for chemical analysis of all main constituents and selected trace elements.
4 Monitoring in the field of the quality of the influent on both sites.
5. Monitoring in the field of the break-through of the injected water on both sites, by chemical analysis of water samples and by resistivity measurements with 13 fixed electrodes in each observation well.

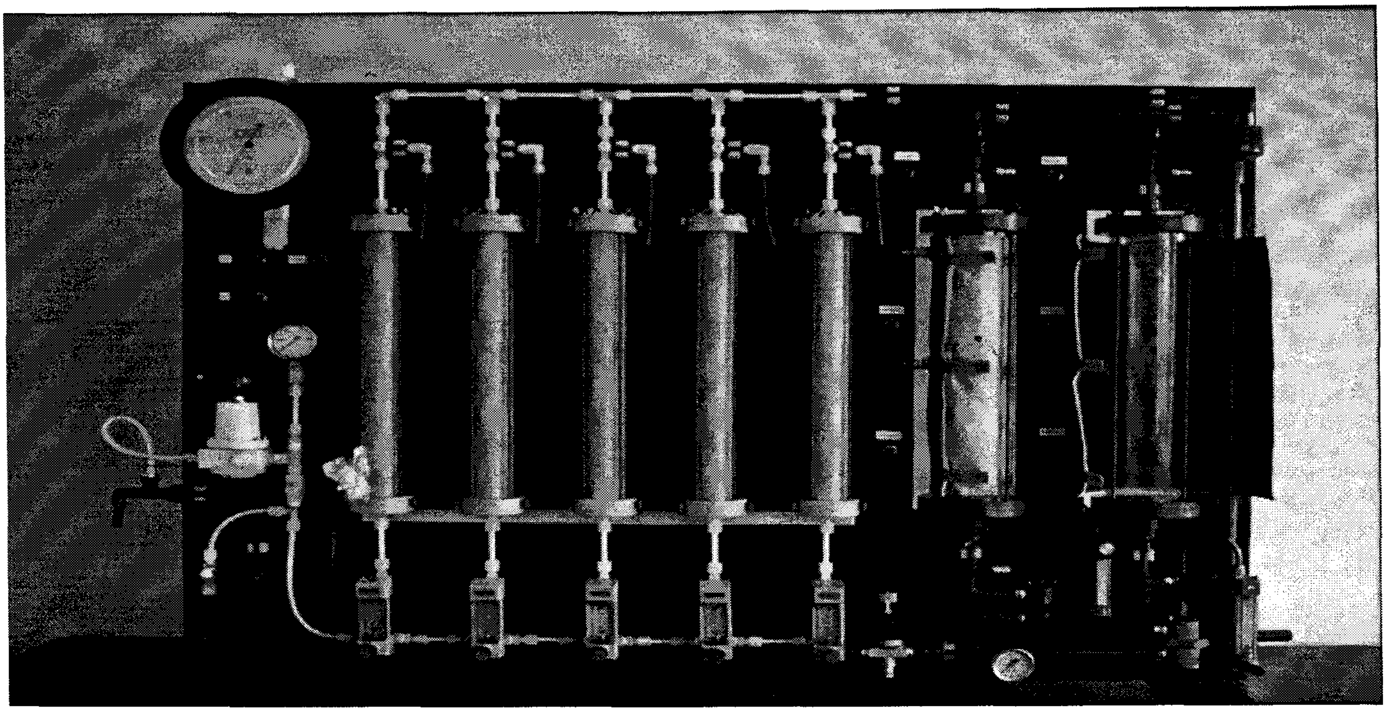

FIG. 2.5 The 5 chemical parallel columns (CPC; left) and 2 hydrological parallel columns (right) filled with sediment cores from the Langerak and Nieuwegein target aquifer. These columns were flushed with the same pretreated Rhine water which was injected in Nieuwegein. Internal dimensions of each CPC: 4 cm diameter, 43 cm high. Mean recharge rate of CPCs was 0.96 L/d resulting in a residence time of 0.225 d.

6. Monitoring in the field on both sites for about 1.5 years, of the quality changes of the influent during aquifer passage (main constituents and selected trace elements), using a row of observation wells (at different distances from the injection well) and the recovery well itself.
7. Monitoring in the field of the effluent quality of 5 chemical parallel filters at the Nieuwegein site.

Regarding clogging of the injection well:

a. Automatic registration of injection rate, temperature and turbidity of the influent, and water pressure in the injection screen, gravel pack and a close observation well.
b. Regular measurements of hydraulic heads in the aquifer using the piezometers of all observation wells.
c. Regular measurement of MFI and AOC in the influent.
d. Regular measurements of the discharge from and pressure decline within the 4 hydrological parallel filters.
e. A single particle size scan of the influent, on 3 September 1997.
f. Chemical analysis of the water back-flushed after surging the injection well on 18 September 1997 and 17-18 December 1997.

2.5 REFERENCES

STUYFZAND, P.J., F. LÜERS & H. TIMMER 1997. Development of the water quality using deep well injection, for treatment plant De Steeg in Langerak; 3. Geochemical and hydrochemical situation in Langerak and Nieuwegein prior to injection. Kiwa-rapport KOA 97.010, in dutch, 43p.

STUYFZAND, P.J., F. LÜERS & H. TIMMER 1998. Development of the water quality using deep well injection, for treatment plant De Steeg in Langerak; 5. Final report after 1.5 years of monitoring. Kiwa-report KOA 98.137, in dutch, 93 p.

TIMMER, H. & P.J. STUYFZAND 1998. Experiments with deep well infiltration along the river Rhine, for drinking water supply. In: Peters J.H. (ed), Artificial Recharge of groundwater, Proc. 3rd Intern. Symp. on Artificial Recharge, Amsterdam the Netherlands, Balkema, 181-185.

TIMMER, H. & J.D VERDEL 1998. Clogging of injection well ZS De Steeg, Langerak. WZHO-report, in dutch.

3 Deep well injection: reactions in pyritiferous sands at the Langerak and Nieuwegein sites (Netherlands)

Pieter J. Stuyfzand
Kiwa Research and Consultancy, Nieuwegein, Netherlands
Harrie Timmer
Water Supply Zuid-Holland Oost, Gouda, Netherlands

ABSTRACT: In the period July 1996 till March 1998 Water Supply Company WZHO carried out 2 deep well recharge experiments, one in Langerak and the other in Nieuwegein (Netherlands). At both test sites the influent was oxic and the anoxic sandy target aquifer contained pyrite. Both experiments revealed a typical quality evolution due to sequential leaching of aquifer constituents. The main processes were, in mean order of increasing duration: displacement of native groundwater, cation exchange, pyrite oxidation, acid-buffering by calcite dissolution, and oxidation of organic matter. Differences in quality changes between both sites relate to their deviating aquifer geochemistry and influent quality. The reactions were quantified using the mass balance approach.

Pyrite oxidation was kinetically hindered, it took about 10 days to deplete O_2 and 100 days to deplete NO_3^- in the influent. Oxygen was reacting faster with pyrite than with labile organic matter, for nitrate the reverse holds. Pyrite oxidation led to mobilization of As, Ni and Zn, but they are largely fixed by neoformed $Fe(OH)_3$. The main geochemical heterogeneity was related to variations in the reactivity of both pyrite (high in lower parts of aquifer) and organic matter (high in upper parts of aquifer).

3.1 INTRODUCTION

Water quality changes after injection in general

A characteristic aspect of deep well recharge is, in most cases, the introduction of pretreated, oxic surface water (saturated with oxygen and containing nitrate), into an anoxic deep aquifer (without any oxygen and nitrate). The target aquifer may contain groundwater deviating from the water injected in other hydrochemical respects as well: like ionic strength, pH, cationic composition (especially Fe^{2+}, Mn^{2+} and NH_4^+), hydrogencarbonate and methane, phosphate and dissolved organic carbon. This leads to various reactions, like cation exchange, the oxidation of pyrite and organic matter, acid buffering by dissolution of calcium carbonate or the conversion of hydrogencarbonate into carbonic acid, sorption of siliciumdioxide, fluoride and phosphate, and sorption and degradation of organic micropollutants (Sniegocki, 1963; Wood & Signor, 1975; Vecchioli et al., 1975; Ehrlich et al., 1979; Van Beek & Van Puffelen, 1987; Stuyfzand, 1998a,b).

Deep well recharge leads to a relatively rapid leaching of the reactive solid phases from the aquifer (Stuyfzand, 1998b) for 3 reasons: the high flow rates as compared to natural groundwater flow, direct introduction of the influent into the target aquifer (without buffering sludge or upper soil layer), and the relatively high reactivity of fine grained deposits in a sandy aquifer in comparison with hardrock or gravels.

The quality changes of injected drinking or waste water during movement in aquifer systems, and particularly the extinction of these changes with time, were never quantitatively linked to the initial amounts of reactive phases in the aquifer matrix. This linking is attempted in the second part of this study (Ch.5), and is a prerequisite for predicting the quality of the water being recovered on the long term.

This study

On 2 sites in the Netherlands, at Langerak and Nieuwegein, an experiment was carried out for 1.5 years with deep well injection of oxic water into an anoxic aquifer. Both test sites are described in detail in Ch.2. Information is given there on the specific interests of Water Supply Company WZHO, the relation between both experiments, several operational matters and the data collection. The results of 2 full reports are summarized here: the first (Stuyfzand et al. 1997) deals with the original (native) geochemistry and hydrochemistry of the target aquifer at both test sites, the second

(Stuyfzand et al. 1998) treats the water quality changes during aquifer passage, their quantitative interpretation and modelling. Both reports include a complete listing of all chemical analyses. The modelling results are not dealt with here but in Ch.5 (using EASY-LEACHER), Saaltink et al. 1998 (using RETRASO) and Brun et al. 1998 (using the MIKE SHE system). The objectives of both experiments are to: (a) quantify the migration rate of the nitrate and oxygen fronts in the anoxic target aquifer and relate their retardation to the relevant redox reactions and the initial amount of the reactive redox constituents of the aquifer material; and (b) quantify all relevant water-aquifer interactions and thereby predict the dynamic water quality evolution in the recovery well.

3.2 SITES, TESTS AND METHODS

The 2 sites and their tests

Detailed information on the location of both deep well injection test sites is given in Ch.2. They are located in the fluvial plain of the Rhine River, about 20 km apart. Characteristic data for both sites and experimental details are listed in Table 3.1.

Hydrochemical monitoring

Water quality monitoring consisted of frequent (daily to monthly) analysis of: (a) the oxic influent, (b) groundwater from observation wells at various distances from the recharge well, and (c) the percolate of 5 parallel columns filled with aquifer cores and flushed with injection water on the Nieuwegein site. Most monitoring wells were situated along the shortest flow paths between injection and recovery well. Groundwater samples were obtained by suction lift from PVC-piezometers (well screen 1 m long). The water content of riser plus well screen was purged 3 times prior to sampling. Temperature, EC, pH and O_2 were measured on site. Alkalinity, pH and EC were measured in the laboratory, on the day of sampling. The portion to be analyzed for most trace elements, Ca^{2+}, Mg^{2+}, Fe^{2+} and Mn^{2+} was filtrated in situ over 0.45 μm, directly acidified to pH=1,5 using HNO_3-suprapure and was stored in the dark at 4 °C in polyethylene vessels rinsed out with HNO_3 and the water to be sampled. Main constituents were analysed with conventional, well-standardized analytical methods, most trace elements were analyzed using Atomic Absorption Spectrophotometry (AAS) with graphite furnace.

Geochemical analyses

From each site 5 sediment cores from the target aquifer were obtained using the Ackerman core catcher in advance of the auger, during bailer drilling of the monitoring wells. The sediment cores including their pore water were immediately sealed on site using lids and liquidized paraffin, and kept at 4°C in the dark till analysis. Samples were opened and pretreated in an anoxic glove-box. The samples were analysed for amongst others: total content of 27 elements by X-Ray Fluorescence, organic matter and calcium carbonate by thermogravimetry (resp. 550 and 1000°C), $CaCO_3$ by HCl-extraction of Ca^{2+} (correcting for exchangeable Ca; ppm level), organic carbon by pyrolysis, exchangeable cations using $SrCl_2$, sulphide species (especially pyrite) with the sequential extraction method of Begheijn (1978), non-Si-bound trace elements by aqua regia extraction and amorphous Al-, Fe- and Mn-(hydr)oxides by ammonium oxalate/oxalic acid.

TABLE 3.1. Description of the deep well injection tests at Langerak and Nieuwegein.

Recharge site **pumping station**		**Langerak** **'De Steeg'**	**Nieuwegein** **'WRK'**
EXPERIMENTAL DETAILS			
injection period		22-7-96/23-2-98	19-8-96/23-2-98
recharge rate	[m^3/h]	35	40
recovery rate[$]	[m^3/h]	60	40
source of injection water		drinking water	Rhine (pretreated)
distance between wells[@]	[m]	190	130
number of observation wells		3	2
number of observation screens		12	9
hydrological parallel columns		-	5 (4N)[#]
chemical parallel columns		-	5 (3L + 2N)[#]
period of chem. parallel columns		-	23-10-96/18-12-96
MEAN CHARACTERISTICS TARGET AQUIFER			
position	[m-LS][*]	67-92	93-139
altitude Land Surface	[m+MSL][*]	-1.0	3.8
thickness	[m]	25	46
permeability	[m/d]	40	50
geological formation		Harderwijk/Kedichem	Harderwijk

@ = between injection and main recovery well; $ = of the main recovery well; # : L = cores from Langerak, N = cores from Nieuwegein; * : LS = Land Surface, MSL = Mean Sea Level.

Problems in maintaining anoxic conditions during the various stages of sample preparation, led in most cases to a serious dissolution of calcite during the $SrCl_2$-extraction of exchangeable cations and losses of exchanged Fe^{2+}, Mn^{2+} and NH_4^+. This necessitated to calculate the exchangeable Ca^{2+}, Fe^{2+}, Mn^{2+} and NH_4^+ content by equilibrium calculations using the approach given in the footnote of Table 3.2. The exchange coefficients $K_{X/Y}$ (Gaines-Thomas convention) derive from Appelo & Postma (1993).

In addition, 5 sediment cores were shaken for 72 hours with 2 different solutes.

3.3 CHARACTERISTICS OF THE TARGET AQUIFER

Hydro(geo)logy

The target aquifer is composed on both sites of Middle Pleistocene sands belonging to the same sedimentary unit (mainly Harderwijk Formation; Fig.2.3 in § 2.2). Excluding the finer-grained sands in the toplayer, these sands have a mean grain size of 300-400 µm, and contain 0.5-2% clay (<2 µm) and 0-3% gravel (>2 mm). The resulting permeability in these layers is 40-70 m/d, while porosity averaged 31% in 5 cores. In both cases the target aquifer is (semi)confined. Detailed cross sections are shown in Fig.3.8 (see also Figs.2.3-2.4).

Geochemical composition

The mean chemical composition of the target aquifer on both sites, excluding the finer grained toplayer, is shown in Table 3.2. Both aquifers are composed of deep anoxic, mainly quartz sands, poor in organic carbon (0.09-0.12%), containing a small amount of pyrite (70-200 mg S/kg) and calcite (0.3-0,6%). CEC is low (8-12 meq/kg), dominated by Ca^{2+} (69-77% of CEC) and Mg^{2+} (17%).

The top layer on both sites contains 2-30 times more organic carbon, calcite and pyrite (Table 5.2 in § 5.3).

The maximum trace element content of pyrite was estimated by linear regression of the pyrite content (expressed as S) and the amounts of As, Co, Ni and Zn extracted with aqua regia (which does not significantly dissolve these elements from the crystal lattice of silicate minerals). As an example the plot for arsenic is shown in Fig.3.1. The Y-intercept is interpretated as the contribution from non-pyritic material and the inclination as the maximum amount deriving from pyrites. This yields As = 0,00619 S_{FeS2}, resulting in 620 µg As/100 mg S or 207 µg As/100 mg SO_4, or 0.0053 mole As/mole FeS_2. The most probable stoichiometry of pyrite for Langerak and Nieuwegein then becomes: $Fe_{0,98}Co_{0,0037}Ni_{0,01}Zn_{0,01}S_2As_{0,0053}$. This composition compares very well with results presented by Stuyfzand & Vogelaar (1997) and Van Beek & Van der Jagt (1996).

TABLE 3.2 Comparison of the mean composition of the target aquifer (excl. the less permeable upper layer) at Langerak and Nieuwegein. Mean based on 4 samples each.

	unit	Langerak	Nieuwegein
clay fraction (<2 µm)	**% d.w.**	**1.9**	**0.7**
mean grain size	**µm**	**329**	**364**
pH-H_2O	**-**	**8.61**	**8.68**
organic matter[$]	**% d.w.**	**0.22**	**0.16**
organische carbon	**% d.w.**	**0.12**	**0.09**
$CaCO_3$	**mg/kg d.w.**	**5820**	**3085**
CEC	**meq/kg d.w.**	**12.36**	**7.75**
Na_{EXCH}	**meq/kg d.w.**	**0.64**	**0.36**
K_{EXCH}	**meq/kg d.w.**	**0.52**	**0.29**
Ca_{EXCH} #	**meq/kg d.w.**	**8.54**	**6.00**
Mg_{EXCH}	**meq/kg d.w.**	**2.09**	**0.89**
$NH4_{EXCH}$ #	**meq/kg d.w.**	**0.18**	**0.08**
Fe_{EXCH} #	**meq/kg d.w.**	**0.36**	**0.10**
Mn_{EXCH} #	**meq/kg d.w.**	**0.03**	**0.03**
FeS	**mg S/kg d.w.**	**12**	**4**
FeS_2	**mg S/kg d.w.**	**176**	**57**
ΣS	**mg S/kg d.w.**	**198**	**67**
As_{AR}	**mg/kg d.w.**	**1.9**	**1.1**
Co_{AR}	**mg/kg d.w.**	**1.7**	**1.4**
Ni_{AR}	**mg/kg d.w.**	**3.2**	**2.3**
Zn_{AR}	**mg/kg d.w.**	**15**	**13**
Fe_{OX} †	**mg/kg d.w.**	**1156**	**659**
Mn_{OX} †	**mg/kg d.w.**	**32**	**16**

[$] = loss on ignition at 550°C corrected for inorganic losses by subtracting 0.07 * clay [% d.w.];

[#] = calculated assuming equilibrium with native groundwater, with the following exchange coefficients (Gaines-Thomas convention): $K_{Na/Mg}$ = 0.5, $K_{Na/Ca}$ = 0.4, $K_{Na/Fe}$ = 0.6, $K_{Na/Mn}$ = 0.55; $K_{Na/K}$ = 0.2, $K_{Na/NH4}$ = 0.25.

† = corrected for contribution from groundwater and Fe_{EXCH}, but could derive from $Fe_{1-x}Mn_xCO_3$ too.

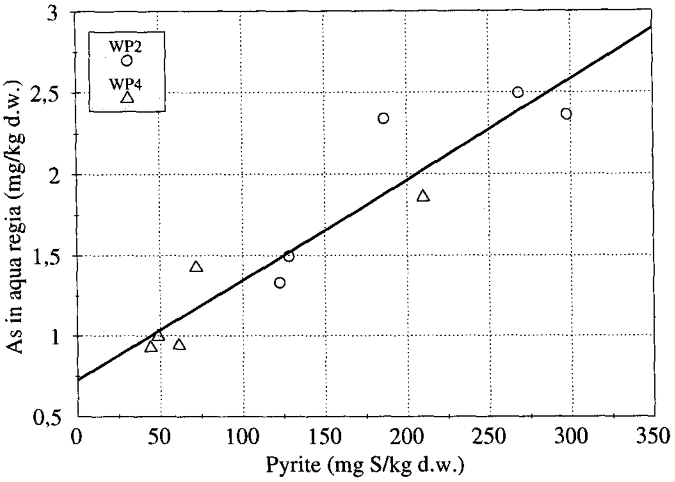

FIG. 3.1 Plot of the As content (dependent variable) versus the pyrite content expressed as S (independent variable) for 10 samples from the target aquifer (WP.2 and WP.4).

The aquifers are suspected to contain manganous siderites ($Fe_{1-x}Mn_xCO_3$) in small amounts. Their quantification and reactivity are matter for future research.

The target aquifer at Langerak is on average finer grained than the one at Nieuwegein, and consequently contains more reactive compounds, especially regarding calcite, organic matter, pyrite, and adsorbed Fe^{2+} and NH_4^+ (Table 3.2). The CEC is higher as well. The differences are rather small, however, without disrupting the comparability of both experimental sites!

Aquifer reactivity

Batch experiments were carried out with 5 of the 10 examined aquifer samples. For 72 hours the samples were shaken with pretreated Rhine River water (WRK-water) in closed vials with a N_2-gas cap, with and without addition of 2 mmol $NaNO_3$/l. The addition of $NaNO_3$ in a second run was intended to raise the oxidative capacity of the WRK-water. The main results are summarized in Table 3.3.

The main reaction was the oxidation of pyrite. This reaction was kinetically hindered, because 3 days of shaking with WRK-water resulted in a consumption of oxygen by 30% and of nitrate by 16%, whereas 9-50% of the pyrite was oxidized. Oxidation of organic matter proceeded at a much slower rate, because DOC and TIC were not produced at all. Addition of 2 mmol nitrate to WRK-water did not lead in 3 days, to any additional oxidation of pyrite or organic matter.

Arsenic and nickel, from oxidizing pyrite, were largely fixed in solid phases again, probably in neoformed ironoxyhydroxides.

Macrochemically there were no significant differences in reaction with WRK-water, between the cores from Langerak and Nieuwegein. Supersaturation of the WRK-water (due to shaking in a N_2-atmosphere) prevented the acid formed during pyrite oxidation, to dissolve calcite.

TABLE 3.3 Averaged results of batch experiments with cores from the target aquifer: 3 samples from well WP.2 (Langerak) and 2 from well WP.4 (Nieuwegein) were shaken for 72 hours with O_2-saturated WRK-water (pretreated Rhine River) and a N_2-gas cap, with and without addition of $NaNO_3$.

		without $NaNO_3$ addition			with 2 mmol $NaNO_3$/l added		
sample	unit	blanc	Nieuwegein	Langerak	blanc	Nieuwegein	Langerak
location		WRK-	WP.4	WP.2	WRK-	WP.4	WP.2
depth	m-LS	water	106-119	76-89	water	106-119	76-89
pH	-	8.15	8.02	8.03	8.14	8.07	8.03
O_2	mg/l	2.7	2.0	1.7	1.9	1.7	1.7
SO_4^{2-}	mg/l	73.0	74.9	75.7	72.2	73.7	73.2
HCO_3^-	mg/l	183	178	181	180	177	179
NO_3^-	mg/l	18.9	16.8	16.7	131	137	132
NO_3^--corr[@]	mg/l	-	16.6	16.3	-	137	132
Ca^{2+}	mg/l	86.9	85.2	85.5	85.2	85.2	85.0
Mn_t	mg/l	<0.005	0.09	0.10	<0.005	0.08	0.09
NH_4^+	mg/l	0.08	0.06	0.08	0.06	0.07	0.08
As	µg/l	<0.5	<0.5	<0.5	<0.5	<0.5	<0.5
Ba	µg/l	71	74	71	68	83	67
Ni	µg/l	5.6	4.1	3.7	4.6	3.8	5.4
Zn	µg/l	3	18	11	3	16	12
$SI_{calcite}$	-	0.74	0.59	0.61	0.69	0.61	0.58
TIC	mmol/l	3.02	2.96	3.00	2.97	2.94	2.97
ΔO_2 corr[**]	mg/l	-	0.4	0.4	-	0.0	0.0
ΔSO_4 sample	mg/l	-	1.9	2.7	-	1.5	1.0
ΔSO_4 max[#]	mg/l	-	2.9	3.6	-	5.2	1.4

[@]: correction for complete oxidation of adsorbed NH_4^+ to NO_3^-: $-(NH_{4EXCH}) * (40/1000) * (\text{dry residue}/100) * (1000/800) * 62$.

[**]: $= (O_2)_{blanc} - (O_2)_{sample} + 3.55\Delta NH_4 + 2.72(NH_4)_{EXCH} + 0.17\ Fe_{EXCH}$ (assumed: mean dry residue = 85%)

[#]: = calculated using: $\Delta SO_4 - max = 1.7\ \Delta O_2 + 1.1\ \Delta NO_3^-$ (all mg/L).

TABLE 3.4 Comparison of the composition of (a) the native groundwater in the target aquifer at Langerak (based on 13 samples) and Nieuwegein (based on 9 samples), and (b) the water injected during the first year on both sites (based on resp. 54 and 24 samples).

	unit	NATIVE GROUNDWATER		INFLUENT	
		Langerak	Nieuwegein	Langerak	Nieuwegein
Temp	°C	13.0	12.5	12.6	13.7
EC (20°C)	µS/cm	610	505	506	728
pH	-	7.25	7.3	7.70	7.55
O_2	mg/L	<0.5	<0.5	9.5	5.8
CH_4	mg/L	8600	3300	0	0
DOC	mg/L	4.9	2.9	3.0	1.3
colour	mg/L Pt/Co	12	4.7	15.9	1.5
SiO_2	mg/L	21	20	20.0	4.0
SI_c #	-	0.03	0.18	0.34	-0.05
Cl^-	mg/L	7.5	8	34	126
SO_4^{2-}	mg/L	<1	<0.1	7.6	61.5
HCO_3^-	mg/L	430	370	298	158
NO_3^-	mg/L	0	0	14.9	14.1
Na^+	mg/L	51	10.6	45.9	65.0
K^+	mg/L	6.8	1.3	6.5	5.4
Ca^{2+}	mg/L	69	98	60.2	72.7
Mg^{2+}	mg/L	12	9.0	11.0	11.0
NH_4^+	mg/L	1.05	0.16	0.015	0.035
Fe^{2+}	mg/L	2.7	1.9	0.04	0.01
Mn^{2+}	mg/L	0.3	0.5	0.012	0.002
Al	µg/L	4	6	2	27
As	µg/L	1	4	0.8	0.7
Ni	µg/L	1	0.5	1.1	2
Zn	µg/L	5	15	4	5

#: SI_c = calcite saturation index = log ($[Ca^{2+}][CO_3^{2-}]/K_{CaCO_3}$)

Hydrochemistry

The mean chemical composition of the groundwater in the target aquifer, prior to the start of deep well injection, is given for both sites in Table 3.4. On both sites the native groundwater shows a very high preindustrial quality, which is characterized further as 'chloride-poor, deep anoxic (high in methane, without any oxygen, nitrate and sulphate) and calcite-saturated. The water at Nieuwegein contains, however, less sodium, potassium and magnesium, probably due to a more prolonged flushing of the aquifer during the Quarternary epoch with fresh groundwater or less salinizination in a remote past. The water also contains less ammonium, DOC, methane and colour, but more dissolved calcite (calcium and hydrogencarbonate), manganese and a little more arsenic.

There is some hydrochemical stratification on both sites (Stuyfzand et al., 1997). The upper layer shows the highest concentrations of methane, colour-components and NH_4^+ (from the aquitard above probably), and the middle parts the highest Fe^{2+}- and lowest CH_4-concentrations.

3.4 QUALITY AND TRACING OF INFLUENT

Quality of influent

The injection water is composed of drinking water in Langerak, and of pretreated Rhine River water (WRK-water) in Nieuwegein. Their mean quality is given in Table 3.4.

The drinking water approaches the native groundwater in Langerak, because it is prepared from that groundwater. The differences are mainly due to the effects of aeration and rapid sand filtration (removal of Fe^{2+}, Mn^{2+}, NH_4^+, CH_4), mixing of different groundwaters within the well field, the addition of NaCl during the first month for tracing purposes and the continuous addition of $NaNO_3$ to make the oxidative capacity comparable to WRK-water.

The WRK-water differed more from the native groundwater due to resp. a fluvial and atmospheric origin. The pretreatment of WRK-water consists of subsequently: aeration and settling, coagulation (using aluminium sulphate), rapid sand filtration and pH-correction. In addition, thus prepared WRK-water was further treated by granular active carbon filtration in a provisional unit, in order to eliminate organic micropollutants.

The injected drinking water had on average a lower salinity (Na^+, Cl^-, Ca^{2+}, SO_4^{2-}), a higher oxygen, SiO_2 and DOC content, higher saturation index for calcite, a higher oxidation capacity (due to more O_2), stronger colour, much less quality and temperature fluctuations.

Tracers and their breakthrough

Chloride, electrical conductivity, sulphate, methane and hydrogencarbonate proved to be very useful tracers of the injection water on both sites (Table 3.4). Although only chloride behaved as a perfectly conservative tracer, the others were conservative enough for use (see methane in Fig.3.2). At the Langerak site where sodium chloride was added for a short time (30 days), sulphate (high in influent) and methane (low in influent) were especially useful for the recovery well where dispersion of the tracer added and mixing with native groundwater faded away the initial chloride contrast (Stuyfzand et al., 1998). The break-through at levels in between observation screens was established using frequent resistivity measurements (of formation plus groundwater; latter variable) with 13 fixed electrodes in each observation well. These measurements compared very well with tracer sampling (Fig.3.2).

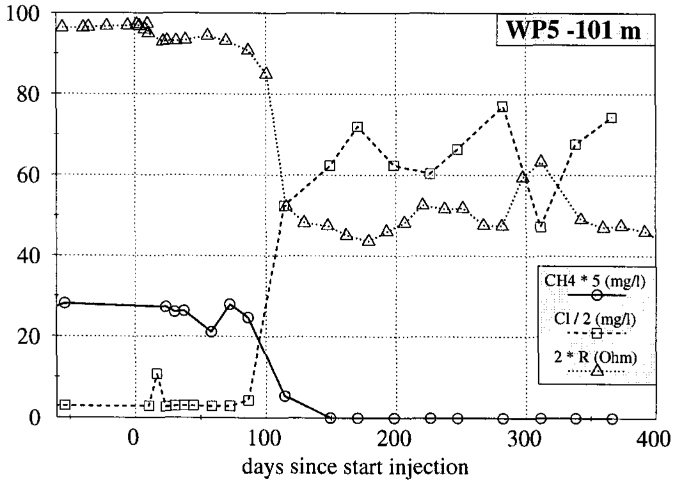

FIG. 3.2. The break-through curves of chloride and methane (in groundwater sampled with a 1 meter long well screen), and electrical resistivity (measured with a fixed electrode couple in gravel pack of well) yield the same mean travel time and longitudinal dispersivity for observation well WP.5-101: resp. 105 days and 0.3 m.

The break-through curves of Cl^-, CH_4 and resistivity yielded the mean (t_{50}), near-shortest (t_{20}) and near-longest travel time (t_{80}), by taking the moments of respectively 50, 20 and 80% break-through. The mean travel times as derived from the 3 tracers compared very well. The spatial pattern of mean travel times to all observation points is shown for Langerak in Fig.3.3. The shorter travel times correspond with zones of coarser sand.

The mean travel time was used to calculate for each observation the amount of pore flushes (PFs) with the injection water during the injection period (Δt_{inj}):

$$PF = \Delta t_{inj}/t_{50} \qquad (1)$$

One pore flush means that the whole sand body, from injection to monitoring well, has been flushed with the infiltration water exactly one time.

Dispersion

The longitudinal dispersivity α_L of the porous medium was calculated from the break-through curve by taking its mean inclination in between t_{20} and t_{80}:

$$\alpha_L = X\,(t_{80}-t_{20})/(\pi\, \Delta C^2\, t_{50}) \qquad (2)$$

with: X = distance of flow path between injection well and observation point [m]; ΔC = concentration change of tracer from t_{20} to t_{80} [mg/L].

Eq.2 is based on Fick's second law and assumes stationary, uniform, laminar flow in a homogeneous soil with negligible diffusion (Appelo & Postma, 1993). Although not all assumptions are satisfied, they are approximated sufficiently to apply Eq.2 in between injection and recovery well.

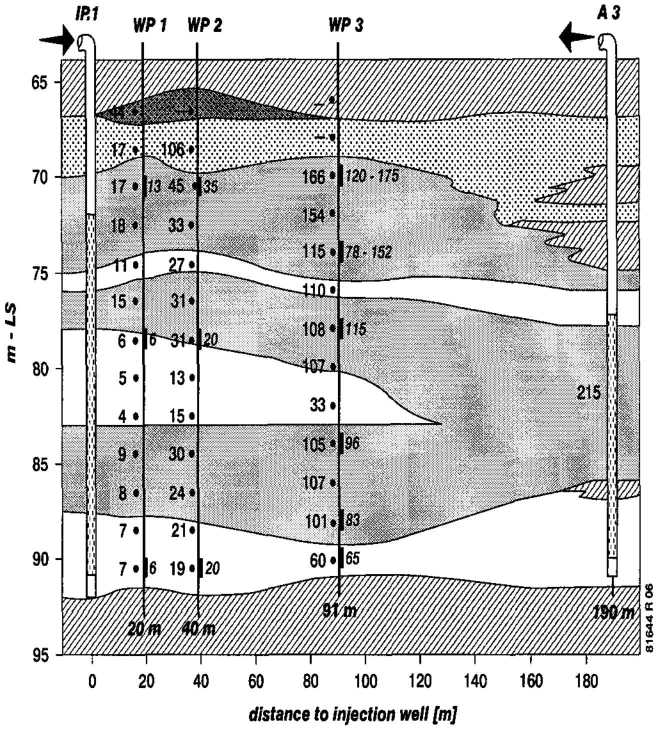

FIG. 3.3 The observed mean travel times of the injected drinking water (in days), in the target aquifer at Langerak.

The α_L-values as derived from the break-through curves of Cl^-, CH_4 and resistivity can be compared in Fig.3.4. Clearly, the 3 parameters yield, contrary to the mean travel time, varying differences in α_L, with on average the highest values for CH_4 and the lowest for Cl^-. The differences mainly relate to: (a) differences in sampling frequency (interpolation errors); (b) differences in the amount of water flushed prior to sampling (zero for resistivity!); (c) difficulties in reading the t_{20} and t_{80} values due to quality fluctuations in both the influent and the native groundwater prior to break-through of the influent; and (d) the possibility of non-conservative behaviour for methane, which may be released for instance from small gas-pockets (this explains some of its anomalously long t_{80} values).

In a selection of the best measurements, α_L-values exhibit a range of 0.3 - 5.5 m, without any relation with the mean travel time or distance travelled. This agrees with observations by Broermann et al. (1997) who studied dispersivity during deep well injection in coarse fluvial sands in the USA. They arrived at an α_L of 0.1-6.5 m using well screens of 0.6 m length. Uffink (1990), however, deduced much lower values (0.01-0.1 m) and found a clear positive relation of α_L with mean travel time (8-87 d), from a deep well injection experiment using miniscreens (screen length 0.01 m).

We therefore conclude that our and Broermann's high α_L-values and the lack of a positive relation with the travel time, result from dispersion introduced by the observation well and sampling! The order of magnitude of α_L roughly corresponds to the screen length used.

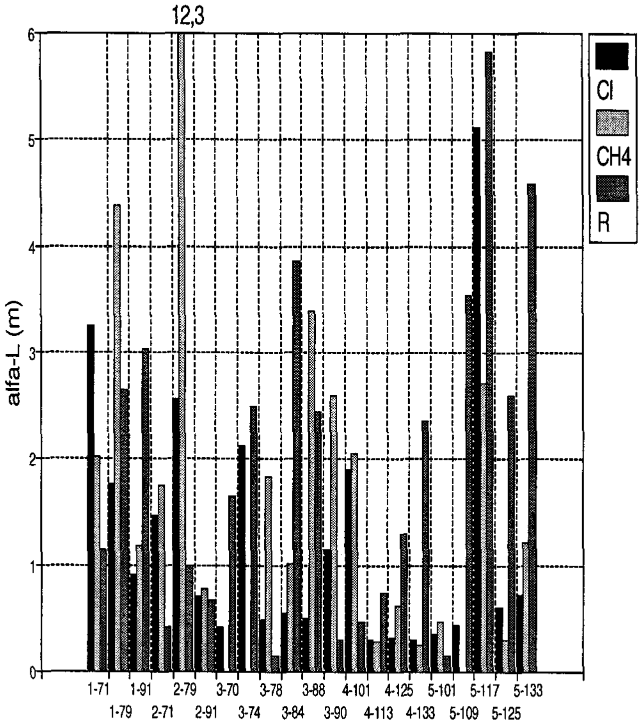

FIG. 3.4 Comparison of the longitudinal dispersivity (α_L) of water injected in Langerak (WP.1-3) and Nieuwegein (WP.4-5), as derived from water samples (chloride and methane) and resistivity measurements on permanent electrode couples. Coding: 4-133 = WP.4 at 133 m-Land Surface.

3.5 QUALITY CHANGES DURING AQUIFER PASSAGE

3.5.1 *Presentation of results*

All results of chemical analysis pertaining the both field tests and the chemical parallel columns are listed in Annex 1 of Stuyfzand et al. (1998). Table 3.5 gives a compact synthesis of the results, showing the mean composition, during the first year, of: (1) the injection water on both sites; (2) the injected water from all observation wells (WP.1-5 at 3-6 depths); (3) the influent of the chemical parallel columns (WRK-water); and (4) the effluent of these 5 columns.

In Table 3.5, for each observation well the average is taken over the period 'injection start + 2 times its travel time till one year later'. The mean concentrations therefore pertain to a PF≥2, which means that any initial admixing with native groundwater can be excluded.

In a similar way for each parallel column the quality of the effluent was averaged over a shorter period, as measurements stopped on 18 December 1996 due to technical problems.

Retardation factors R (for O_2, NO_3^-, Na^+, K^+, Mg^{2+}) or leach factors L (for Fe^{2+}, Mn^{2+}, NH_4^+, CH_4, As) were simply deduced from concentration plots against PFs, because the definition of these factor^s is as follows:

$$R_i = \frac{t_i}{t_{H2O}} \qquad (3) \qquad\qquad L_i = \frac{t_L}{t_{H2O}} \qquad (4)$$

with: t_i = time for 90% breakthrough of solute "i" [days]; t_L = time required for 90% leaching or till equilibrium is attained with the injection water [days]; t_{H2O} = mean travel time for water or a conservative tracer like chloride [days].

For practical reasons 90 in stead of 100% breakthrough or leaching has been chosen.

The results of all R- and L-readings are listed for each monitoring point in Table 3.6.

3.5.2 *The main redox parameters*

The main redox sensitive parameters monitored were: O_2 , NO_3^-, SO_4^{2-}, CH_4 , Fe^{2+}, Mn^{2+}, and NH_4^+. The results in Table 3.5, Fig.3.5 (Langerak) and Fig.3.6 (Nieuwegein) demonstrate that O_2 and NO_3^- were consumed, and SO_4^{2-}, Fe^{2+}, Mn^{2+} and NH_4^+ released (produced). Methane behaved nearly conservatively: there was no reaction with oxidants (O_2, NO_3^- or SO_4^{2-}) but possibly some contribution by slowly dissolving gas pockets. Nitrate is breaking through prior to oxygen, and when their breakthrough is significant the release of SO_4^{2-},

TABLE 3.5. *Mean composition of the injected drinking water (influent Langerak) and WRK-water (influent pretreated Rhine water Nieuwegein), the injected water during aquifer passage, and the percolate of 5 chemical parallel columns (CPCs), during the first year.*

LOCATION	t$_{50}$	PFs	No. of samples	Al	As	Ca	CH4	Cl	DOC	EGV-lab	Fe	HCO3	K	colour	Mg	Mn	Na	NH$_4$	Ni	NO$_3$	O$_2$-lab	pH-field	SI	SO$_4$	TEMP	TIC	Zn
	d	-	-	µg/l	µg/l	mg/l	µg/l	mg/l	mg C/l	mS/m	mg/l	mg/l	mg/l	mg Pt/l	mg/l	mg/l	mg/l	mg/l	µg/l	mg/l	mg/l	-	-	mg/l	°C	m-mol/l	µg/l
LANGERAK																											
influent	0,0	-	54	2	0,8	60,2	0	34	3,0	50,6	0,04	298	6,5	15,9	11,0	0,012	45,9	0,02	1,1	14,9	9,5	7,70	0,34	7,6	12,6	5,11	4
WP.1-72	13,0	2-28	18	3	7,5	63,5	2543	22	4,4	53,9	3,83	333	4,5	9,8	9,1	0,339	54,5	1,32	2,1	1,1	0,5	7,31	-0,03	19,0	11,6	6,17	4
WP.1-80	6,0	2-64	20	4	1,8	59,6	118	25	2,7	51,7	0,62	295	6,7	10,1	11,0	0,098	49,6	0,12	2,9	8,9	2,5	7,45	0,04	17,4	11,7	5,26	5
WP.1-87	5,0	2-57	21	3	17,0	60,7	46	29	2,7	53,0	1,19	288	6,0	6,7	10,3	0,118	54,2	0,31	1,9	1,5	0,8	7,41	-0,01	30,9	12,0	5,19	5
WP.2-72	33,0	2-10	14	3	5,9	59,0	130	14	2,6	49,2	2,42	295	6,2	7,3	10,7	0,176	40,4	0,48	2,5	0,2	0,7	7,42	-0,00	29,5	11,0	5,31	4
WP.2-80	13,0	2-18	18	4	4,9	61,4	473	21	2,8	51,4	1,36	304	6,7	7,9	10,9	0,134	42,9	0,37	1,6	1,6	0,6	7,37	-0,02	22,6	11,6	5,52	9
WP.2-90	18,0	2-19	17	3	7,4	61,2	43	20	2,5	50,9	1,33	291	5,8	5,6	10,3	0,086	44,1	0,39	1,4	0,0	0,6	7,40	-0,02	32,6	11,6	5,26	5
WP.3-71	120,0	2,2	2	-	1,0	62,2	3435	13	3,9	51,0	4,17	318	4,1	-	9,4	0,625	47,0	1,69	-	0,0	0,4	7,30	-0,07	23,4	11,3	5,87	3
WP.3-74	90,0	2-3	3	3	2,5	58,2	19	11	2,7	47,4	1,35	293	6,3	5,6	12,0	0,077	37,7	0,80	2,5	0,0	0,7	7,30	-0,10	27,0	11,6	5,38	3
WP.3-77	113,0	2-3	5	3	1,0	58,0	0	11	2,5	47,1	1,26	295	6,5	5,8	12,2	0,112	38,3	0,85	2,5	0,1	0,6	7,40	-0,03	24,1	11,5	5,32	3
WP.3-82	91,0	2-4	7	3	1,6	60,6	0	11	2,4	48,4	2,49	308	6,4	6,6	11,9	0,211	36,8	0,65	2,5	0,0	1,0	7,40	-0,00	21,5	10,9	5,56	3
WP.3-86	77,0	2-4	8	3	1,0	60,7	986	11	2,1	48,2	1,46	298	6,5	4,3	11,6	0,269	39,3	0,45	2,5	0,0	0,7	7,37	-0,02	28,6	10,9	5,42	3
WP.3-89	65,0	2-6	9	2	3,0	60,9	128	11	2,8	48,3	1,44	294	5,2	7,6	10,2	0,123	40,2	0,69	1,8	0,2	0,9	7,38	-0,04	30,4	11,1	5,33	3
NIEUWEGEIN: COLUMNS																											
influent	0,0	-	4	-	0,5	77,5	0	149	1,5	77,9	0,00	151	6,1	-	11,8	0,000	79,0	0,01	-	15,9	7,7	7,48	-0,36	66,1	8,4	2,72	5
CPC.1	0,2	5-253	6	-	1,3	76,6	-	147	1,7	82,0	0,05	168	6,5	-	11,0	0,266	82,8	0,09	-	14,6	-	-	0,08	67,0	12,0	2,85	20
CPC.2	0,2	5-253	6	-	1,3	78,2	-	149	1,3	82,0	0,03	167	7,1	-	11,1	0,397	82,0	0,38	-	13,6	-	-	-0,13	67,2	12,0	3,12	29
CPC.3	0,2	5-253	6	-	1,8	79,1	-	152	1,1	81,2	0,04	163	6,2	-	11,1	0,347	82,2	0,29	-	12,6	-	-	-0,02	69,3	12,0	2,71	31
CPC.4	0,2	5-253	6	-	1,5	75,0	-	147	1,6	81,8	0,02	166	6,4	-	10,9	0,240	82,4	0,03	-	15,0	-	-	-0,02	66,4	11,8	2,87	34
CPC.5	0,2	5-253	6	-	1,5	74,8	-	147	1,4	81,1	0,01	165	6,4	-	10,9	0,202	82,0	0,03	-	15,1	-	-	-0,15	64,8	11,8	2,98	25
NIEUWEGEIN																											
influent	0	-	24	27	0,7	72,7	0	126	1,3	72,8	0,01	158	5,4	1,5	11,0	0,002	65,0	0,04	2,0	14,1	5,8	7,55	-0,05	61,5	13,7	2,79	5
WP.4-95	59,0	2-6	9	3	1,0	100,0	52	128	1,4	79,4	1,70	228	2,0	1,6	10,1	0,426	69,4	0,33	2,5	0,0	0,9	7,61	0,36	68,2	11,9	4,02	3
WP.4-110	5,0	2-64	20	13	2,5	80,6	2	128	1,0	75,8	0,39	173	5,4	1,7	10,6	0,304	69,3	0,05	3,3	8,0	1,5	7,42	-0,12	69,8	12,1	3,13	11
WP.4-120	3,0	2-114	21	5	10,1	77,9	0	127	0,7	75,5	0,43	168	5,0	1,0	10,2	0,445	67,2	0,05	6,3	7,6	1,9	7,37	-0,17	70,5	12,2	3,08	27
WP.4-130	6,0	2-65	19	6	1,8	82,5	0	128	0,9	77,0	0,03	181	5,6	1,9	10,4	0,253	66,2	0,04	2,8	8,7	1,9	7,49	0,01	68,7	12,1	3,20	8
WP.5-95	106,0	2-4	6	3	1,0	101,3	0	131	1,4	80,1	1,15	216	1,2	1,9	8,7	0,313	64,9	0,27	2,5	0,0	0,8	7,74	0,37	73,4	12,5	3,71	3
WP.5-106	19,0	2-17	16	-	4,5	88,0	0	129	1,1	77,5	1,23	194	4,9	0,8	10,0	0,418	62,9	0,07	-	0,4	1,2	7,52	0,09	72,2	11,2	3,44	9
WP.5-112	31,0	2-11	13	3	3,7	91,2	139	123	1,3	77,5	2,08	217	4,3	1,2	10,4	0,545	65,8	0,12	2,3	0,3	0,9	7,45	0,03	67,9	11,3	3,91	5
WP.5-120	26,0	2-13	14	4	7,6	85,9	0	129	1,2	77,2	1,78	189	4,4	0,9	10,5	0,380	69,3	0,12	2,3	0,1	0,9	7,42	-0,09	76,7	11,3	3,42	7
WP.5-130	27,0	2-13	14	4	9,8	90,9	3	131	1,1	78,8	1,20	200	4,6	1,2	10,6	0,232	68,1	0,11	2,3	0,3	0,8	7,57	0,12	75,7	11,5	3,51	5

TABLE 3.6. *The observed retardation (R) and leach (L) factors for some quality parameters on all observation wells (situation after 1.5 years of injection) and all chemical parallel columns. N.B.: the threshold was fixed at 90% breakthrough c.q. leaching (for O_2 and NO_3^- also 10% given). For definition of retardation and leach factor see resp. Eq.3 and 4.*

observation well	t$_{50}$ d 50%	O$_2$ R 10-90%[@]	NO$_3$ R 10-90%[@]	NH$_4$ L 90%	Fe L 90%	Mn L 90%	Mg L/R 90%	K L/R 90%	Na R 90%	CH$_4$ L 90%	As L 90%
LANGERAK (DE STEEG)											
WP.1-72	13	>43	18->43	>43	>43	>43	36?^{R}	36?^{R}	?	32	15?
WP.1-80	6	15->102	2-101	16	13	88?	3?^{L}	6^L	<1.4	3.2	12
WP.1-87	6	≥81->88	50->88	13	>88	>88[#]	?	13^R	?	1.4	18
WP.2-72	38	>15	>15	9	>15	>15	?	6?^{R}	?	1.6	>15
WP.2-80	20	>29	13->29	24	28	>29	5^L	6^L	?	4.4	18
WP.2-90	20	>29	>29	19	>29	>29	?	?^{R}	?	1.4	17
WP.3-71	166	>3.4	>3.4	>3.4	>3.4	>3.4	>3.4^R	>3.4^R	?	>3.4	>3.4
WP.3-74	115	>5	>5	≥5	>5	>5	4^L	?^{R}	?	1.3	?
WP.3-77	107	>5	>5	>5	>5	>5	≥5^L	3?^{L}	?	1.2	>5
WP.3-82	96	>6	>6	>6	≥6?	>6	?	2?^{L}	?	1.3	>6
WP.3-86	83	>7	>7	7?	>7	>7	2?^{L}	2?^{L}	?	1.2	>7?
WP.3-89	65	>9	>9	7	>9	>9	5?	7^R	?	1.6	≥8?
NIEUWEGEIN (WRK)											
MLF.1	0.2	-	9-27	7	<1	67	<5	<5	<5	-	35-200
MLF.2	0.2	-	27	13	<1	100	<5	<5	<5	-	35-200
MLF.3	0.2	-	30	17	<1	100	<27	<27	<27	-	35-200
MLF.4	0.2	-	9-26	10	<1	80	<5	≤5	<5	-	35-200
MLF.5	0.2	-	9-26	9	<1	60	<5	≤5	<5	-	35-200
WP.4-95	64	>8	>8	>8	>8	>8	5^R	>8^R	3^R	2.3	2.5
WP.4-110	6	23-94	10-30	8	11.5	80	7.5^R	5.3^R	1.8^R	1.4	11
WP.4-120	3	40-170	15-36	7.4	16	127	5?^{R}	5?^{R}	<2.2^R	1.5	20
WP.4-130	6	23->95	8-30	9	4-7	85	5?^{R}	4.2^R	1.2^R	1.1	12
WP.5-95	102	>5.2	>5	>5	>5	>5	5?^{R}	>5^R	1.5^R	1.2	>5.2
WP.5-106	21	>26	25->26	24	26	>26	≤7^R	≤7^R	2^R	1.5	7
WP.5-112	34	>16	>16	8?	>16	>16	4^R	7^R	2.7^R	3	9.5
WP.5-120	28	>19	>19	10?	>19	>19[#]	4.5^R	8^R	<2.1^R	1.2	14
WP.5-130	28	>19	>19	9	>19	>19	5^R	8^R	2.1^R	1.4	14

[@] = if only one value, then for both 10 and 90%; [#] = strong increase.

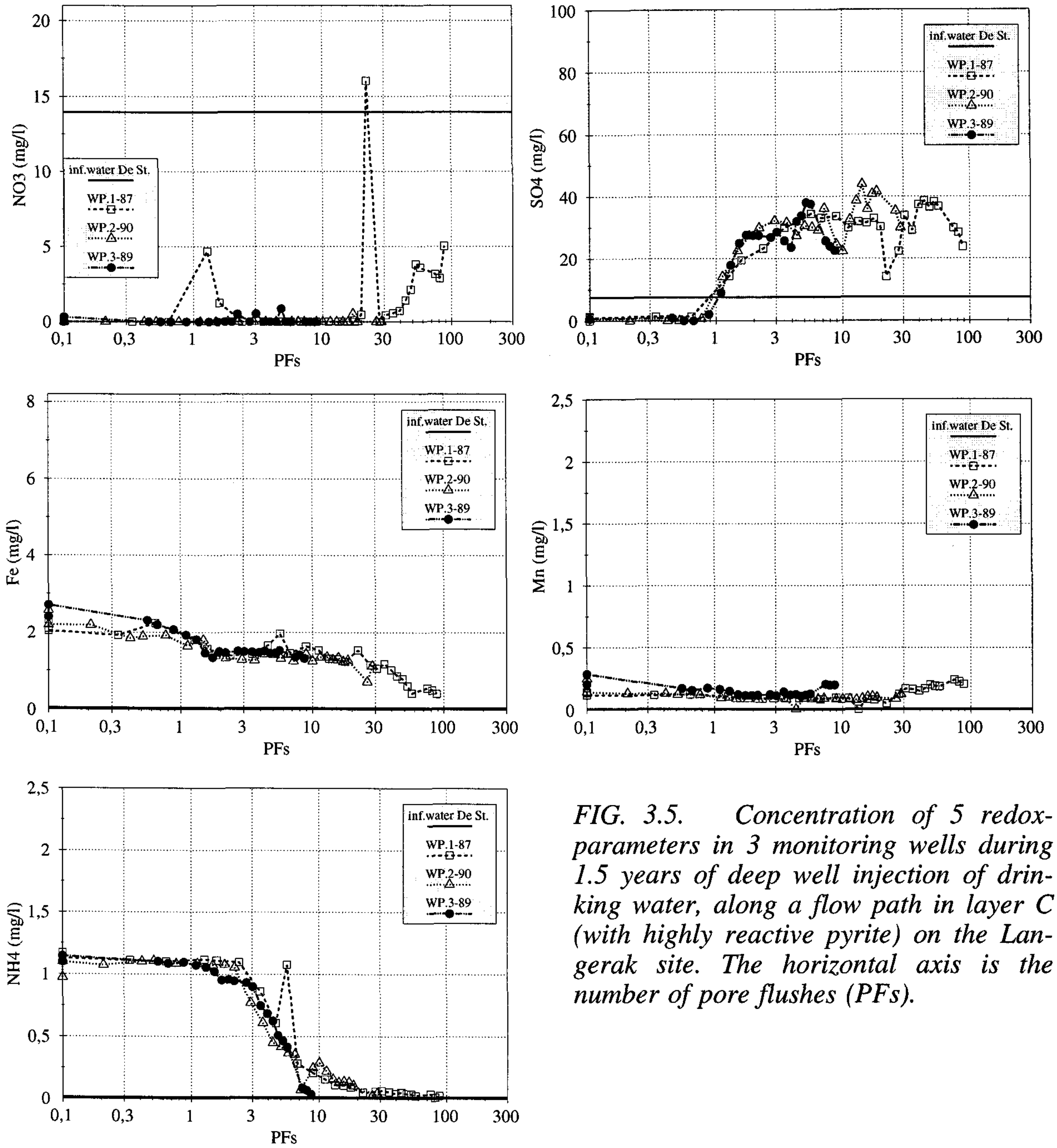

FIG. 3.5. Concentration of 5 redox-parameters in 3 monitoring wells during 1.5 years of deep well injection of drinking water, along a flow path in layer C (with highly reactive pyrite) on the Langerak site. The horizontal axis is the number of pore flushes (PFs).

Fe^{2+}, Mn^{2+} and NH_4^+ strongly declined. Oxygen concentrations below 1-2 mg/l are likely biased by atmospheric introduction during sample transport or analysis (also in the field) notwithstanding efforts to prevent this. O_2-levels <2 mg/l are therefore considered as zero, if accompanied by zero NO_3^- levels.

The rate of O_2-consumption, when temperatures superate 10°C, is typically about 1,2-5 mg/l/d, and the rate of NO_3^- consumption approximates 1-4 mg NO_3/l/d. When temperatures in the infiltration water drop below 10°C, as happened only at the Nieuwegein site in between 30 and 100 pore flushes (Fig.3.6), oxidation reactions slow down significantly (for O_2 and NO_3^- <0.5 mg/l/d). The mean behaviour is primarily dictated by oxidation of pyrite (O_2 and NO_3^- consumed, SO_4^{2-} and Fe^{2+} produced), oxidation of organic matter (NO_3^- consumed, TIC [= HCO_3^- + CO_3^{2-} + CO_2] produced) and cation exchange (desorption of Fe^{2+}, Mn^{2+} and NH_4^+). The increases for Fe^{2+} and Mn^{2+} may also relate to the reduction of (hydr)oxides ($Fe(OH)_3$ and MnO_2) or dissolution of manganous siderites. Measurable NO_3^- concentrations combined with measurable Fe^{2+} concentrations only in those few wells with the highest leach factor for methane, indicating that some mixing occurred with native groundwater. As expected, Fe^{2+} and O_2, Mn^{2+} and O_2 and NH_4^+ and O_2 were never noticed together during aquifer passage. Nitrate and Mn^{2+} were observed together, however, close to the injection well, indicating that Mn^{2+} and NO_3^- do not react sufficiently fast to reach thermodynamic equilibrium.

The chemical parallel columns showed similar but less pronounced behaviour. This is due to the very short contact time (0.2 d) and sluggish oxidation of pyrite and organic matter (see below).

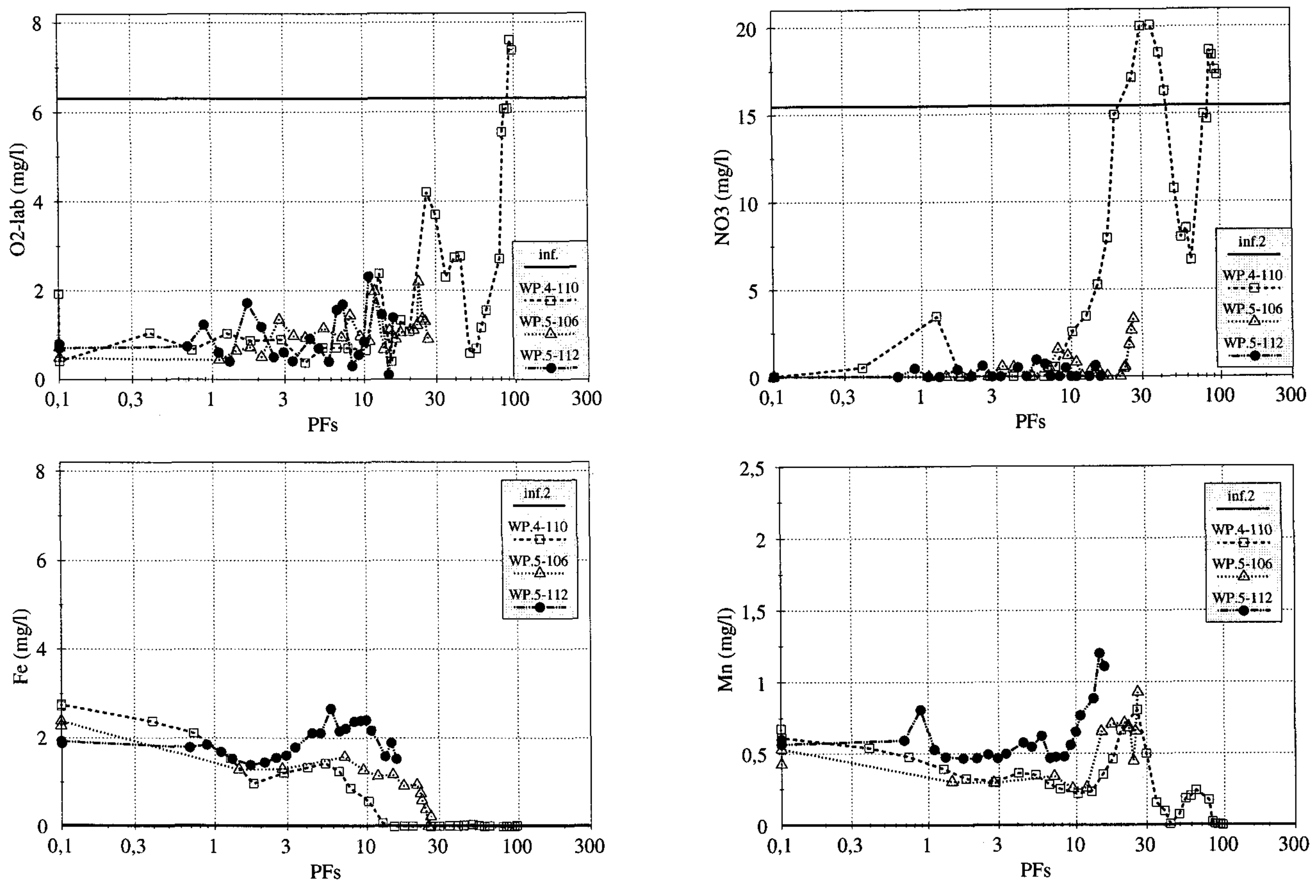

FIG. 3.6. Concentration of 4 redox-parameters in 3 monitoring wells during 1.5 years of deep well injection of pretreated Rhine River water, in layer D (with moderately reactive pyrite) on the Nieuwegein site. The horizontal axis is the number of pore flushes (PFs).

Zoning in vertical plane

The pyrite and organic matter content are highest in the upper aquifer zone, and lowest in the lowest aquifer zone (Stuyfzand et al., 1997). Yet there is less pyrite oxidation in the upper and middle zones than in the lower parts (compare ΔSO_4 in Fig.3.7), especially in Langerak. The upper zone shows, however, on both sites a relatively high TIC-production coupled to a high O_2- and NO_3^- consumption. This indicates that the oxidation of organic matter predominates over pyrite oxidation in the upper zone, and that the reverse holds for the lower zone (especially in Langerak). De middle parts of the aquifer in Langerak contain more pyrite and organic matter than the lower zone, but show the lowest production rate of SO_4^{2-} and the lowest consumption rate of O_2 and NO_3^-. This indicates that the pyrite in the lower zone should be more reactive than in both other zones, probably by a more favourable crystal structure or size (smaller) and exposition (less coatings of organic matter).

Zoning in horizontal plane

Sulphate concentrations did increase significantly with increasing travel time or distance in the aquifer on both sites (Fig.3.7). This proves that pyrite oxidation proceeds at a slow rate (considerably slower than water transport), which agrees with experience elsewhere (Nicholson et al., 1988, 1990; Bronswijk et al., 1993). It is concluded from Fig.3.7 that the complete consumption of O_2 and NO_3^- by pyrite oxidation in the lower aquifer zone

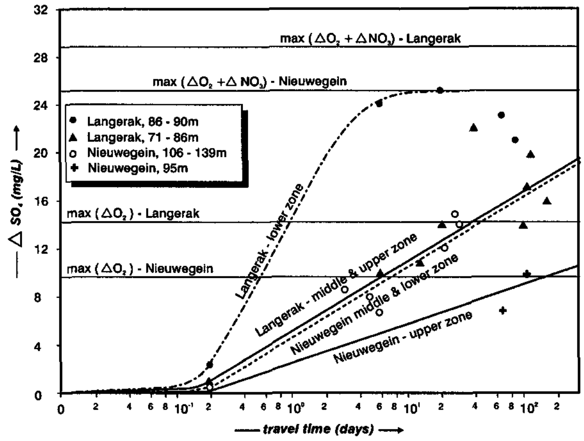

FIG. 3.7. Mean increase in sulphate concentration (by pyrite oxidation) as a function of the travel time, for Langerak and Nieuwegein. The maximum SO_4^{2-} increase is indicated for 2 cases: (a) all O_2 oxidizes pyrite, or (b) all O_2 and all NO_3^- oxidize pyrite. SO_4^{2-} concentrations and travel times derive from Table 3.5.

requires <6 days in Langerak, and above this layer 40-100 days. In Nieuwegein it takes 20-100 days. Both oxygen and nitrate oxidize pyrite, but they are not exclusively used up by pyrite oxidation, the lower zone in Langerak excluded.

The spatial distribution of redox environments in February 1998 (after 1.5 years of injection) is depicted for both sites in Fig.3.8. It follows that the oxygen front, along the most favourable flow path, advanced more in Langerak than in Nieuwegein (ca. 25 against 20 m), and this also holds for the nitrate front (ca. 50 versus 35 m).

Trends

At least a partial break-through of nitrate is observed in 8 of the 21 sampled monitoring wells, of which 4 show complete break-through (Fig.3.8). The retardation factor (R_{90}) for nitrate was 30-100 for wells with t_{50} <10 d (Table 3.6).

Oxygen break-through lagged behind nitrate (Table 3.6, Fig.3.6). On average its retardation factors R_{10} and R_{90} are 3 times higher than those for nitrate. Pyrite was more or less completely leached after 1.5 years of injection, only up to WP.4-110, WP.4-120 and WP.4-130. This is evidenced by the concentrations of SO_4^{2-} (no production), NO_3^- and O_2 (both no or hardly losses).

Complete leaching of NH_4^+, Fe^{2+} and Mn^{2+} necessitated on average resp. 15, 13-88 and ≥90 PFs in Langerak, and 9, 7-26 and 85 PFs in Nieuwegein (Table 3.6). The faster leaching of NH_4^+ is due to rapid exhaustion of its single source, the cation exchange complex. Both metals are in addition released by solid phases like pyrite (mainly Fe^{2+}), $Fe(OH)_3$ (both), MnO_2 (Mn^{2+}) and siderite ($Fe_{1-x}Mn_xCO_3$; both). The leach factor of Fe^{2+} is smaller than the one for Mn^{2+}, because traces of O_2 or NO_3^- are sufficient to halt Fe^{2+} mobilization, whereas Mn^{2+} still clearly mobilizes in the presence of minor amounts of both oxidants (Fig.3.6).

Fluctuations

A remarkable seasonal fluctuation is noticed for NO_3^- and O_2 in WP.4 (Nieuwegein; Fig.3.6). Their peak around 30 and 100 PFs is connected with temperatures <10°C, indicating a slowing down of the redox reactions. Simultaneously the TIC-increase was more suppressed than the SO_4^{2-} increase. This means that the oxidation of organic matter was more sensitive than pyrite oxidation in this case (the reverse was observed during deep well injection in older deposits; Stuyfzand, 1998b).

Nitrate and SO_4^{2-} developed during the first year in Langerak some irregularities due to variations in the $NaNO_3$-dosage (Fig.3.5). Higher sulphate levels were connected with a higher $NaNO_3$-input, demonstrating that nitrate was capable of oxidizing pyrite in the field (the batch experiments with $NaNO_3$ addition did not show this; Table 3.3).

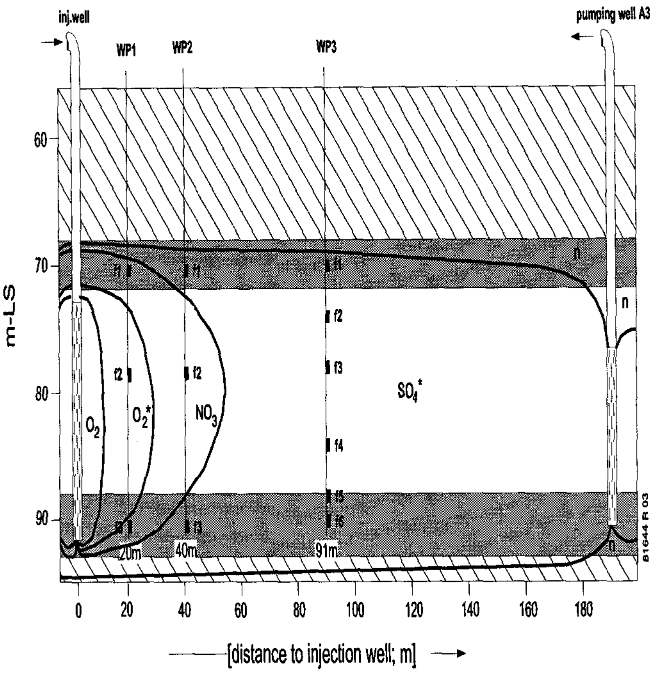

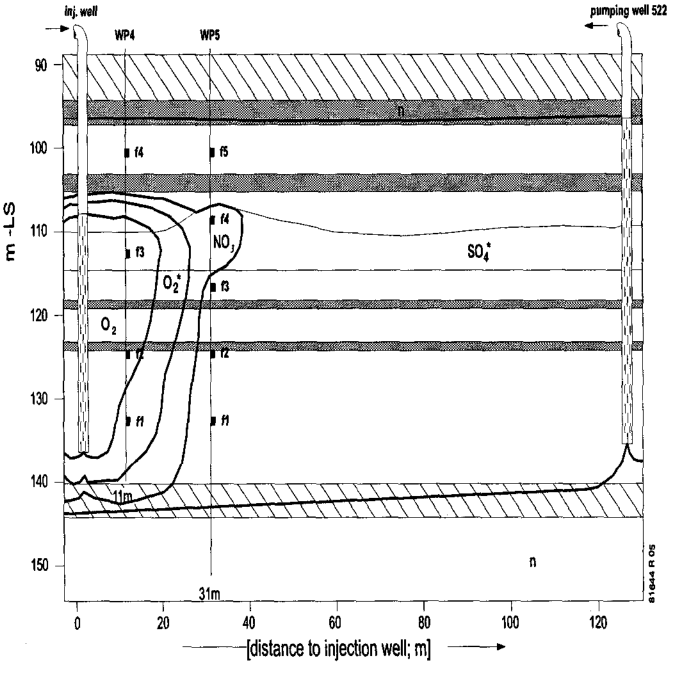

FIG. 3.8. Redox zoning in the target aquifer in Langerak and Nieuwegein in february 1998 (after 1.5 years of injection). O_2 = oxic (O_2-concentration about equal to the influent); O_2^* = penoxic (O_2-concentration diminishing with distance from ca. 10 tot 0 mg/L, and containing all nitrate); NO_3 = (sub)oxic (O_2 = 0, nitrate diminishing with distance from 15 to 0 mg/l); SO_4^* = anoxic (O_2 = NO_3^- = 0 mg/L, SO_4^{2-} above influent level due to pyrite oxidation); n = native groundwater.

On both sites a partial break-through of nitrate was observed close to the injection well, only during the break-through phase of the influent (0.5-1.5 PFs; Figs.3.5 and 3.6). This phenomenon was also reported by Stuyfzand & De Ruiter (1998). The isolated peak indicates that denitrification requires some time to reach its full size, either by diffusion through coatings or by adaptation of a mediating bacterial population.

3.5.3 *The cations Na^+, K^+ and Mg^{2+}*

Sodium, potassium and magnesium are retarded at the Nieuwegein site during the initial 2-8 pore flushes as a result of cation exchange (releasing Ca^{2+}, Fe^{2+}, Mn^{2+} and NH_4^+). The retardation factors are there on average 2 for sodium, 8 for potassium and 4-5 for magnesium (Table 3.6 and Fig.3.9). Notwithstanding a smaller contrast between the influent and native groundwater in Langerak, cation exchange dominated the behaviour of these cations there as well. The vertical zoning of the native hydrochemistry resulted in either adsorption (retardation) or desorption (leaching), with factors similar to those observed in Nieuwegein.

After the initial cation exchange Na^+, K^+ and Mg^{2+} behaved conservatively, apart from minor exchange reactions due to quality fluctuations in the influent. This means that the dissolution of silicates containing these cations can be ignored.

3.5.4 *Parameters of the $CaCO_3$-CO_2 system*

The following parameters of the $CaCO_3$-CO_2 system are listed in Table 3.5: pH, Ca^{2+}, HCO_3^-, SI_c (calcite saturation index; explained in footnote of Table 3.4) and TIC (= $HCO_3^- + CO_3^{2-} + CO_2$). The results in Table 3.5 show that Ca^{2+} and HCO_3^- hardly changed in Langerak, TIC increased slightly (0.1-0.4 mmol/l), pH (0.3-0.4) and SI_c (0.3-0.4) decreased. Obviously calcite did not dissolve, notwithstanding its presence and acid formation by pyrite oxidation. This is explained by supersaturation of the influent.

The results in Table 3.5 and Fig.3.10 show that calcite dissolved in Nieuwegein: there was an increase for calcium (2-25 mg/l), HCO_3^- (10-60 mg/l) and TIC (0.3-1.2 mmol/l), whereas pH decreased (0.1-0.2) and SI_c remained ca. 0.0.

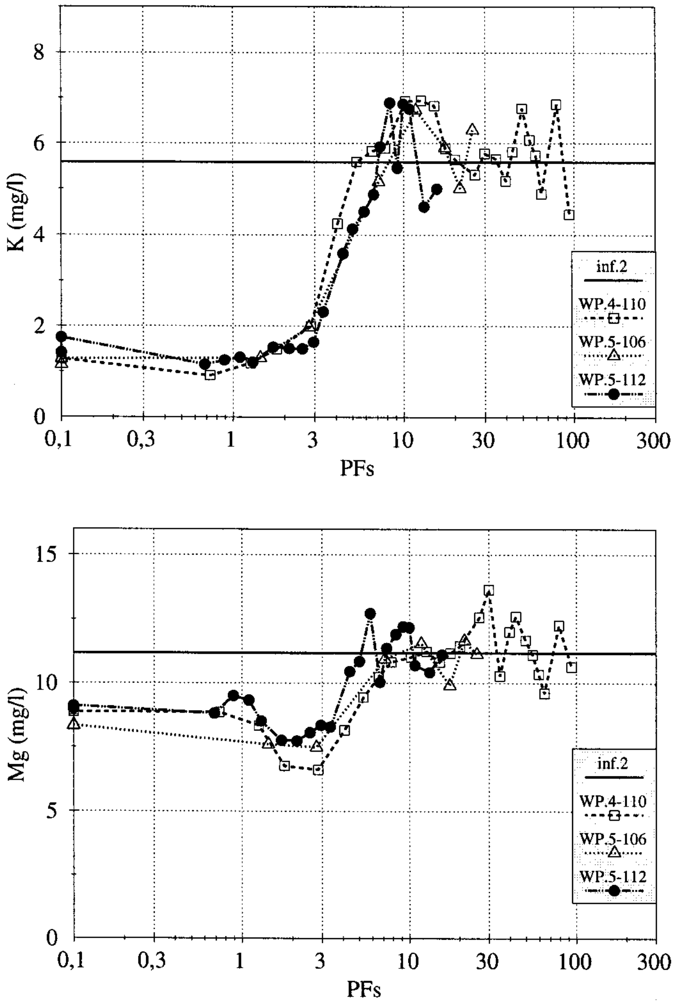

FIG. 3.9. Concentration of exchanging potassium and magnesium in 3 monitoring wells during 1.5 years of deep well injection of pretreated Rhine River water, in layer D (with moderately reactive pyrite) on the Nieuwegein site. The horizontal axis is the number of pore flushes (PFs).

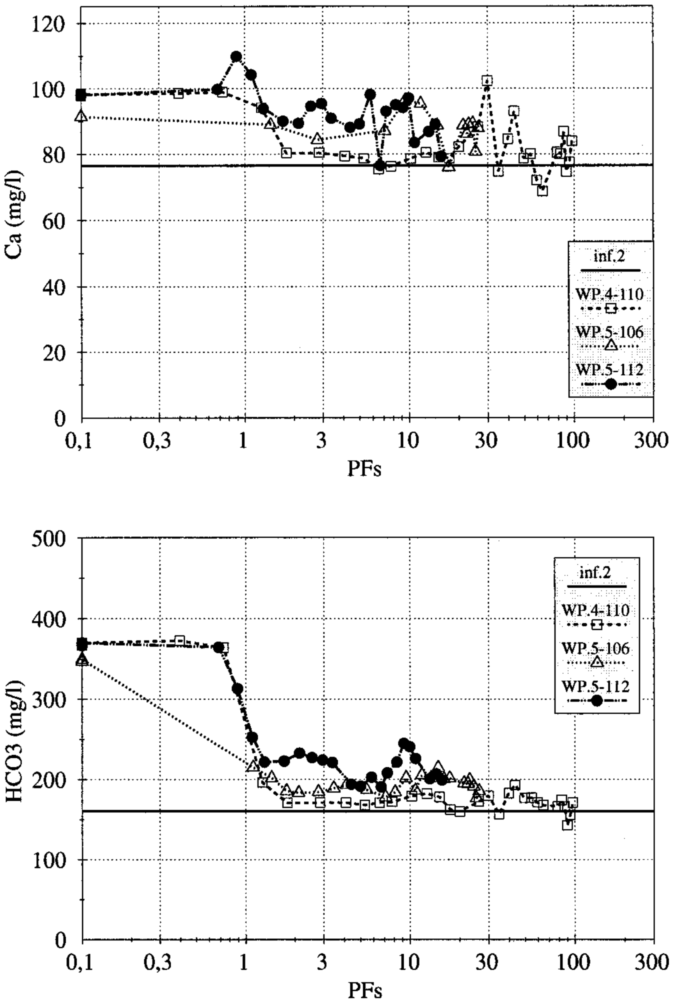

FIG. 3.10 Concentration of 2 parameters for calcite dissolution in 3 monitoring wells during 1.5 years of deep well injection of pretreated Rhine River water, in layer D on the Nieuwegein site. The horizontal axis is the number of pore flushes (PFs).

Calcium was also involved in cation exchange: in Nieuwegin it desorbed due to relatively high concentrations of Na^+, K^+ and Mg^{2+} in the influent. In Langerak Ca^{2+} desorbed from 0.5-1.5 PFs due to NaCl-dosage, and adsorbed from 1.5-4 PFs due to displacement of adsorbed Fe^{2+}, Mn^{2+} and NH_4^+.

3.5.5 *Dissolved organics*

Dissolved Organic Carbon (DOC) and colour became progressively reduced upon aquifer passage (Table 3.5), probably by degradation. DOC-removal (up to 18% in Langerak, and 15% in Nieuwegein) was less than colour-reduction (up to 65% in Langerak, and 40% in Nieuwegein). Although the first meters of aquifer passage contribute most to DOC and colour reduction, the subsequent 25-85 m lead to significant further losses.

In the upper zone of the aquifer on both sites, which contains more organic matter than the other zones, less organics were removed. In this layer DOC increased in Langerak, and the colour in Nieuwegein. The aquifer layer with the lowest organic matter content performed best in removing DOC and colour on both sites.

DOC showed minor retardation during breakthrough of the influent (Fig.3.11), colour did not. The leach factor for DOC was about 2. DOC and colour removal were more or less constant, indicating that degradation is the main mechanism.

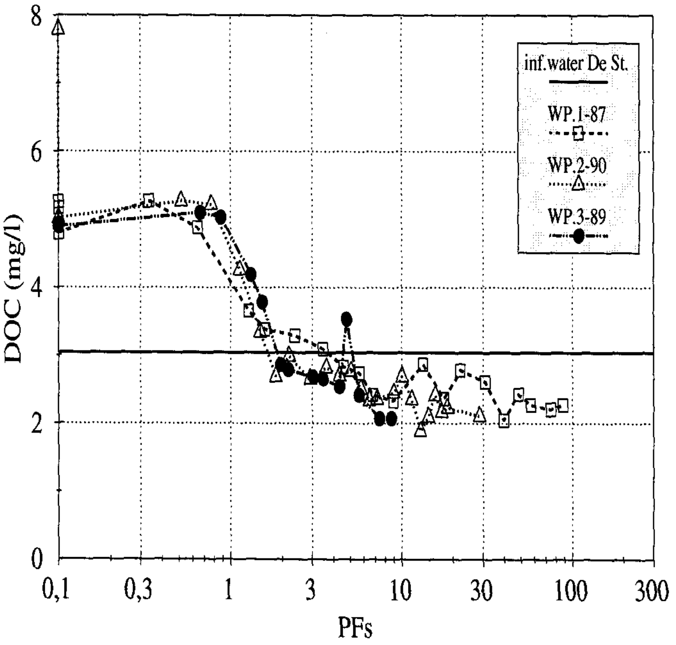

FIG. 3.11. Concentration of Dissolved Organic Carbon (DOC) in 3 monitoring wells during 1.5 years of deep well injection of drinking water, in layer C (very reactive pyrite) on the Langerak site. The horizontal axis is the number of pore flushes (PFs).

3.5.6 *Trace elements*

Aluminium hardly changed at the Langerak site, the concentration remained low at ca. 2 µg/l as expected in a pH 7.3-7.4 environment. At the Nieuwegein site aluminium concentrations were somewhat higher in the injection water due to aluminium colloids deriving from coagulation in the pretreatment. Aquifer passage resulted here in filtration of these colloids and reduced the aluminium concentrations significantly. Cadmium was analysed but showed in all samples concentrations below detection (<0.05 µg/l).

Arsenic (as H_3AsO_3 or mainly $HAsO_4^{2-}$), nickel (as Ni^{2+}) and zinc (as Zn^{2+}) are released during aquifer passage (Table 3.5 and Fig.3.12). This is explained by oxidation of pyrite, which was shown in geochemical analyses to contain significant amounts of arsenic, cobalt, nickel and zinc (§ 3.3). Upon stoichiometric oxidation this pyrite in Langerak (with an observed maximum release of 25 mg SO_4^{2-}/L) would add 52 µg As/L, 28 µg Co/L, 76 µg Ni/L, and 85 µg Zn/L. In Nieuwegein (with an observed maximum release of 15 mg SO_4^{2-}/L) this would add 40% (100*[1-15/25]) less of these trace elements. Only As actually approximated these levels, however exclusively close to the injection well during the first 1-3 or 1-10 PFs (Fig.3.12). This is explained by a higher mobility of As in the beginning due to (a) its reduced state (H_3AsO_3) which prevents it to sorb to neoformed iron(hydr)oxides, and (b) a limited amount of these iron(hydr)oxides. After some time the advancing oxygen and nitrate fronts convert the dissolving arsenic into the oxidized state (AsO_4^{3-}) which is much less mobile due to preferential sorption to neoformed iron(hydr)oxides. In addition the amount of neoformed iron(hydr)oxides steadily increases with time, supplying a growing amount of sorption sites.

Downstream the As peak shrinks, probably due to continued interaction with iron(hydr)oxides. The latter could be transported as particles over some distance and then become filtered away by the aquifer. In fact filtration of the water samples in the field led to an obvious removal of iron(hydr)oxides evidenced by a brownish coating of the filters.

The expected nickel front is retarded by sorption, it breaks through in between 10 and 100 PFs (Fig.3.12). The bulk of nickel released by pyrite is probably incorporated in the neoformed iron(hydr)oxides as well. Peak levels approaching the stoichiometric release concentration were not observed here and neither during other experiments (Stuyfzand, 1998b). The behaviour of zinc was blurred by a significant release from the PVC risers.

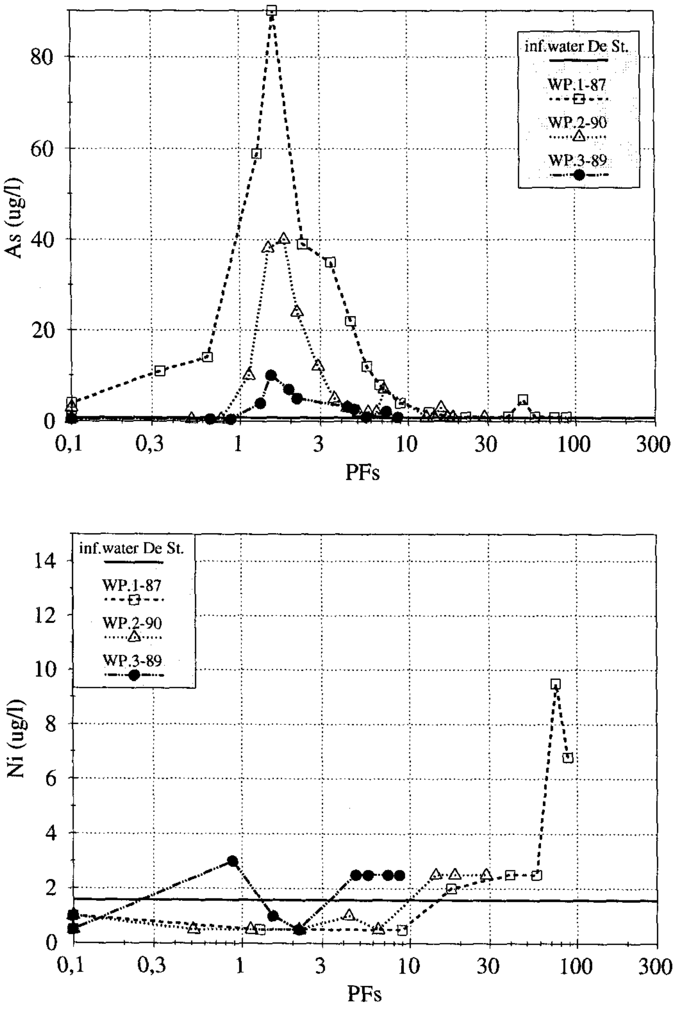

FIG. 3.12. Concentration of arsenic and nickel during 1.5 years of deep well injection of drinking water, in 3 monitoring wells in layer C (very reactive pyrite) on the Langerak site. The horizontal axis is the number of pore flushes (PFs).

3.6 QUANTIFYING THE REACTIONS

3.6.1 *The mass balance approach*

Chemical mass balances are drawn up by using a set of reaction equations in appropriate order and summing up all resulting mass transfers between an arbitrary starting and ending point in a flow system (Garrels & Mackenzie, 1967; Plummer & Back, 1980; Plummer et al., 1991). In the present case the observed composition of the injected water in the aquifer is simulated by adding to its initial composition (prior to recharge) the losses and gains by all relevant reactions with the aquifer matrix. If such a simulated transformation of water prior to injection into the observed groundwater succeeds well, we may have confidence in the model applied and we obtain insight into the relative contribution of each process.

Such a simulation approach is, however, never unequivocal and requires further independent evidence from geochemical inspection and laboratory experiments (Stuyfzand, 1993). In this well defined case of deep well injection an additional way of validation exists: validation by calculating the leaching of reactive aquifer components and comparing this with the observed breakthrough of the reactants which caused the leaching.

The procedure as applied at Kiwa, involves 6 steps (Stuyfzand et al., 1998). The first 4 steps regard the normal mass balance for the liquid phase and are discussed in this section. As a tool the simple spread sheet model 'REACTIONS+' (Stuyfzand et al., 1998) is used to perform several tedious calculations. Steps 5 and 6 regard the mass balance for all reactive solid phases and are discussed in § 5.3. Those balances were calculated using the model 'EASY-LEACHER' (Ch.4).

3.6.2 *Selecting samples and precalculations (phase 1)*

Sample selection

Those samples were selected which satisfied the following criteria: (1) the analysis covers at least all main constituents and resulted in a square ionic balance; (2) break-through is completed (no mixing with native groundwater; PF≥2); (3) sample can be unambiguously related to the influent (after a time shift); and (4) most reactive phases are still present in the aquifer. Quality fluctuations and analytical noise in influents and water samples taken during aquifer passage, forced to compare the mean hydrochemistry before and after some aquifer passage (resp. in- and output) instead of comparing individual samples.

Three monitoring wells were selected as output, using their mean water quality during the first year excluding the first 2 PFs: from Langerak WP.2-80 (pyrite moderately reactive, t_{50} 20 d, 2-20 PFs), and WP.2-90 (pyrite very reactive, t_{50} 20 d, 2-20 PFs), and from Nieuwegein WP.5-120 (pyrite moderately reactive, t_{50} 28 d, 2-14 PFs). Their mean input quality (of influent) was taken, applying a time shift to the period selected equal to their respective t_{50}. This procedure does not prevent that minor differences arise for conservative tracers between in- and output couples. Such differences are balanced in the term 'convective transport'.

Precalculations using REACTIONS+

All concentrations in water are converted from mg/l into micromoles per liter. The measured alkalinity (often expressed as HCO_3^-) is converted into total HCO_3^- and CO_3^{2-}, and if not measured, the $H_2CO_3^*$ (=CO_2 + H_2CO_3) concentration is calculated according to Stuyfzand (1989). Subsequently the ionic balances are squared completely, by a proportional change for each cation or anion or both. Inorganic carbon speciation is then recalculated.

Results of these precalculations are presented for the INPUT-rows and middle OUTPUT-row in Table 3.8. They are performed by Kiwa's computer code REACTIONS+, a spread-sheet (in QPRO+ or EXCEL), which is used for calculating the whole mass balance.

Equilibrium calculations using WATEQ4F

Mineral equilibria were calculated using the computer code WATEQ4F (Ball & Nordstrom, 1991). It is concluded that the water injected remained in the aquifer supersaturated with respect to gibbsite ($Al(OH)_3$) and amorphous $Fe(OH)_3$, and undersaturated with respect to siderite ($FeCO_3$) and rhodochrosite ($MnCO_3$). This makes it highly unlikely that the waters injected would dissolve gibbsite or $Fe(OH)_3$. They could dissolve, however, a manganous siderite if present. With respect to calcite, the influent in Langerak was supersaturated and the influent in Nieuwegein was in equilibrium or slightly agressive. Aquifer passage conduced to equilibrium, which means -- in an acid producing system -- that in Nieuwegein calcite dissolved. Arsenic was calculated to be present mainly as $HAsO_4^{2-}$ in waters containing nitrate, and mainly as H_3AsO_3 in anoxic waters ($O_2 = NO_3^- = 0$ mg/L).

3.6.3 *Looking for the right reactions (phase 2)*

The most important reactions as observed during deep well injection in the Netherlands (Stuyfzand, 1998b), are listed in Table 3.7. The reactions involving F^-, PO_4^{3-} and SiO_2 are not considered here due to lack of their analysis. The presence of reactive calcite eliminates the alternative acid buffering by HCO_3^-. Siderite or a manganous siderite could be present in small amounts, but if so, its reactivity needs to be demonstrated as well (it is known to react much slower than calcite). These uncertainties and the possibility to use other reactions, made us skip siderite reactions.

The oxalate extractions demonstrated that MnO_2 and $Fe(OH)_3$ or related phases may be present in the aquifer (Table 3.2). It cannot be excluded, however, that this extraction actually dissolved a manganous siderite! Anyhow, MnO_2-reduction was selected and $Fe(OH)_3$-reduction was disregarded, because the water was either supersaturated with respect to $Fe(OH)_3$ or other Fe-sources explained the observations well enough.

Some of the reactions typical for mixing (1-4b in Table 3.7) remain important also beyond the breakthrough phase (0.5-1.5 PFs), because desorbing Fe^{2+}, Mn^{2+} and NH_4^+ can be oxidized when not all O_2 or NO_3^- has been consumed earlier by reaction with pyrite or organic matter.

TABLE 3.7 Listing of possible reactions between on the one hand the injected water and native groundwater (upon mixing), and on the other hand injected water and solid constituents of the target aquifer. Quantitatively the most important reactions are marked with an asterix. N.B.: acidifying reactions can be recognized by presence of CO_2 (=carbonic acid) on the right side of the reaction equation.

Reactions with oxygen	
$O_2 + 4\ Fe^{2+} + 8\ HCO_3^- + 2\ H_2O \rightarrow 4\ Fe(OH)_3 + 8\ CO_2$	(1)
$2\ O_2 + NH_4^+ + 2\ HCO_3^- \rightarrow NO_3^- + 2\ CO_2 + 3\ H_2O$	(2)
$3{,}75\ O_2 + FeS_2 + 4\ HCO_3^- \rightarrow Fe(OH)_3 + 2\ SO_4^{2-} + 4\ CO_2 + 0{,}5\ H_2O$	* (3a)
$3{,}5\ O_2 + FeS_2 + 2\ HCO_3^- \rightarrow Fe^{2+} + 2\ SO_4^{2-} + 2\ CO_2 + H_2O$	* (3b)
$O_2 + 4\ FeCO_3 + 6\ H_2O \rightarrow 4\ Fe(OH)_3 + 4\ CO_2$	(4)
$O_2 + CH_2O \rightarrow CO_2 + H_2O$	(5)
Reactions with nitrate	
$0{,}2\ NO_3^- + Fe^{2+} + 1{,}8\ HCO_3^- + 0{,}6\ H_2O \rightarrow Fe(OH)_3 + 0{,}1\ N_2 + 1{,}8\ CO_2$	* (6a)
$NO_2^- + 3\ Fe^{2+} + 5\ HCO_3^- + 2\ H_2O \rightarrow 0{,}5\ N_2 + 3\ Fe(OH)_3 + 5\ CO_2$	(6b)
$2{,}8\ NO_3^- + FeS_2 + 0{,}8\ H^+ \rightarrow Fe^{2+} + 2\ SO_4^{2-} + 1{,}4\ N_2 + 0{,}4\ H_2O$	* (7a)
$3\ NO_3^- + FeS_2 + HCO_3^- + H_2O \rightarrow Fe(OH)_3 + 2\ SO_4^{2-} + 1{,}5\ N_2 + CO_2$	* (7b)
$NO_3^- + 5\ FeCO_3 + 8\ H_2O \rightarrow 5\ Fe(OH)_3 + \frac{1}{2}N_2 + HCO_3^- + 4\ CO_2$	(8)
$NO_3^- + 1{,}25\ CH_2O \rightarrow 0{,}5\ N_2 + 0{,}25\ CO_2 + HCO_3^- + 0{,}75\ H_2O$	* (9a)
$NO_3^- + 0{,}5\ CH_2O \rightarrow NO_2^- + 0{,}5\ CO_2 + 0{,}5\ H_2O$	(9b)
Other redox reactions	
$MnO_2 + 0{,}5\ CH_2O + 1{,}5\ CO_2 + 0{,}5\ H_2O \rightarrow Mn^{2+} + 2\ HCO_3^-$	(10)
$Fe(OH)_3 + 0{,}25\ CH_2O + 1{,}75\ CO_2 \rightarrow Fe^{2+} + 2\ HCO_3^- + 0{,}75\ H_2O$	(11)
$SO_4^{2-} + 2\ CH_2O + Fe^{2+} \rightarrow FeS + 2\ CO_2 + 2\ H_2O$	(12)
$CO_2 + 2\ CH_2O \rightarrow CH_4 + 2\ CO_2$	(13)
Exchange reactions	
$[Fe,NH_4,Mn,Mg]\text{-EXCH} + Ca^{2+} + K^+ + Na^+ \leftrightarrow [Ca,K,Na]\text{-EXCH} + Fe^{2+} + NH_4^+ + Mn^{2+} + Mg^{2+}$	* (14)
$[OH]\text{-EXCH} + F^- + CO_2 \leftrightarrow [F]\text{-EXCH} + HCO_3^-$	* (15)
$[H_4SiO_4]\text{-EXCH} + X^- \leftrightarrow [X]\text{-EXCH} + H_4SiO_4$	* (16)
$[H_2PO_4]\text{-EXCH} + HCO_3^- \leftrightarrow [HCO_3]\text{-EXCH} + H_2PO_4^-$	* (17)
Dissolution/precipitation and pH-buffering	
$CaCO_3 + H_2CO_3 \leftrightarrow Ca^{2+} + 2\ HCO_3^-$	(18)
$FeCO_3 + H_2CO_3 \leftrightarrow Fe^{2+} + 2\ HCO_3^-$	(19)
$Ca_5(PO_4)_3OH + 7\ CO_2 + 6\ H_2O \rightarrow 5\ Ca^{2+} + 3\ H_2PO_4^- + 7\ HCO_3^-$	(20)
$SiO_2 + 2H_2O \rightarrow H_4SiO_4$	(21)
$Fe(OH)_3 + x\ H_4SiO_4 + H_2O \leftrightarrow Si_xFe(OH)_{3+4x} \cdot H_2O$	(22)
$CaAl_2Si_2O_8 + CO_2 + 8H_2O \rightarrow Ca^{2+} + 2HCO_3^- + H_4SiO_4 + 2Al(OH)_3$	(23)
$H^+ + HCO_3^- \leftrightarrow H_2CO_3 \leftrightarrow CO_2 + H_2O$	* (24)

$CaCO_3$ = calcite; CH_2O = organic matter; EXCH = exchanger; $Fe(OH)_3$ = ironhydroxide; $FeCO_3$ = siderite; FeS_2 = pyrite; $CaAl_2Si_2O_8$ = anorthite; H_4SiO_4 = dominant silicon species dissolved in water.

TABLE 3.8. Mass balance, using the REACTIONS+ spread-sheet, for observation screen WP.2-f2 at 80 m-LS at 40 m from the injection well (travel time 20 d), with the mean composition for period 27 August 1996 till 22 July 1997. The calculated OUTPUT is equal to the water injected (INPUT) plus the reaction products during aquifer passage. The observation well is representative for the middle parts of the target aquifer. Concentrations in μmol/l. Insignificant reactions have been omitted.

balance term μmol/l		O_2	CO_2	CH_4	H^+	SO_4^{2-}	NO_3^-	HCO_3^-	Cl^-	Na^+	K^+	Ca^{2+}	Mg^{2+}	NH_4^+	Fe	Mn	As	DOC
INPUT = Drinking water produced from well field Langerak, averaged as WP.2-f2, however period shifted back 20 days																		
mg/L: measured		9.5	10.7$^{\#}$	0	7.7^{pH}	7.5	14.3	297	19.4	41.6	6.52	60.1	11.1	0.015	0.04	0.012	0.0008	3.1
μmol/L: calculated		297	242	0	0	78	231	4876	547	1809	167	1500	457	1	1	0	0.011	258
μmol/L: corr. for I.B.$^{@}$		297	242	0	0	79	232	4905	551	1796	165	1488	453	1	1	0	0.011	258
CONVECTIVE TRANSPORT		-	-	-	-	-	-	-	17	17	-	-	-	-	-	-	-	-
REACTIONS	(Eq.)**																	
FeS_2 oxidation O_2	(3a)	-246	262	-	-	131	-	-262	-	-	-	-	-	-	0	-	0	-
DOC-oxidation O_2	(5)	-25	25	-	-	-	-	-	-	-	-	-	-	-	-	-	-	-25
OC-oxid (aquifer)	(5)	-25	25	-	-	-	-	-	-	-	-	-	-	-	-	-	-	-
Fe^{2+} + NO_3^-	(6a)	-	18	-	-	-	-2	-18	-	-	-	-	-	-	-10	-	-	-
FeS_2 oxid. NO_3	(7a)	-	-7	-	-	18	-25	7	-	-	-	-	-	-	9	-	0.048	-
OC-oxidat. NO_3	(9a)	-	42	-	-	-	-169	169	-	-	-	-	-	-	-	-	-	-
cation exchange	(14)	-	-	-	-	-	-	-	-	30	6	-51	-1	18	23	2	-	-
dissol. calcite	(18)	-	-91	-	-	-	-	182	-	-	-	91	-	-	-	-	-	-
OUTPUT WP.2-80				7.39^{pH}														
calculated$^{\delta}$		0	**518**	0	0	228	41	**4981**	595	1870	172	1529	452	19	23	2	0.060	233
measured: μmol/l (corr. I.B.$^{@}$)		0	**528**	0	0	228	41	**4983**	595	1870	172	1529	452	19	23	2	0.060	233
measured: mg/l		0	23.2$^{\#}$	0	7.38^{pH}	21.9	2.54	304	21.1	43.0	6.74	61.3	11.0	0.35	1.29	0.132	0.0045	2.8

** = reaction equation in Table 3.7.

$^{\#}$ = calculated from HCO_3, pH, EGV and temp; $^{@}$ = correction for a not 100% squaring Ionic Balance;

$^{\delta}$: OUTPUT = INPUT + CONVECTIVE TRANSPORT + reaction terms = calculated hydrochemistry for WP2-f2.

3.6.4 *The total reaction scheme (phases 3+4)*

Procedures

Phase 3 of the mass balance approach is composed of putting together all selected reactions and add the resulting losses and gains to the mean quality of the influent. This is done with the spread-sheet model REACTIONS+ discussed earlier. Each reaction requires the input of either the reactant or one reaction product, after which the total mass balance is directly recalculated. The distribution of a reactant or reaction product over various reactions may need various trials. The best distribution and the best mass balance are obtained when the result, the simulated water quality after interaction with the aquifer, closely approximates, in this case, the observed water quality as sampled from a monitoring well. The most important calibration terms in the balance are CO_2 and HCO_3^-, because they are not balanced them selves but result from balancing the other parameters.

Phase 4 represents the evaluation of the final mass balance, followed by its acceptance or rejection. In case of rejection phase 2 should be repeated by selecting other reactions.

Results

The best mass balance for observation well WP.2-80 is presented in Table 3.8. The mass balances for WP.2-90 and WP.5-120 are presented in Stuyfzand et al. (1998). In all cases an excellent mass balance could be obtained. The results in Table 3.8 show that the following reactions are quantitatively most important for WP.2-80, in decreasing order: (a) oxidation of organic matter from the aquifer by nitrate; (b) pyrite oxidation mainly by O_2 and little by NO_3^-; (c) cation exchange mainly with Na^+, K^+, NH_4^+, Fe^{2+} and Mn^{2+} being desorbed and Ca^{2+} adsorbing; (d) calcite dissolution; (e) oxidation of DOC and organic matter from the aquifer by O_2; and (f) denitrification by oxidation of mobilized Fe^{2+}.

Expressing all these reactions in μmol/L leads to the total reaction scheme for WP.2-80 indicated in Table 3.9. This scheme is also shown for the 2 other wells. Wells WP.2-80 and WP.5-120 are representative for the middle aquifer zone, well WP.2-90 for the lower zone (higher reactivity of pyrite). The middle aquifer zone showed in Langerak, as compared to Nieuwegein, much less calcite dissolution, no MnO_2 reduction, less oxidation of organic matter, and more oxidation of Fe^{2+} and DOC. Pyrite oxidation and cation exchange had a similar size. These differences are mainly connected with the composition of the influent (SI_c and DOC higher in Langerak) and the aquifer (more exchangeable Fe^{2+} in Langerak).

The lower aquifer zone showed in Langerak, as compared with the middle aquifer zone, much more pyrite oxidation, less oxidation of organic matter and more DOC removal. The latter could be due to losses by sorption to neoformed iron(hydr)oxides.

TABLE 3.9. Comparison of the total reaction scheme for injected water arriving in monitoring wells WP.2-80, WP.2-90 and WP.5-120 during the first year.

well	Reactions with aquifer in µmol/L (+ = formation; - = loss of phase)							
	FeS_2	CH_2O	OS	$Fe(OH)_3$	$CaCO_3$	EXCH	Fe^{2+}	Mn^{2+}
LANGERAK (drinking water)								
WP.2-80	-75	-169	-25	+85	-46	±66	-10	0
WP.2-90	-131	-48	0	+125	-46	±131	-10	0
NIEUWEGEIN (pretreated Rhine River water)								
WP.5-120	-75	-225	0	+57	-260	±60	0	-3

FeS_2 = pyrite oxidation mainly by O_2 and little by NO_3^-; CH_2O = oxidation of organic matter from the aquifer by nitrate; OS = oxidation of organic matter from the aquifer by O_2; $Fe(OH)_3$ = oxidation product of pyrite and desorbing Fe^{2+}; $CaCO_3$ = calcite dissolution; EXCH = cation exchange mainly with Na^+, K^+, NH_4^+, Fe^{2+} and Mn^{2+} being desorbed and Ca^{2+} adsorbing; Fe^{2+} = denitrification by oxidation of mobilizing Fe^{2+}; Mn^{2+} = dissolution of MnO_2.

3.7 CONCLUSIONS

The influent could be traced down in the aquifer using Cl^-, CH_4 and electrical resistivity. Their break-through curves yielded a longitudinal dispersivity (α_L) of the sands varying from 0.3 to 5.5 m, without any relation with travel time or distance. This is explained by dispersion introduced by the observation facilities (screen length 1 m).

The quality of the aerobic influent changed during passage of the anoxic aquifer by oxidation of pyrite and organic matter, calcite dissolution and cation exchange. In the 1.5 years of injection, pyrite and the labile fraction of organic matter were completely leached up to several monitoring wells. This resulted in the break-through first of NO_3^- (after 30-100 PFs) and subsequently of O_2 (3 times later), which decreased simultaneously the production of TIC and SO_4^{2-}.

Pyrite oxidation also mobilized As, Ni and Zn, however not in accordance with its chemical composition ($Fe_{0.98}Co_{0.0037}Ni_{0.01}Zn_{0.01}S_2As_{0.0053}$). They were fixed to a large extent by neoformed Fe-$(OH)_3$. In the course of time this fixation increased, especially regarding As.

The geochemical heterogeneity of the aquifer mainly consisted of a higher reactivity of pyrite in the lower aquifer zone, and a higher reactivity of organic matter in the upper parts. In the lower aquifer zone in Langerak pyrite oxidation was relatively fast (all O_2 and NO_3^- used up within 6 days mainly by pyrite), and elsewhere their elimination took 40-100 days (most NO_3^- used by organic matter). When temperatures dropped below 10°C the oxidation of organic matter decreased more than pyrite oxidation.

The leaching of NH_4^+, Fe^{2+} and Mn^{2+} took on average resp. 9-15, 7-88 en ≥90 PFs on both sites. Cation exchange supplied most NH_4^+, oxidizing pyrite most Fe^{2+}, and MnO_2 or a manganous siderite ($Fe_{1-x}Mn_xCO_3$) most Mn^{2+}. The leaching of Fe^{2+} and Mn^{2+} stopped prior to complete leaching of their sources due to penetration of aerobic conditions. Cation exchange of Na^+, K^+, and Mg^{2+} was in general completed within resp. 2, 7 and 5 PFs. DOC (Dissolved Organic Carbon) and colour showed a permanent reduction (10-30% for DOC, and 30-60% for colour) due to degradation and perhaps some incorporation in neoformed $Fe(OH)_3$.

The mass balance approach clearly quantified the most important reactions.

3.8 REFERENCES

APPELO, C.A.J. & D. POSTMA 1993. Geochemistry, groundwater and pollution. Balkema, 536p.

BALL,J.W. & D.K. NORDSTROM 1991. User's manual for WATEQ4F, with revised thermodynamic data base and test cases for calculating speciation of major, trace and redox elements in natural waters. US Geol. Surv., Open-File report 91-183.

BROERMANN, J., R.L. BASSETT, E.P. WEEKS & M. BORGSTROM 1997. Estimation of α_L, velocity, K_d and confidence limits from tracer injection test data. Ground Water 35, 1066-1076.

BRUN, A., F.D. CHRISTENSEN, J.S. CHRISTIANSEN, P.J. STUYFZAND & H. TIMMER 1998. Water quality modelling at the Langerak deep-well recharge site. In: Peters J.H. (ed), Artificial Recharge of groundwater, Proc. 3rd Intern. Symp. on Artificial Recharge, Amsterdam the Netherlands, Balkema, 305-310.

EHRLICH, G.G., E.M. GODSY, C.A. PASCALE & J. VECCHIOLI 1979. Chemical changes in an industrial waste liquid during post-injection movement in a limestone aquifer, Pensacola, Florida. Groundwater 17, 562-573.

NICHOLSON, R.V., R.W. GILLHAM & E.J. REARDON 1988. Pyrite oxidation in carbonate-buffered solution: 1. Experimental kinetics. Geochim. Cosmochim. Acta 52, 1077-1085.

NICHOLSON, R.V., R.W. GILLHAM & E.J. REARDON 1990. Pyrite oxidation in carbonate-buffered solution: 2. Rate control by oxide-coatings. Geochim. Cosmochim. Acta 54, 395-402.

PLUMMER, L.N., E.C. PRESTEMON & D.L. PARKHURST 1991. An interactive code (NETPATH) for modeling net geochemical reactions along a flow path. US Geol. Surv. Water Resour. Invest. Rep., 91-4078.

SAALTINK, M.W., C. AYORA, P.J. STUYFZAND & H. TIMMER 1998. Modelling the effects of deep artificial recharge on groundwater quality. In: Peters J.H. (ed), Artificial Recharge of groundwater, Proc. 3rd Intern. Symp. on Artificial Recharge, Amsterdam the Netherlands, Balkema, 423-425.

SNIEGOCKI, R.T. 1963. Problems in artificial recharge through wells in the Grand Prairie Region, Arkansas. U.S. Geol. Survey Water Supply Paper 1615F, 25p.

STUYFZAND, P.J. 1989. An accurate, relatively simple calculation of the saturation index of calcite for fresh to salt water. J. Hydrol. 105, 95-107.

STUYFZAND, P.J. 1993. Hydrochemistry and hydrology of the coastal dune area of the Western Netherlands. Ph.D. Thesis, edited by Kiwa, ISBN 90-74741-01-0, 366p.

STUYFZAND, P.J. 1998a. Fate of pollutants during artificial recharge and bank filtration in the Netherlands. In: Peters J.H. (ed), Artificial recharge of groundwater, Proc. 3rd Intern. Symp. on Artificial Recharge, Amsterdam the Netherlands, Balkema, 119-125.

STUYFZAND, P.J. 1998b. Quality changes upon injection into anoxic aquifers in the Netherlands: evaluation of 11 experiments. In: Peters J.H. (ed), Artificial recharge of groundwater, Proc. 3rd Intern. Symp. on Artificial Recharge, Amsterdam the Netherlands, Balkema, 283-291.

STUYFZAND, P.J. 1998c. Simple models for reactive transport of pollutants and main constituents during artificial recharge and bank filtration. In: Peters J.H. (ed), Artificial recharge of groundwater, Proc. 3rd Intern. Symp. on Artificial Recharge, Amsterdam the Netherlands, Balkema, 427-434.

STUYFZAND, P.J., F. LÜERS & H. TIMMER 1997. Development of the water quality using deep well injection, for treatment plant De Steeg in Langerak; 3. Geochemical and hydrochemical situation in Langerak and Nieuwegein prior to injection. Kiwa-rapport KOA 97.010, in dutch, 43p.

STUYFZAND, P.J., F. LÜERS & H. TIMMER 1998. Development of the water quality using deep well injection, for treatment plant De Steeg in Langerak; 5. Final report after 1.5 years of monitoring. Kiwa-report KOA 98.137, in dutch, 93 p.

STUYFZAND, P.J. & C.J DE RUITER 1997. Kwaliteitsveranderingen van drinkwater bij diepinfiltratie te St. Jansklooster; 2. Tussenrapport over de metingen van april 1996 t/m juli 1997. Kiwa-rapport KOA 97.176, 54p.

STUYFZAND, P.J. & A.J. VOGELAAR 1997. Kwaliteitsveranderingen van drink- en Maaswater na bodempassage bij Lith; deelstudie in kader van Project Infiltratie Maaskant (PIM). Kiwa-rapport KOA 97.070.

UFFINK, G.J.M. 1990. Analysis of dispersion by the random walk method. Proefschrift TU Delft, 150p.

VAN BEEK, C.G.E.M. 1989. Rehabilitation of clogged discharge wells in the Netherlands. Quart. J. Eng. Geol. London, 22, 75-80.

VAN BEEK, C.G.M.M. & H. VAN DER JAGT 1996. Mobilization and speciation of trace elements in groundwater. AQUA in press.

VAN BEEK, C.G.E.M. & J. VAN PUFFELEN 1987. Changes in the chemical composition of drinking water after well infiltration in an unconsolidated sandy aquifer. Water Resources Research 23, 69-76.

WOOD, W.W. & D.C. SIGNOR 1975. Geochemical factors affecting artificial groundwater recharge in the unsaturated zone. Transactions ASAE 18, 677-683.

4 Principles of EASY-LEACHER

Pieter J. Stuyfzand
Kiwa Research and Consultancy, Nieuwegein, Netherlands

ABSTRACT: At Kiwa the model EASY-LEACHER was developed for simulating the dynamic quality changes of an infiltrating solute which 'leaches' the aquifer. It is an analytical 2D-spread sheet model, based on: (1) the mass balance approach, for both reactive solutes in the water recharged and solid reactive phases in the aquifer system; and (2) some empirical rules regarding the sequence of reactions, reaction kinetics and mobility of elements.

4.1 INTRODUCTION

The model EASY-LEACHER is an alternative to reactive 2-D transport codes which require a high skill, tedious data input and powerful computers. It is easy to work with and generates quick answers which are ready for manipulation in a spread-sheet environment. It was developed at Kiwa specifically for use in artificial recharge and bank filtration, where the rapid leaching of reactive aquifer constituents needs consideration and variations in the input signal can be neglected. As it is partly based on empirical rules pertaining to the situation in the Netherlands, it cannot be used without adaptations in strongly deviating environments. However, the principles should be applicable anywhere.

4.2 MAIN CHARACTERISTICS

EASY-LEACHER is an analytical 2D-spread sheet model, simulating the dynamic quality changes of an infiltrating solute which 'leaches' the aquifer (Figs.4.1-4.2). It is based on:
(1) the mass balance approach, for both reactive solutes in the water recharged and solid reactive phases in the aquifer system (Fig.4.1); and (2) some empirical rules regarding the sequence of reactions, reaction kinetics and mobility of elements. These rules are based on 20 years of experience with water quality changes in aquifer systems in the Netherlands, especially regarding basin recharge, deep well injection, and bank filtration (Stuyfzand, 1989a,b, 1998a,b,c).

The required data input consists of: (i) mean composition of the influent; (ii) mean composition of native groundwater in each layer of the target aquifer; (iii) native geochemistry of each layer of the target aquifer (content of reactive solid phases); (iv) the cumulative frequency curve of detention times in each model layer or flow path, as derived from either a separately run hydrological model or tracer breakthrough data; and (v) specific information derived from the mass balance of the water phase (which reactions are needed, how do O_2 and NO_3^- distribute over the various redox reactions).

The model then calculates, (primarily) for a site with artificial recharge or bank filtration, the development of the water quality of the raw water recovered, either as a whole (mixed) or for each individual aquifer layer or flow path, since the start of infiltration.

The model simulates for as many strata as desired: (a) displacement of the native groundwater by the influent, including effects of dispersion; (b) leaching of reactive aquifer constituents: exchangeable cations, calcite, organic matter, iron sulphides and MnO_2; (c) breakthrough of solutes; and (d) sorption and breakdown of organic micropollutants. The composition of the recharge water is assumed constant, which means that the input signal takes the shape of a step function. The leaching of reactive solid phases is also taken into account when modelling the behaviour of organic pollutants, because the advance of redox fronts determines the overall breakdown rates.

As shown in Fig.4.2 there are essentially 2 options for running EASY-LEACHER. When flow parallels the discerned aquifer layers, as in case of deep well injection, the model is built up by the indivi-

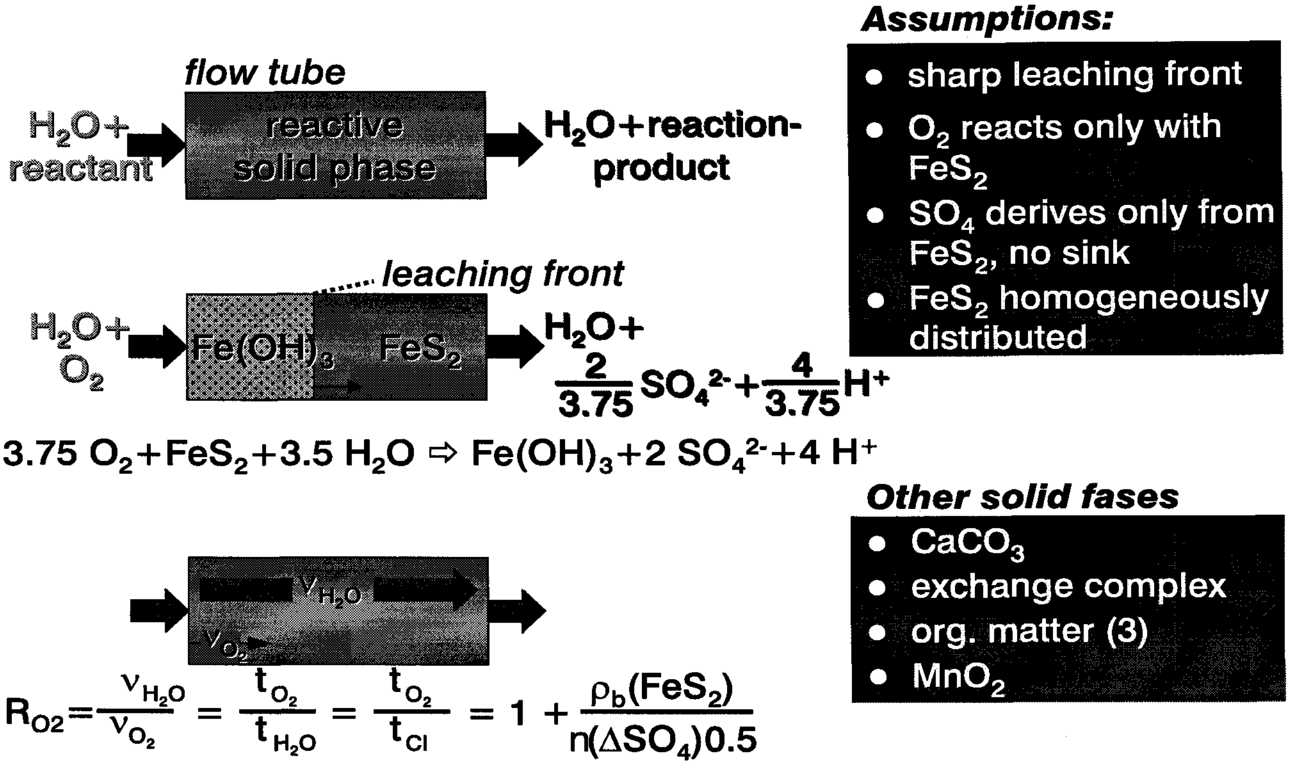

Assumptions:

- sharp leaching front
- O_2 reacts only with FeS_2
- SO_4 derives only from FeS_2, no sink
- FeS_2 homogeneously distributed

$$3.75\ O_2+FeS_2+3.5\ H_2O \Rightarrow Fe(OH)_3+2\ SO_4^{2-}+4\ H^+$$

Other solid fases

- $CaCO_3$
- exchange complex
- org. matter (3)
- MnO_2

$$R_{O2}=\frac{v_{H_2O}}{v_{O_2}}=\frac{t_{O_2}}{t_{H_2O}}=\frac{t_{O_2}}{t_{Cl}}=1+\frac{\rho_b(FeS_2)}{n(\Delta SO_4)0.5}$$

FIG. 4.1. The basic concept behind 'EASY-LEACHER' is the steady leaching of reactive phases in the aquifer, as described by the mass balance approach.

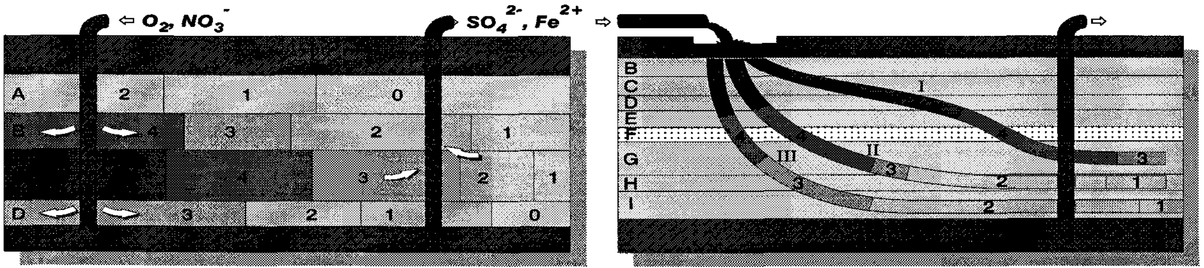

model constructed using layers **model constructed using flow paths**

the shifting of geohydrochemical zones (0 ⇨1 ⇨2 etc.)

0=native groundwater 1=EXCH + FeS_2-ox + CH_2O-ox +$CaCO_3$ dissolution + rest
2=as 1 - EXCH 3=as 2 - CH_2O-ox 4=as 3 - FeS_2-ox
5=as 4 - $CaCO_3$ dissolution
N.B. 3-5 depend on leaching sequence

for each model layer: A-D

a	own native hydrochemistry
b	own original geochemistry
c	own travel time
d	own flux (contribution to Q_{out})
e	same injection water

for each flow path: I-III

a	native hydrochemistry of layer at well screen
b	weighted mean geochemistry of involved strata (by travel time)
c-e	as left

FIG. 4.2. Essential features of EASY-LEACHER in case flow parallels the stratified medium (left) or crosses it (right).

dual layers. If flow crosses the discerned aquifer layers, as in case of basin recharge, the model is built up by selected flow paths. In the latter case some problems may arise and information on the exact position of leaching fronts is lost, due to the necessity to average the geochemistry along each flow path (excluding sludge at the bottom of recharge basins, which is treated separately).

The basic assumptions or conditions of the model are summarized in Table 4.1. The 6 main switches of EASY-LEACHER for validating the model, are discussed in § 5.2 (see Table 5.1).

For running the program the following is needed: PC ≥486, DOS or Windows, Internal memory ≥8 Mb. The software is written for QPRO+ and EXCEL.

TABLE 4.1. The 10 basic assumptions or conditions of EASY-LEACHER

(1) suspended solids are filtrated at the water/sediment interface and do not play a further role, because of inert behaviour or removal by either natural erosion or man;
(2) steady hydrology (travel times, water depth in ponds, flow path, etc.);
(3) there is no unsaturated zone (if any, then take the upper groundwater as influent or add the expected changes to the influent);
(4) bottom sludge in a recharge basin remains in steady state leading to constant O_2 and NO_3^- losses by oxidizing organic material;
(5) DOC and NH_4^+ in influent are (partly) oxidized first; the remaining O_2 and NO_3^- can oxidize aquifer materials;
(6) exchange reactions and the dissolution of inorganic aquifer phases are without kinetic hinderance (sharp fronts);
(7) the leachable phases are all homogeneously distributed within each layer or along each flow path;
(8) organic material in the aquifer matrix is composed of a labile (highly reactive), tough (little reactive) and inert fraction, with the tough fraction being oxidized only after total consumption of the labile fraction;
(9) the oxidation rate of organic material depends on the presence of O_2 and NO_3^-, and the original amount of the labile c.q. tough fraction; and
(10) the leaching sequence is such that when pyrite is completely leached, tough organic material is still present.

TABLE 4.2. Some of the most important transport equations used in EASY-LEACHER.

The retardation and leach factor in general

Sorbing and oxidizing solutes are retarded during aquifer passage, and similarly desorbing and dissolving compounds are delayed by leaching. In the latter case raised concentrations drop to the influent level long after passage of the chloride front. These delays are quantified by respectively the retardation factor R_i and leach factor L_i:

$$R_i = \frac{t_i}{t_{H2O}} \qquad (1) \qquad\qquad L_i = \frac{t_L}{t_{H2O}} \qquad (2)$$

with: t_i = time for 90% breakthrough of solute "i" [days]; t_L = time required for 90% leaching or till equilibrium is attained with the injection water [days]; t_{H2O} = mean travel time for water or a conservative tracer like chloride [days].

For practical reasons 90 in stead of 100% breakthrough or leaching has been chosen.

The general formula for a stationary and fast leaching of a homogeneously distributed reactive phase in the aquifer, is:

$$L = 1 + \frac{\rho_b(solid)}{n(reac)\, r_r} \qquad (3)$$

with: (solid) = content of reactive phase in aquifer [mmol/kg dry weight]; (reac) = concentration of reactant in flushing fluid [mmol/L]; r_r = reaction coefficient, i.e. number of mmoles of solid phase leached by 1 mmol of reactant [-]; ρ_b = bulk density = $(1-n)\rho_s$ with ρ_s = density of solids [kg/L];
n = porosity [-].

In stead of the concentration of the reactant (reac) and its reaction coefficient r_r, also the concentration of a reaction product (prod) and its reaction coefficient r_p can be taken, so that Eq.8 becomes:

$$L = 1 + \frac{\rho_b(solid)}{n(prod)\, r_p} \qquad (4)$$

Of course, (reac) or (prod) should have no other sinks or sources, unless these can be properly accounted for.

Cation exchange

The period of cation exchange reactions (here Base EXchange) can be estimated by:

$$R_{BEX} = L_{BEX} = 1 + \frac{\rho_b CEC}{n\Sigma c} \qquad (5)$$

with: CEC = cation exchange capacity [meq/kg d.w.]; Σc = sum of cations in flushing liquid, the influent [meq/L].

For the individual, adsorbed cations like Fe^{2+}, Mn^{2+} and NH_4^+ the following approximation holds:

$$L_{X\text{-}EXCH} = 1 + \frac{\rho_b X_{EXCH}}{0.75 n X_o} \qquad (6)$$

with: X_{EXCH} = content of X in cation exchange complex [meq/kg d.w.]; X_0 = concentration of X in anoxic, native groundwater prior to displacement [meq/L]. The factor 0.75 is empirical and assumes the influent to be without X.

Pyrite oxidation

The leach factor for pyrite (FeS_2) is the result of oxidation by O_2 and/or NO_3^-:

$$L_{FeS2} = 1 + \frac{\rho_b(FeS_2)}{0.5n(\Delta SO_4)} \qquad (7)$$

with: (FeS_2) = pyrite content [mmol/kg d.w.]; ΔSO_4 = sulphate-increase due to pyrite oxidation [mmol/L].

Oxidation of organic matter

The leach factor for organic matter (C_0) is the result of oxidation by O_2 and/or NO_3^-:

$$L_{Clab} = 1 + \frac{\rho_b f_{lab}(C_0)}{n(0.8\Delta NO_3 + \Delta O_2)} \qquad (8)$$

with: (C_0) = total organic carbon content [mmol/kg d.w.];
f_{lab} = fraction of easily degradable (labile) organic carbon [kg/kg]; ΔNO_3 = nitrate-decrease due to oxidation of labile organic matter [mmol/L]; ΔO_2 = oxygen-decrease due to oxidation of labile organic matter [mmol/L].

After leaching of the labile fraction of organic matter (sometimes 2%), the tough fraction (assumed 100 - 20 - 100 f_{lab}) is to be leached. About 20% is considered inert then.

Dissolution of calcite

The leach factor for calcite (or $CaCO_3$) is the result of dissolution by CO_2:

$$L_{CaCO3} = 1 + \frac{\rho_b(CaCO_3)}{n f_{CO2} CO_2} \qquad (9)$$

with: ($CaCO_3$) = total calcite content [mmol/kg d.w.];
f_{CO2} = fraction of carbonic acid reacting with calcite [-]; CO_2 = CO_2-concentration prior to reaction with $CaCO_3$ but after its production upon oxidation of pyrite, organic matter (and DOC), and nitrification [mmol/L].

4.3 CALCULATIONS

Contrary to most transport codes, the situation after each time step is directly calculated with analytical formulae, i.e. without iterations, finite elements and equilibrium calculations. Only calcite and CO_2/H_2O equilibria are calculated, in an easy direct way (nearly as accurate as speciation and mineral equilibria programs like WATEQ4F) by a method proposed by Stuyfzand, 1989c). Some of the most important transport equations regarding inorganics are collected in Table 4.2. The equations regarding organic micropollutants are not presented here (see Table 2 in Stuyfzand 1998c), as trace organic contaminants are not considered during the experiments with deep well injection. The transport equations involving calcite dissolution and the oxidation of organic matter strongly depend on the leaching sequence (see Annex 4 in Stuyfzand et al., 1998), as this changes resp. the amount of CO_2 produced and the amount of O_2 and NO_3^- available for organic matter.

How to assess the mass balance for the water phase, is explained in § 3.6.

4.4 REFERENCES

STUYFZAND P.J., 1989a. Quality changes of river Rhine and Meuse water upon basin recharge in The Netherlands' coastal dunes: 30 years of experience. In "Artificial recharge of groundwater", Johnson & Finlayson (eds), Am. Soc. Civ. Eng., New York, 235-247.

STUYFZAND, P.J. 1989b. Hydrology and water quality aspects of Rhine bank ground water in The Netherlands. J. Hydrol. 106, 341-363.

STUYFZAND, P.J. 1989c. An accurate, relatively simple calculation of the saturation index of calcite for fresh to salt water. J. Hydrol. 105, 95-107.

STUYFZAND, P.J. 1998a. Fate of pollutants during artificial recharge and bank filtration in the Netherlands. In: Peters J.H. (ed), Artificial recharge of groundwater, Proc. 3rd Intern. Symp. on Artificial Recharge, Amsterdam the Netherlands, Balkema, 119-125.

STUYFZAND, P.J. 1998b. Quality changes upon injection into anoxic aquifers in the Netherlands: evaluation of 11 experiments. In: Peters J.H. (ed), Artificial recharge of groundwater, Proc. 3rd Intern. Symp. on Artificial Recharge, Amsterdam the Netherlands, Balkema, 283-291.

STUYFZAND, P.J. 1998c. Simple models for reactive transport of pollutants and main constituents during artificial recharge and bank filtration. In: Peters J.H. (ed), Artificial recharge of groundwater, Proc. 3rd Intern. Symp. on Artificial Recharge, Amsterdam the Netherlands, Balkema, 427-434.

STUYFZAND, P.J., F. LÜERS & H. TIMMER 1998. Development of the water quality using deep well injection, for treatment plant De Steeg in Langerak; 5. Final report after 1.5 years of monitoring. Kiwa-report KOA 98.137, in dutch, 93 p.

5 Modelling chemical reactions during deep well injection at Langerak and Nieuwegein with EASY-LEACHER

Pieter J. Stuyfzand
Kiwa Research and Consultancy, Nieuwegein, Netherlands

ABSTRACT: On 2 sites in the Netherlands, at Langerak and Nieuwegein, an experiment was carried out for 1.5 years with deep well injection of oxic water into an anoxic aquifer. The resulting water quality changes during aquifer passage and the leaching of reactive solid phases from the aquifer have been successfully simulated for each site, using the model EASY-LEACHER. The main reactions included were: pyrite oxidation, oxidation of organic matter, cation exchange and calcite dissolution. The general leaching sequence was, starting with the first to be leached: exchangeable cations, labile organic matter, pyrite, tough organic matter and calcite.

In addition, the results are presented of a prognosis of the quality development over 100 years, for the raw water recovered by a fictive deep well injection plant on the Langerak site. A rapid clogging of the recovery wells by mixing of aerobic with anaerobic, ferrogenous water was feared. The presence of oxidizable pyrite and organic matter in the aquifer are expected to protect the recovery wells from a cumbersome clogging for at least 50 years.

5.1 INTRODUCTION

On 2 sites in the Netherlands, at Langerak and Nieuwegein, an experiment was carried out for 1.5 years with deep well injection of oxic water into an anoxic aquifer. Both test sites are described in detail in Ch.2. Information is given there also on the specific interests of Water Supply Company WZHO, the relation between both experiments, several operational matters and the data collection. The results of monitoring and interpretation of the water quality changes in the target aquifer at both sites, are summarized in Ch.3, and reported fully by Stuyfzand et al. (1998). In this section these water quality changes and the resulting leaching of the aquifer are simulated using the model EASY-LEACHER, which is explained in Ch.4. In addition, the results are presented of a prognosis of the quality development over 100 years, for the raw water recovered by a fictive deep well injection plant on the Langerak site.

5.2 SIMULATION OF WATER QUALITY CHANGES IN OBSERVATION WELLS

General set-up

The water quality measurements have been simulated in detail for one well on each injection site: observation well WP.1-90 in Langerak (20 m from injection well, travel time 6 days in aquifer layer C), and observation well WP.5-120 in Nieuwegein (31 m from injection well, travel time 28 days in aquifer layer E). The position of these wells and the discerned aquifer layers are shown in Fig.2.4 of § 2.3. The geochemical and other characteristics of the discerned layers are listed in Table 5.2. During most of the experimental period the water sampled at both wells was not aggressive anymore towards pyrite, i.e. all O_2 and NO_3^- was used up earlier.

The influent was resp. drinking water to which $NaNO_3$ was added, and WRK-water (pretreated Rhine River water). Although their concentration varied with time (especially the WRK-water), their concentration had to be assumed constant, so that their respective mean concentration was taken. The native groundwater quality for each observation point was assumed equal to the measurements prior to the start of injection.

The mass balances for the water phase as discussed in § 3.6 were used to quantify the various reactions and distribute the oxidants O_2 and NO_3^- over reactions with DOC, pyrite, organic matter and desorbing or dissolving Fe^{2+}. These results and the observed break-through data have been combined to tune the 6 main 'switches' of EASY-LEACHER as indicated in Table 5.1.

TABLE 5.1. The 6 main 'switches' of EASY-LEACHER for matching the simulations to the observed quality evolution: principles and specific settings for this case.

f_{lab}	adjusts the fraction of labile organic matter. This was set at 0.02 (2% of C_{org}), because this resulted in the best simulation of the break-through of oxygen and nitrate.
f_{tough}	regulates the fraction of tough organic matter. This switch is much less sensitive than f_{lab}, and without clear experimental proof it was set at 78% (this means that 20% of all organic matter is considered inert).
dO_2-C_{lab}	defines the rate of oxygen consumption (in mg O_2 L^{-1} d^{-1}) by labile organic matter. This rate was set at 5 times the original fraction of total organic carbon in the aquifer (f_{OC} on kg/kg basis), because this resulted in the best simulation of the break-through of oxygen and nitrate. The dO_2-C_{lab} switch also fixes: dNO_3-C_{lab} (= 0.5*dO_2-C_{lab}), dO_2-C_{tough} (= 0.1*dO_2-C_{lab}) and dNO_3-C_{tough} (= 0.05*dO_2-C_{lab}), all on mg/L/d basis.
f_{CO2}	regulates the fraction of all resulting CO_2 which reacts with calcite ($CaCO_3$). This is done by forcing the calcite saturation index (SI_c) of the water after aquifer passage to approach '0' (indicating equilibrium with calcite) or a slightly higher value when some supersaturation is noticed. In case of WP.1-90 there was actually a slight supersaturation (SI = 0.3), which necessitated adjustment of f_{CO2} to a value of 0.3. In WP.5-120 the influent was in equilibrium with calcite (SI = 0), which made f_{CO2} = 0.8.
f_{O2}	adjusts the fraction of oxygen which reacts with pyrite. In case of competition between pyrite and labile organic matter for oxygen, the larger part is in general consumed by pyrite. The f_{O2} switch has to be set such that the observed sulphate concentration is approached. Because nitrate can be used for pyrite oxidation as well (see below), the mass balance[1] needs to be consulted. For both monitoring wells f_{O2} was 0.91.
f_{NO3}	fixes the fraction of nitrate reacting with pyrite. In case of competition between pyrite and labile organic matter for nitrate, the larger part is in general consumed by organic matter. The f_{NO3} switch has to be set such that the observed sulphate concentration is approached. Because oxygen can be used for pyrite oxidation as well (see above), the mass balance[1] needs to be consulted. For monitoring well WP.1-90 f_{NO3} was 0.83 (pyrite much more reactive than organic matter), for WP.5-120 it was 0.27 (organic matter much more reactive than pyrite).

1 = see § 3.6

The break-through of the influent was simulated by only taking the measured mean travel time (t_{50}; 50% break-through) to the observation point, and divide the whole frequency distribution of travel times into 5 equal parts in between $0.5t_{50}$ and $1.5t_{50}$. This results in a break-through curve composed of 5 parts of 20% of the water with a mean travel time of resp. 0.6, 0.8, 1.0, 1.2 and 1.4 times t_{50}. In EASY-LEACHER, in stead of running one layer for each observation point (see Fig.4.2 on p.34) 5 equal layers were run each with its own travel time.

Results

Some of the modelling results are shown for WP.1-90 (Langerak) in Fig.5.1, and for WP.5-120 (Nieuwegein) in Fig.5.2. The simulation compares in general very well with the observed quality evolution, especially considering the folowing complications:

a the model was run with a constant quality of the influent notwithstanding fluctuations: drinking water especially regarding nitrate, WRK-water regarding all parameters;

b the model had to yield a good fit also for other monitoring wells; and

c complications due to the NaCl-addition for one month at Langerak, and variations in recharge and recovery rate had to be ignored.

In Fig.5.1 the pyrite leaching front is approaching WP.1-90, which can be deduced from the break-through of first nitrate and then oxygen in combination with a declining sulphate production after about 400 days. Ammonia and potassium clearly exchange for each other, 20% of DOC is continuously removed, and methane closely follows the break-through of the influent. Below 0.1 mg CH_4/L, however, methane shows a minor contribution of either semi-stagnant water or gas pockets. In Fig.5.2 the pyrite leaching front is still far upstream of WP.5-120, because oxygen and nitrate were completely used up and the sulphate production was stable. The oxidation of pyrite is largely responsible for the continuous mobilization of Fe^{2+} and arsenic. Initially they show a peak or bulge due to more escape from capture by precipitating $Fe(OH)_3$. Calcite is clearly dissolved over the whole period, and methane closely follows the break-through of the influent (without complications).

5.3 CALCULATED VERSUS OBSERVED LEACHING

Another way of validating the predictions of EASY-LEACHER is to check for the actual leaching of reactive solid phases in the aquifer. As geochemical analyses were only performed on aquifer cores taken prior to injection, the hydrochemistry is used to indicate when these phases are practically leached. The thus observed leach factors can be compared in Table 5.2 with the leach factors calculated by the model. The calculation of leach factors and their comparison with observed leach factors form steps 5 and 6 respectively, in the mass balance approach as presented in § 3.6.1.

It is important to notice that the leach factors are

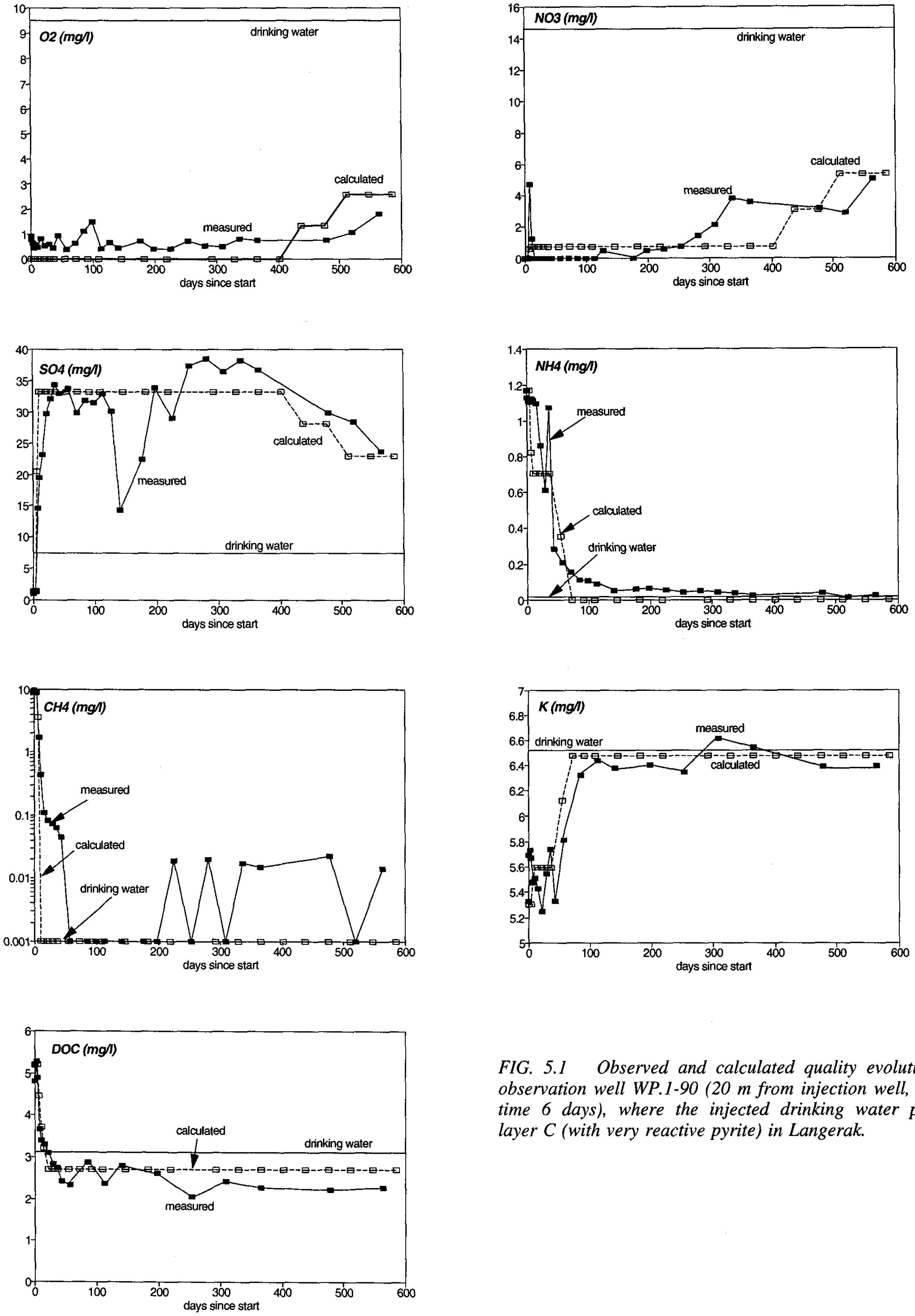

FIG. 5.1 Observed and calculated quality evolution in observation well WP.1-90 (20 m from injection well, travel time 6 days), where the injected drinking water passed layer C (with very reactive pyrite) in Langerak.

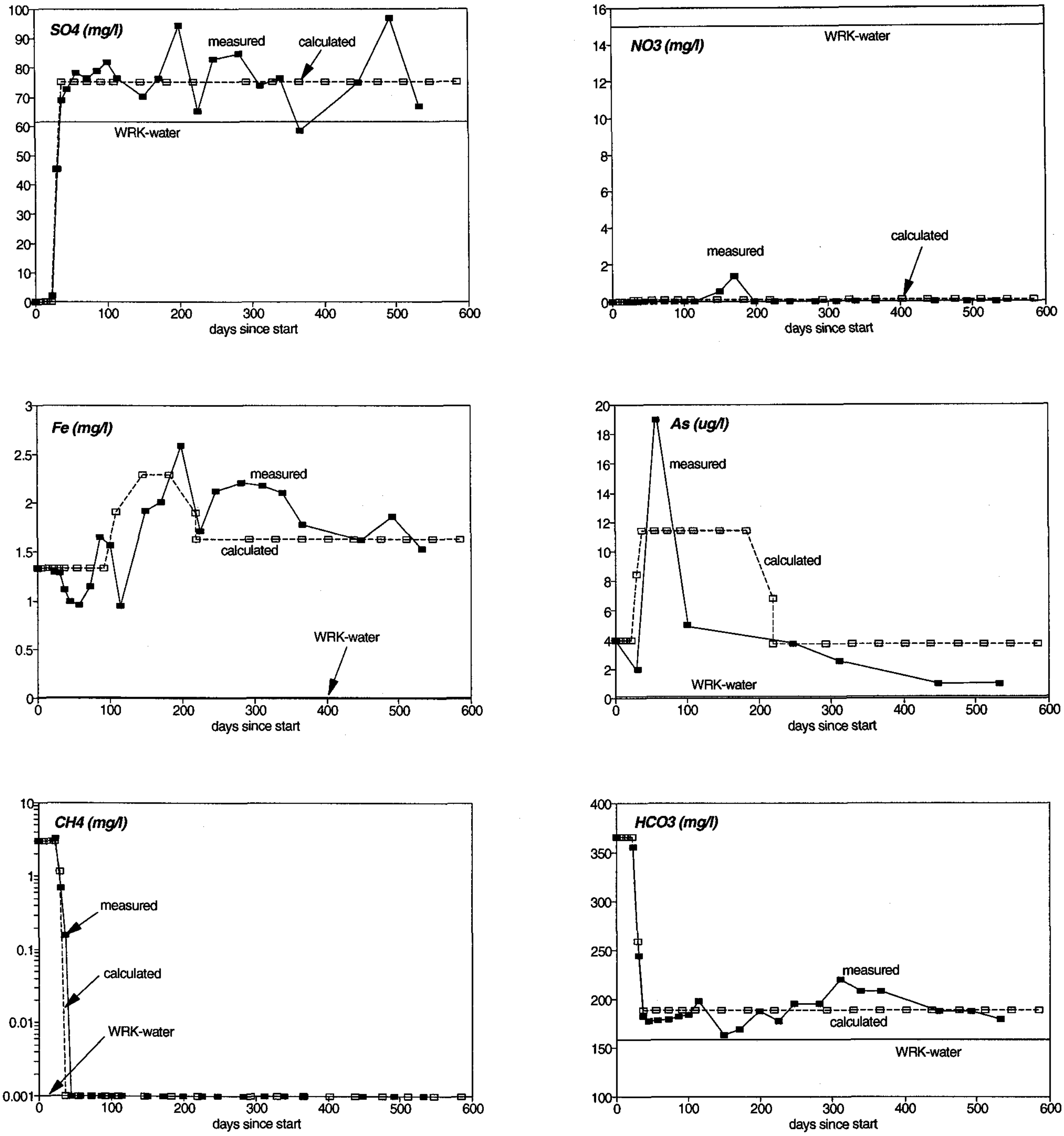

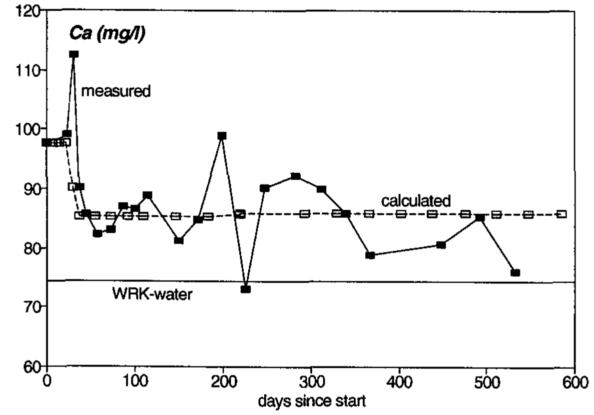

FIG. 5.2 Observed and calculated quality evolution in observation well WP.5-120 (31 m from injection well, travel time 28 days), where injected WRK-water passed layer E in Nieuwegein.

TABLE 5.2. Calculated and observed leach factors for the most important reactive phases in 3 zones of the target aquifer in Langerak and Nieuwegein, which were flushed with resp. drinking water and WRK-water. Based on the schematization of the geochemistry and hydrology as given below, and calculated with the model EASY-LEACHER.

		Langerak			Nieuwegein		
model-layer no.	unit	A	B	C	B	D	E
Depth	m-MV	68-72	72-88	88-93	96-102	104-117	118-137
Permeability (K_h)	m/d	15	40	65	20	50	70
Travel time in aquifer †	d	1027	384	280	1050	420	300
Geochemistry: see footnote #	-	$2.67{*}B_L$	B_L	C	B_N	D	E
Hydrochemistry	-	WP1-72 WP2-72 WP3-72	WP1-80 WP2-80 WP3-74 WP3-77 WP3-82	WP1-87 WP2-90 WP3-86 WP3-89	WP4-95 WP5-95	WP5-112	WP4-110 WP4-120 WP4-130 WP5-106 WP5-120 WP5-130
GEOCHEMISTRY (before the start)							
CEC	meq/kg	40.3	15.1	9.3	65.4	11.8	6.6
Fe_{EXCH}	meq/kg	0.85	0.32	0.09	0.41	0.10	0.04
Mn_{EXCH}	meq/kg	0.11	0.04	0.01	0.16	0.03	0.02
NH_{4EXCH}	meq/kg	0.43	0.16	0.06	0.28	0.03	0.02
$CaCO_3$	mmol/kg	204.3	76.6	41.2	481	44.3	15.4
Org. carbon	mmol/kg	300	117	83	133	75	67
FeS_2	mmol/kg	9.75	3.65	2.06	3.87	1.56	2.37
CALCULATED LEACH FACTORS (with resp. mean drinking water and mean WRK-water)							
CEC	-	42	16	10	51	10	6
Fe_{EXCH}	-	198	21	9	65	12	6
Mn_{EXCH}	-	44	14	8	77	13	10
NH_{4EXCH}	-	32	24	9	154	25	20
$CaCO_3$	-	140820	35290	14310	274760	8670	1071
Org. matter: labile[1]	-	198	88	218	84	53	58
Org. matter: tough[2]	-	6369	2957	6896	2745	2430	3220
FeS_2	-	912	280	92	518	159	193
OBSERVED LEACH FACTORS (from Table 3.6 on p.22)							
Fe	-	>43	21	>88	>8	>16	7-26
Mn	-	>43	88?	>88	>8	>16	100
NH_{4CEC}	-	9->43	20	7-19	>8	8?	9
$CaCO_3$	-	@	@	@	>8	>16	**
Org. matter: labile	-	>43	100	>88	>8	>16	32
FeS_2	-	>43	>102	>88	>8	>16	95-170

[1] = this fraction is leached first, before the tough fraction starts to be leached;

[2] = this fraction starts to leach only, after complete leaching of the labile fraction;

#: reference to samples indicated in Fig.2.4 on p.12. In Langerak: $A = 2.67{*}B_L$; $B_L = \{WP2\text{-}73 + WP2\text{-}76 + WP2\text{-}82 + WP2\text{-}84\}/4$; C = WP2-89; in Nieuwegein: B_N = WP4-98; D = (WP4-106 + WP4-119)/2; E = (WP4-112 + WP4-130)/2.

†: modal travel time from injection to recovery well.

@ = cannot be established due to insufficient calcite dissolution in consequence of supersaturation of the influent;

** = after ca. 70 pore flushes calcite dissolution seems to diminish, which is only due to a reduced production of acid in consequence of a partial leaching of pyrite.

equal to the amount of pore flushes needed to remove the reactive phase, and that the total amount of pore flushes achieved during both experiments (ca. 1.5 years) varied for all observation wells between 2 and 102 for Langerak, and between 2 and 167 for Nieuwegein. This explains the many '>' values reported in Table 5.2 for the observed leach factors.

Nevertheless there is in general a good agreement between the observed and calculated leach factors. The larger deviations are seen for iron and manganese, which are related, however, to differences in definition: the observed leach factors are not solely dictated by the leaching of exchangeable Fe^{2+} and Mn^{2+}, as their calculated phases are, but also by dissolution of resp. pyrite and MnO_2 or a manganous siderite.

It can be deduced from Table 5.2 that calcite and the tough fraction of organic matter survived the whole injection period on all observation points (leaching not completed). The leaching of ammonia is in most cases representative enough for the leaching of most exchangeable cations (CEC; Fe^{2+} and Mn^{2+} only close to the injection well). Its leaching proved to be completed during the experiments up to most observation points, except those with a very low flow rate and high CEC (layer A in Langerak, and layer B in Nieuwegein). The labile fraction of organic matter was completely leached during the experiments up to WP.1 in layer B (Langerak) and up to WP.4 in layer E (Nieuwegein). Pyrite was completely oxidized up to WP.4 in layer E (Nieuwegein), and this leaching front was approaching WP.1 in layer C (Langerak). The general leaching sequence was, starting with the first to be leached: exchangeable cations (mainly NH_4^+), labile organic matter, pyrite, tough organic matter and calcite.

5.4 PROGNOSIS FOR A FUTURE INJECTION PLANT

Boundary conditions

Water supply company South-Holland East (WZHO) aims at a deep well injection facility integrated into its existing well field in Langerak (see § 2.1). A first design of this facility is shown in Fig.5.3: 10 future injection wells are projected in between the existing 2 rows of 10 recovery wells each. About 3 Mm^3/a of WRK-water (pretreated Rhine River water) is to be injected.

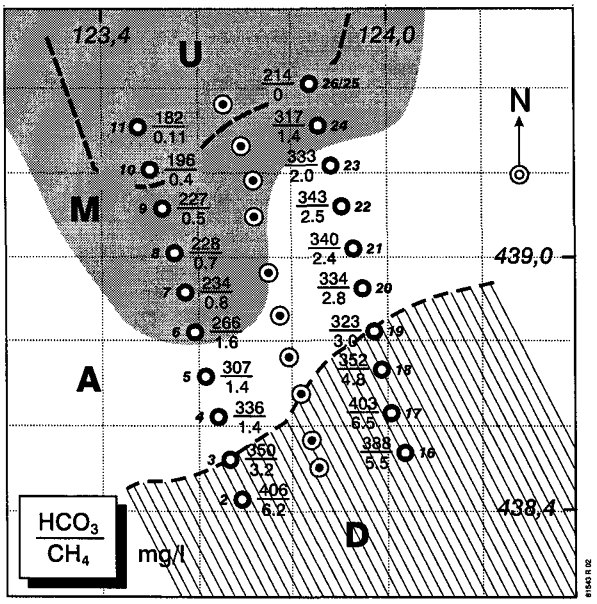

FIG. 5.3. Provisional WZHO-design of the injection plant for well field Langerak, with the distribution of groundwater types in 1996 (without injection). The inner row of dots is composed of the future injection wells, both outer rows are the actual 20 pumping wells. A = deep-anoxic, authochtonous groundwater; D = as A, however with more methane; M = mixture of A and U; U = Rhine bank filtrate (which infiltrated prior to 1953).

For this facility WZHO made preliminary hydrological calculations using the 3D-model MICROFEM. This resulted in the frequency distribution of travel times for the discerned aquifer layers A, B and C, which is required for running EASY-LEACHER.

The target aquifer was schematized exactly as indicated in Table 5.2. The native hydrochemistry of the target aquifer was based on an inventory of the water produced by the 20 existing pumping wells in 1996. This survey resulted in the recognition of the 4 watertypes depicted in Fig.5.3. The areal distribution of these watertypes was incorporated in EASY-LEACHER by subdividing each of the 3 aquifer layers into 5 sublayers and fill these layers with one of the 4 watertypes, such that the areal distribution was simulated well. The 5 sublayers were also used to simulate the frequency distribution of travel times of the injected WRK-water. The mean quality of WRK-water, as observed during the experiment in Nieuwegein, was taken for the influent during 100 years, the forecast period.

An important, additonal boundary condition was that the injection wells do not clogg significantly, because this could cause a notable consumption of oxygen and nitrate close to the injection wells in and downstream of the clogged parts. The model was run with the 6 model switches listed in Table 5.1, in the same position as during the simulation of the experimental results at Langerak.

The predicted quality evolution of the water recovered

The results obtained with EASY-LEACHER are presented in Fig.5.4. It shows the quality evolution for the total mixture of recovered groundwater since the start of injection till 100 years of continuous operation.

Displacement of the native groundwater by the influent is mainly responsible for the quick responses, in between 0.5 to 3 years, of the tracers Cl^-, CH_4, DOC and HCO_3^-, as well as SO_4^{2-} and Ca^{2+}. The latter ions show of course also a concentration increase due to respectively pyrite oxidation and calcite dissolution. Oxygen is completely consumed during the entire 100 years, but nitrate shows some break-through after 50 years due to leaching of labile organic matter in layer B. Cation exchange causes the delay in ammonia leaching and a small retardation for sodium. Arsenic is mobilized by pyrite oxidation, but its mobility is reduced in the course of time due to expansion of the oxidized zone. This creates an increasing amount of sorption sites (to neoformed iron(hydr)oxides) and oxidizes an increasing amount of arsenite into the less mobile arsenate.

The strongest uncertainties in the prediction regard the behaviour of iron and especially manganese, because these ions already exhibited some unexpected behaviour during the experiment in Nieuwegein. This behaviour seemed to relate to fluctuations in the O_2- and NO_3-concentrations and in temperature of the WRK-water. The observed concentration range of manganese has been included in Fig.5.4 by showing 2 curves for Mn^{2+}: the lower one as predicted by EASY-LEACHER and the upper curve as based on the measured concentration levels in Nieuwegein.

Other uncertainties in the predicted quality evolution are connected with amongst others the correctness of (a) the imported hydrological model, (b) the geochemical schematization, and (c) the chemical transport code. The main problem connected with the latter is, that it assumes all leaching fronts to be sharp. In reality a broad pyrite leaching front is seen already during the first 1.5

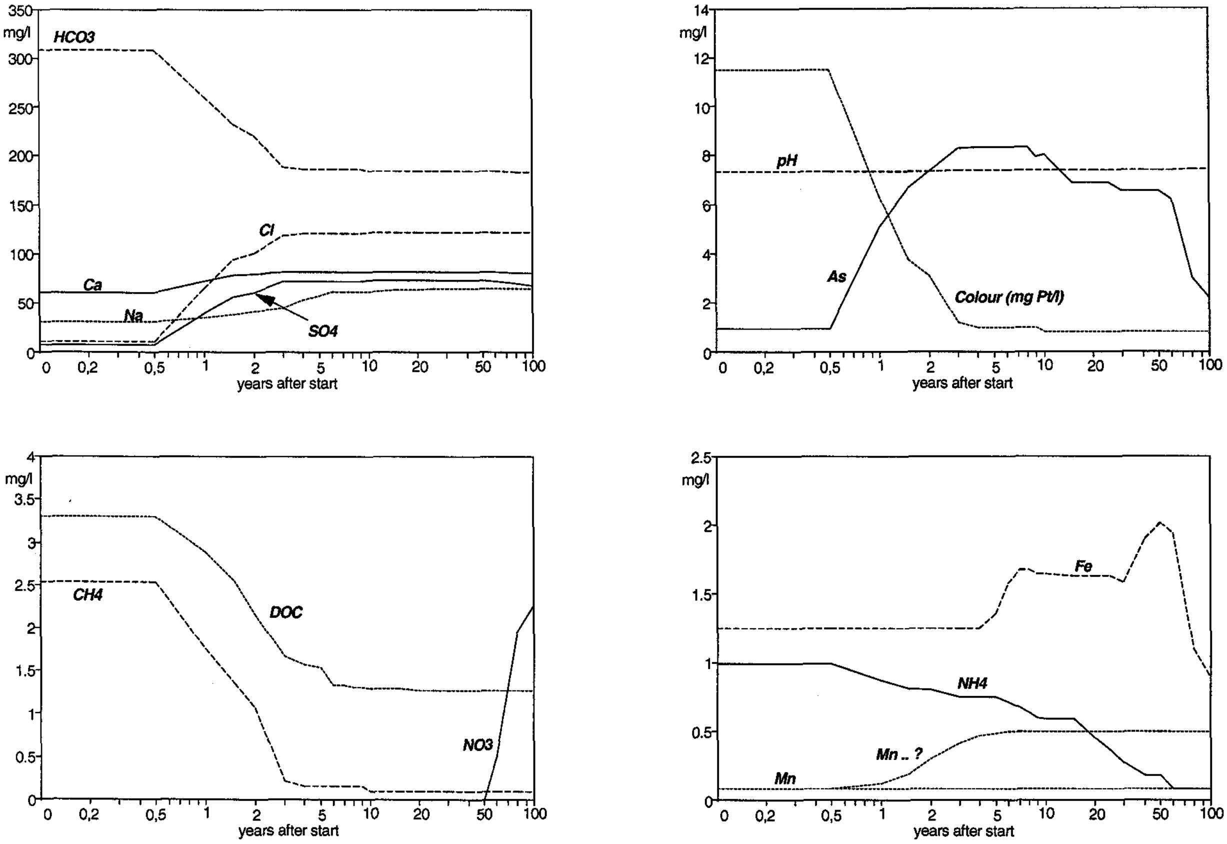

FIG. 5.4 Predicted quality evolution of WRK-water which is recovered in a future plant at Langerak, after deep-well injection and aquifer passage of 200-3550 days (calculated with EASY-LEACHER).

years (Fig.3.7 on p.24). This front could be broadening further in the course of time due to coating of pyrite by fresh precipitates of iron(hydr)oxides. This could also happen to organic matter and will happen with calcite leaching as this is strongly depending on pyrite oxidation.

The consequence of a further broadening of the leaching fronts is, that nitrate and oxygen may break-through in the recovery wells earlier than predicted. This is compensated, however, to some extent by an expected fouling of the aquifer in the vicinity of the injection well which will consume part of the oxygen and nitrate.

Well clogging by mixing of water types

Clogging of the injection wells by mixing of the influent with the native groundwater is considered impossible, which is corroborated by field experience. More realistic, however, is the clogging of recovery wells by mixing of aerobic injectate with anoxic waters containing dissolved Fe^{2+}. In that case the well-known reaction of oxygen with Fe^{2+} proceeds to form a clogging precipitate of amorphous iron(hydr)oxides together with a considerable mass of bacteria and their slimes (Van Beek, 1989). As nitrate should arrive in recovery wells ahead of oxygen, an important question arises: 'does the mixing of water containing nitrate but no oxygen, with anoxic waters containing dissolved Fe^{2+} lead to a sufficiently fast reaction to clog a well?'. The answer is unknown.

Anyhow, Fig.5.4 shows that nitrate might arrive after 50 years of injection and is to be followed by oxygen centuries later. At worst clogging of the recovery wells by mixing could start then after 50 years, which is not alarming indeed. It can be concluded that the presence of oxidizable pyrite and organic matter in the aquifer protects the recovery wells from a cumbersome early clogging.

5.5 CONCLUSIONS

The simple analytical 2D-spread sheet model EASY-LEACHER is very well capable of simulating the dynamic quality changes of an infiltrating, oxidizing solute which leaches an anoxic aquifer. The main processes simulated here were: displacement of the native groundwater and the leaching of exchangeable cations, calcite, organic matter and pyrite.

The best fit was obtained by assuming that only 2% of all organic matter was really labile, i.e. reacting fast with an oxygen consumption rate (in mg O_2/L/d) of ca. 5 f_{OC} (original fraction of total organic carbon in aquifer, on kg/kg-basis).

The main problems encountered, are connected with front-broadening and the behaviour of iron and manganese. Pyrite oxidation is not resulting in a sharp oxygen and nitrate front, as assumed in EASY-LEACHER. This front is occupying actually (after 1.5 years of injection) a zone of 20-30 m wide. With a minimum total travel distance in the aquifer of 130-190 m the actual size of this zone is not too worrying. But it should not widen further. Future research should focus on the possibility of front-broadening. The second point is that the behaviour of dissolved Fe^{2+} and Mn^{2+} seems to depend on fluctuations of O_2 and NO_3^- in the influent, and that a manganous siderite could contribute to their supply. These aspects need further investigation as well.

5.5 REFERENCES

STUYFZAND P.J., 1989a. Quality changes of river Rhine and Meuse water upon basin recharge in The Netherlands' coastal dunes: 30 years of experience. In "Artificial recharge of groundwater", Johnson & Finlayson (eds), Am. Soc. Civ. Eng., New York, 235-247.

STUYFZAND, P.J. 1989b. Hydrology and water quality aspects of Rhine bank ground water in The Netherlands. J. Hydrol. 106, 341-363.

STUYFZAND, P.J. 1989c. An accurate, relatively simple calculation of the saturation index of calcite for fresh to salt water. J. Hydrol. 105, 95-107.

STUYFZAND, P.J. 1998a. Fate of pollutants during artificial recharge and bank filtration in the Netherlands. In: Peters J.H. (ed), Artificial recharge of groundwater, Proc. 3rd Intern. Symp. on Artificial Recharge, Amsterdam the Netherlands, Balkema, 119-125.

STUYFZAND, P.J. 1998b. Quality changes upon injection into anoxic aquifers in the Netherlands: evaluation of 11 experiments. In: Peters J.H. (ed), Artificial recharge of groundwater, Proc. 3rd Intern. Symp. on Artificial Recharge, Amsterdam the Netherlands, Balkema, 283-291.

STUYFZAND, P.J. 1998c. Simple models for reactive transport of pollutants and main constituents during artificial recharge and bank filtration. In: Peters J.H. (ed), Artificial recharge of groundwater, Proc. 3rd Intern. Symp. on Artificial Recharge, Amsterdam the Netherlands, Balkema, 427-434.

STUYFZAND, P.J., F. LÜERS & H. TIMMER 1998. Development of the water quality using deep well injection, for treatment plant De Steeg in Langerak; 5. Final report after 1.5 years of monitoring. Kiwa-report KOA 98.137, in dutch, 93 p.

VAN BEEK, C.G.E.M. 1989. Rehabilitation of clogged discharge wells in the Netherlands. Quart. J. Eng. Geol. London 22, 75-80.